METABOLIC ENGINEERING OF MICROBIAL BIOCATALYSTS FOR FERMENTATIVE PRODUCTION OF NEXT GENERATION BIOFUELS

By

PHI MINH DO

A DISSERTATION PRESENTED TO THE GRADUATE SCHOOL
OF THE UNIVERSITY OF FLORIDA IN PARTIAL FULFILLMENT
OF THE REQUIREMENTS FOR THE DEGREE OF
DOCTOR OF PHILOSOPHY

UNIVERSITY OF FLORIDA

2009

To my friends, family, colleagues, mentors, and especially Ming Dang for their support and motivation for making this possible

ACKNOWLEDGMENTS

I would like to thank my committee chair, Dr. K.T. Shanmugam and my committee members, Dr. Ingram, Dr. Maupin-Furlow, Dr. Stewart, and Dr. Romeo, for their guidance over these many years, and my lab mates for their time and assistance. I would also like to extend a special thanks to Dr. Hrdy and Dr. Scharf for *T. vaginalis* NADH-dehydrogenase (NDH) DNA and termite gut [Fe]-hydrogenase DNA, respectively, Dr. Angerhofer for conducting Electron Paramagnetic Resonance (EPR) experiments, and the entire Department of Microbiology and Cell Science at the University of Florida for making this a positive experience.

TABLE OF CONTENTS

LIST OF TABLES

LIST OF FIGURES

LIST OF ABBREVIATIONS

Aad	Alcohol-aldehyde dehydrogenase
A	Absorbance
ABE	Acetone butanol ethanol fermentation
Adc	Acetoacetyl-CoA decarboxylase
ADH	Alcohol dehydrogenase
ADP	Adenosine-5'-diphosphate
amp	Ampicillin
amp^R	Ampicillin resistant
ATCC	American type culture collection
AtoB	*E. coli* thioloase
ATP	Adenosine-5'-triphosphate
Bcd	Butyryl-CoA dehydrogenase
Bcd/EtfBA	Butyryl-CoA dehydrogenase – electron transfer flavoprotein complex
BCA	Bicinchoninic acid protein determination assay
BCS	Butyryl-CoA synthesis pathway from acetoacetyl-CoA to butyryl-CoA
Bdh	Butanol dehydrogenase
bp	Base pair
BSA	Bovine serum albumin
BTU	British thermal unit; equals 1.053 kJ of energy
but$^+$	*E. coli* strain carrying butanol biosynthesis genes (chromosomal insertion of *spc*^{R}-P_{trc}-*adhE2*-P_{trc}-*atoB*-P_{trc}-*crt-bcd-etfBA-hbd*-P_{trc}-*ccrA-udhA*)
BV	Benzyl viologen
cal	Calories; equal to 4.184 J

CcrA	Crotonyl-CoA reductase from *Streptomyces*
CoA	Coenzyme-A
Crt	Crotonase
CSC	Commercial solvent corporation
CTAB	Cetyl trimethylammonium bromide
CtfAB	Coenzyme-A transferase
DCPIP	2,6-dichlorophenolindophenol
DNA	Deoxyribonucleic acid
dNTP	Deoxyribonucleotide
DOE	United States Department of Energy
DTT	Dithiothreitol
E	Actual concentration-dependent redox potential
e^-	Electron
E10	Gasoline blend; 10 % ethanol, 90 % gasoline
E85	Gasoline blend; 85 % ethanol, 15 % gasoline
E_o'	Standard redox midpoint potential
EIA	Energy Information Administration; branch of DOE
EPR	Electron paramagnetic resonance
Etf	Electron transfer flavoprotein
etfBA	Genes AB encoding electron transfer flavoprotein subunits
E_{value}	Statistical expect value
F	Faraday constant (96,500 C mol^{-1})
FAD	Flavin adenine dinucleotide
Fd	Ferredoxin

FDH	Formate dehydrogenase
[Fe-S]	Iron-sulfur cluster
FHL	Formate hydrogen-lyase
FMN	Flavin mononucleotide; riboflavin-5′-phosphate
FRT	Flippase recognition target
G3P	Glyceraldehyde-3-phosphate
GC	Gas chromatograph
GRAS	Generally regarded as safe
GutHyd	Symbiont [Fe]-hydrogenase from *R. flavipes* hindgut
H^+	Proton
Hbd	Hydroxybutyryl-CoA dehydrogenase
HPLC	High-performance liquid chromatography; High-pressure liquid chromatography
Hrs	Hours
HYD	Hydrogenase
HYD3	*E. coli* hydrogenase isoenzyme 3
IPTG	Isopropyl β-D-1-thiogalactopyranoside
J	Joules; equals to 0.239 cal ($kg\ m^2\ s^{-2}$)
kan	Kanamycin
kan^R	Kanamycin resistant
K_{cat}	Turnover rate; number of enzymatic reactions catalyzed per second (sec^{-1})
kDa	Kilodaltons (1000 molecular weight)
KFeCN	Potassium ferricyanide; $K_3Fe(CN)_6$
K_m	Michaelis constant; substrate concentration that yields $½V_{max}$ of enzyme activity

LB	Luria-Bertani medium
LHC	Light harvesting complex
Lpd	Dihydrolipoamide dehydrogenase; E3 component of PDH
*lpd101**	*E. coli lpdA* with point mutation E354K
M	Molar concentration (mol L^{-1})
mol	Mole; quantity equal to 6.022×10^{23} atoms or molecules (Avogadro number)
MTT	3-(4,5-Dimethylthiazol-2-yl)-2,5-diphenyltetrazolium bromide
MV	Methyl viologen
MV^R	Methyl viologen resistance
n	Number of electrons as in Nernst equation
N1a	[2Fe-2S] cluster of small subunit of NDH
N3	[4Fe-4S] cluster of large subunit of NDH
NAD^+	Nicotinamide adenine dinucleotide
NADH	Reduced nicotinamide adenine dinucleotide
$NADP^+$	Nicotinamide adenine dinucleotide phosphate
NADPH	Reduced nicotinamide adenine dinucleotide phosphate
ND	Not detected or not determined
NDH	NADH dehydrogenase
NEB	New England Biolabs, Inc.
NFOR	NADH-ferredoxin oxidoreductase
OD	Optical density
Ox	Oxidized
PCR	Polymerase chain reaction

PDH	Pyruvate dehydrogenase
PEP	Phosphoenolpyruvate
PFOR	Pyruvate-ferredoxin oxidoreductase
PS	Photosystem
P_{T7}	T7 promoter
P_{trc}	*trc* promoter
quad	Quadrillion BTU; 10^{15} BTU; equivalent to about 8 billion gallons of gasoline
R	Ideal gas constant (8.314 J K^{-1} mol^{-1})
Red	Reduced
Redox	Reduction / oxidation
RNA	Ribonucleic acid
S-200	Sephacryl-200 gel filtration matrix
SD	Shine-Dalgarno sequence
SDS	Sodium dodecyl sulfate
SDS-PAGE	Sodium dodecyl sulfate polyacrylamide gel electrophoresis
Sp. Act.	Specific activity (U (mg protein)$^{-1}$)
spc	Spectinomycin
spc^R	Spectinomycin resistance
T	Temperature (K)
TCA	Tricarboxylic acid cycle; citric acid cycle; Kreb's cycle
Thl	Thioloase; ThlA and ThlB
U	Unit of enzyme activty (μmole min^{-1})
V	Volt (J C^{-1}; Kg m^2 s^{-2} C^{-1})

V_{max}	Enzymes maximum velocity (U (mg protein)$^{-1}$)
Δ	Gene deletion
ΔE	Change in redox potential; $E_{product} - E_{reactant}$
ΔG	Gibbs free energy (J mol^{-1} or cal mol^{-1})
ε	Molar extinction coefficient

Abstract of Dissertation Presented to the Graduate School
of the University of Florida in Partial Fulfillment of the
Requirements for the Degree of Doctor of Philosophy

METABOLIC ENGINEERING OF MICROBIAL BIOCATALYSTS FOR FERMENTATIVE PRODUCTION OF NEXT GENERATION BIOFUELS

By

Phi Minh Do

August 2009

Chair: Name K.T. Shanmugam
Major: Microbiology and Cell Science

With increasing demand for fuel and a finite supply of petroleum, alternative renewable sources of energy need to be generated in order to free the world from the bond of fossil fuels. New transportation fuels currently in development include hydrogen and higher chain alcohols such as butanol. This study focuses on metabolic engineering of *Escherichia coli* as a microbial biocatalyst for fermentative production of these high energy alternative fuels towards identifying the rate-limiting steps in achieving high product yields. For production of hydrogen at high yield from fermentable sugars, the reducing potential from reduced nicotinamide adenine dinucleotide (NADH) produced during fermentation also needs to be converted to hydrogen. The gene encoding the first enzyme in the NADH-dependent hydrogen pathway, NADH-ferredoxin oxidoreductase (NDH), was cloned from an anaerobic protozoan, *Trichomonas vaginalis*, and expressed. The NDH protein purified from the recombinant *E. coli* and biochemically characterized. The recombinant enzyme reduced several low-potential electron acceptors such as ferredoxin and viologens with NADH as electron donor. The [Fe-S] cluster composition of this heterodimer is apparently responsible for this unique catalytic property. Attempts to couple NADH oxidation to hydrogen production using NDH, methyl viologen and native hydrogenase 3 were not successful due to thermodynamic constraints, which proved to be difficult to overcome

in vivo. Although several microbes produce butanol as a fermentation product, none of them produce butanol as sole fermentation product. Towards constructing a recombinant *E. coli* that produces butanol as the main fermentation product, the genes encoding the enzymes minimally needed for converting acetyl-CoA to butanol were cloned from *Clostridium acetobutylicum* and *Streptomyces avermitilis* and expressed in *E. coli*. The encoded proteins upon purification and mixing *in vitro* established the butanol pathway and converted acetyl-CoA to butanol. *E. coli* carrying the butanol pathway genes produced butanol but the yield of butanol was only about 2 mM. One of the rate-limiting steps in achieving higher yield butanol production was identified as the butyryl-CoA dehydrogenase complex. Other rate-limiting steps in butanol production were the competition for acetyl-CoA between ethanol and butanol pathways as well as generating sufficient amounts of appropriate reductants to support the activity of various enzymes in the butanol pathway while also maintaining proper redox balance.

CHAPTER 1
INTRODUCTION AND SIGNIFICANCE

Fuel Crisis

The United States consumes more energy than it produces, importing 34 % of its total energy needs (65). In 2007, imports accounted for 58.6 % of the petroleum consumed, indicating our dependency on foreign energy suppliers. In order to increase this nation's energy security, there needs to be a shift from foreign imports to domestic production of energy. As of 2007, 40.0 % of the energy consumed by the US was derived from petroleum followed by 23.3 % natural gas, 22.3 % coal, 8.3 % nuclear, and 5.9 % renewable energy (65). Fossil fuel accounts for 85.6 % of the total energy used. Of the petroleum consumed, 58.6 % of the petroleum was imported and 42.4 % and 15.9 % of the total petroleum consumed was used for transportation in the form of gasoline and diesel, respectively (65).

In 2007, The United States consumed 40.75 quadrillion British Thermal Unit (BTU) (quad) of petroleum per year with the predicted increase to 41.60 quad of petroleum per year in 2030 where 1 quad is equivalent to about 8 billion gallons of gasoline (65). The price of crude oil is projected to almost double from $73.33 to $130.43 per barrel in the same time period. However, crude oil price reached higher than $140 per barrel in 2008, 22 years ahead of this prediction. The predicted cost reflects global supply/demand and does not account for instability in the global economy which could radically fluctuate prices. For example, from $137.11 in July 2008 the price declined to $35.70 per barrel five months later in December 2008 (65). With the increase in demand and higher price for oil, domestic production of petroleum is optimistically projected to increase from the current 10.73 to 15.96 quad per year in 2030. This projection of increased production is expected to decrease the petroleum import from the current 28.87 to 21.72 quad per year. In the transportation sector, the expected decrease in use of gasoline for

transportation from 17.29 to 14.49 quad of petroleum per year will be due to a projected use of E85 blends up to 2.18 quad per year in 2030. This 13 % reduction in the transportation gasoline demand outlines the country's anticipated shift to a renewable fuel (65).

Combustion of fossil fuels produces heat plus carbon dioxide, carbon monoxide, and other waste products depending on the fuel source. These undesirable greenhouse gases are released into the atmosphere, which is reported to cause global temperature increase. Alternate sources of energy that are CO_2 neutral are being explored to mitigate these problems associated with fossil fuel use. The ideal fuel would be renewable, domestically produced, non-polluting, and cost effective.

Renewable Biomass to Ethanol

Renewable energy is derived from sources that are constantly replenished by natural processes such as wind, water, geothermal, and solar. Energy from these sources can be converted to a usable form such as electricity. Among these, solar energy can be directly converted to electricity or indirectly to combustible fuels, such as ethanol, H_2, biodiesel, etc. During the process of photosynthesis, plants collect and store solar energy as carbohydrates, lipids, and plant materials. Crude petroleum, a primary source of our present energy, is indeed a derivative of plant materials generated by photosynthesis eons ago and processed at high temperature and pressure. The CO_2 trapped in these plant materials is currently being released into the atmosphere during the liberation of the stored energy. Global warming observed today due to CO_2 release in this loop is caused by the time between the capture and release of this CO_2. By using biomass instead of fossil fuels, plant materials can, once again, serve as the energy intermediate to meet the current energy demand without enhancing CO_2 concentration in the atmosphere that leads to global warming.

As the plants grow, they utilize energy from the sun to fix CO_2 into sugars, which polymerize to form starch and lignocellulosic biomass, the structural components of stalks, stems, and leaves (31). Starch, which is the storage components of plants, is made up of two components, amylose and amylopectin. Amylose polymers are long chains of glucose linked by α-1,4 glycosidic bonds. Amylopectin, the other component of starch, consists of amylose with branched α-1,6 glycosidic bonds of glucose polymers occurring every after 24-30 glucose units (149). Lignocellulosic biomass is composed of three major components: cellulose, hemicellulose, and lignin (77, 188). The largest fraction, cellulose, which makes up about 20-50 % of biomass, comprises long polymers of glucose linked by β-1,4 glycosidic linkages. Hydrogen bonding between cellulose polymers results in insoluble and anhydrous crystalline structure (188). Hemicellulose, which comprises about 20-40 % of biomass, is relatively shorter, and is a highly branched polymer of mainly D-xylose with varying amounts of L-arabinose, D-galactose, D-glucose, and D-mannose (97, 98, 230). Higher percentages of hemicellulose are found in hard woods and lesser percentages are found in soft plants. The other major component, lignin makes up 10-20 % of biomass and is a polymer of mostly aromatic compounds (188).

Starch, cellulose, and hemicellulose can serve as feedstock for ethanol fermentation. The polymers must first be hydrolyzed into their monomeric carbohydrate constituents that are the usable substrates for the ethanol producing microbial biocatalyst. The α-1,4 and α-1,6 glycosidic linkage of starch is easily hydrolyzed by α-amylase, glycoamylase, and pullulanase releasing glucose (149). Hydrolysis of the β-1,4 glycosidic linkage in cellulose is catalyzed by a class of enzymes called cellulases (134, 191). There are different types of cellulases classified by their activities (15). Endocellulases are enzymes that hydrolyze internal β-1,4 glycosidic linkages

producing smaller chains of the cellulose polymer (131, 134). Exocellulase (cellobiohydrolase) hydrolyzes the β-1,4 linkages near the ends of the native cellulose polymer and polymers produced by endocellulase releasing 2, 3, or 4 linked glucose units called cellobiose, cellotriose, or cellotetrose, respectively (134). Cellobiase or β-glucosidase hydrolyzes the exocellulase products such as cellobiose into individual glucose monosaccharides (134). The structural complexity of cellulose hinders the accessibility of cellulases to the polymer, thus requiring pretreatment of the polymer and a higher level of enzymes than used for starch hydrolysis to hydrolyze cellulose to glucose (15, 230). Current hemicellulose hydrolysis involves a non-enzymatic approach. Hemicellulose is hydrolyzed by dilute acid at high temperature and steam treatments (191). This process releases the monomeric carbohydrates; however, due to the harsh conditions needed to hydrolyze hemicellulose, small amounts of the sugars and aromatic compounds of lignin are converted to other compounds that are inhibitory to fermenting organisms. These inhibitory compounds include, but are not limited to, acetate, furfural, 5-hydroxymethylfurfural (HMF), *p*-hydroxybenzoic acid, vanillin, and syringaldehyde (4, 191, 230, 231). There are several studies that are focused on reducing the production of inhibitors and/or increasing the tolerance of fermenting organisms to such compounds (79, 191, 193).

Currently in the United States, greater than 93 % of ethanol production utilizes corn starch as feedstock (31, 77, 127). Other countries with warmer climates such as Brazil, mainly use sucrose from sugarcane; whereas, more temperate regions use sucrose from sugar beets as feedstock (11, 19, 50, 125). Since these dominant feedstock sources are also food items, the increase in global ethanol demand shifts the use of these food items to fuel thus increasing global food prices (31, 91). In order for ethanol to be an economically favorable fuel, its feedstock

must be derived from non-food sources such as lignocellulose – cellulose and hemicellulose fractions of biomass (77, 127, 188).

Yeast, such as *Saccharomyces cerevisiae*, are the industrial ethanol producers (50, 127, 202). *S. cerevisiae*'s historical prevalence and industrial knowledge still makes it the organism of choice for ethanol fermentation; however, its substrate utilization limitations may suggest a shift to non-traditional fermentative organisms. *S. cerevisiae* naturally ferments glucose but not pentoses such as xylose, the second most abundant carbohydrate found in biomass (106, 156, 202, 227). Other yeast, such as *Pichia stipitis* and *Candida tropicalis*, can ferment xylose; however, their low ethanol yields with xylose and inability to ferment other hemicellulose sugars has hindered further strain development (77, 105, 106). Expression of xylose reductase and xylitol dehydrogenase from *P. stipitis* in recombinant strains of *S. cerevisiae* was only partially successful due to the inherent redox constraints of this pathway, which resulted in undesirable byproduct formation, such as xylitol, in the absence of oxygen (7, 115, 181, 203). To mediate this problem, xylose isomerase from yeast *Piromyces sp*. E2 and *Thermus thermophilus* were cloned and expressed in *S. cerevisiae* resulting in strains with similar ethanol yields on xylose as with glucose (25, 36, 203). Attempts in engineering *S. cerevisiae* to ferment pentose such as L-arabinose were less successful due to the poor expression of bacterial source genes in this eukaryote (25, 36, 80, 216, 218).

Bacterial ethanol fermentation also has potential industrial applications. *Zymomonas mobilis* is a traditional bacterial ethanol producer used for fermentation of alcoholic beverages such as tequila. *Z. mobilis* metabolizes sugars by Entner-Doudoroff pathway and produces only ethanol as fermentation product. Advantages of *Z. mobilis* include, but are not limited to, high ethanol production yield of up to 120 g L^{-1}, high ethanol tolerance, and high specific ethanol

productivity (139, 170, 184). *Z. mobilis'* inability to utilize other sugars found in biomass hinders the industrial use of this organism for production of fuels. Like yeast, recombinant strains of *Z. mobilis* were constructed for utilization of xylose and arabinose resulting in strains with broader substrate capability while retaining high ethanol yields; yet, problems of long fermentation times due to low productivity has hindered the development of these strains (30, 54, 127).

Escherichia coli is a Gram-negative facultative anaerobe that catalyzes mixed acid fermentation. The vast accumulated knowledge and available genetic tools makes this organism a feasible platform for metabolic engineering for production of ethanol or other valuable chemicals. This organism has a broad range of substrate utilization, can naturally ferment all carbohydrates found in lignocellulose, and can grow in minimal salts medium which reduces cost of product production. To date, one of the most promising ethanologenic *E. coli*, strain KO11, has a chromosomally integrated pyruvate decarboxylase gene (*pdc*) and alcohol dehydrogenase gene (*adhB*) from ethanologenic bacterium *Zymomonas mobilis* (97, 155, 227). Strain KO11 has the same ethanol specific productivity as yeast using glucose as a substrate and can utilize extremely high xylose concentrations of over 100 g L^{-1} (96-98, 227, 235). However, disadvantage of this recombinant strain include low ethanol tolerance of about 5 % which was about one-third that of yeast's ethanol tolerance.

Problems with ethanol: Ethanol is the first widely used commercially available renewable transportation fuel. The use of ethanol is a first step away from the dependence on fossil fuels and towards a new era of clean, sustainable energy. Ethanol as a fuel however, is not perfect. Pure ethanol cannot be combusted in modern automotive engines due to its chemical properties (199). Ethanol has a higher vapor pressure than gasoline, which at operating

temperatures, could produce vapor bubbles within the fuel lines. The "vapor lock" can cause the car to hesitate and stall due to inadequate fuel delivery. Another main concern with ethanol is that it has a higher latent heat of vaporization which requires more heat to vaporize the ethanol fuel than gasoline which can reduce the ability of the car's engine to ignite the fuel at lower temperatures. High ethanol containing fuels may be a problem for older cars with carburetors due to inadequate fuel delivery if they are not adjusted for the lower combustional energy. Modern fuel injection delivery systems sense the lower energy and adjust by increasing fuel delivery; however, this in turn lower fuel efficiency. Most internal combustion engines can operate with 10 % ethanol mixtures with 90 % gasoline without modifications, but only new engines especially modified for E85 can utilize 85 % ethanol, 15 % gasoline mixture. The chemical properties of ethanol also make ethanol incompatible with current fuel transportation infrastructure and utilization. Ethanol's lower solubility in gasoline, high solubility in water, and hygroscopic nature present an immense problem in fuel transportation (199). Currently, gasoline is primarily transported through pipelines. Moisture that seeps into transportation pipelines is normally not a problem due to water's low solubility in gasoline. Since ethanol is hygroscopic, a gasoline/ethanol mixture permits water contamination in fuel which may cause damage to engine parts. The polar nature of ethanol molecules creates strong hydrogen bonds with water. Since water easily separates from gasoline, water contamination causes a temperature dependent phase separation of gasoline and ethanol/water mixture (199). Low temperature is a major concern since it increases phase separation of water contaminated gasoline/ethanol mixture which may lead to frozen fuel lines during the winter. The added corrosiveness of ethanol and water also makes it less suitable for pipeline transportation. To mediate this problem, ethanol requires its

own separate transportation system and needs to be mixed with gasoline at the pumping station to avoid water contamination and fuel separation.

Another problem with ethanol is that current production requires use of food items as feedstock which in turn drives up the cost of both food and fuel. A shift to lignocellulosic ethanol would remedy this problem; however, more research will be needed to develop improved processes and microbes to handle the harsh scale of industrial fermentation of biomass. Continual usage of ethanol as a fuel will require a drastic overhaul of the fuel infrastructure. A shift to a new "second" generation renewable fuel may be required to move beyond the problems associated with ethanol use. The new fuel must be clean, cost-effective, high in energy, and/or does not require much change in current delivery systems. Potential next generation renewable fuels are hydrogen and butanol.

Second Generation Renewable Fuels

Hydrogen

The use of hydrogen as a fuel has been of great interest since its combustion produces only heat and water, although shift to H_2 as a fuel would also require a new infrastructure. Hydrogen provides more energy per unit mass than all other combustional energy sources (57). The combustional energy of hydrogen is 52,200 BTU/lb whereas gasoline, compressed natural gas, propane, and ethanol yield only 18,600 BTU/lb, 20,200 BTU/lb, 19,900 BTU/lb, and 11,600 BTU/lb, respectively (57). During the energy crisis of the 1970s, hydrogen sources and applications were explored. Hydrogen was, at the time, believed to be the "fuel of the future". Most of the funds for hydrogen research diminished after oil price dropped but resurfaced again in the 1990s with the concern about the greenhouse effect of net CO_2 release into the atmosphere from fossil fuel use (20). In 2003, President Bush announced a $1.2 billion hydrogen fuel

initiative for developing technology associated with creating, storing, distributing, and utilizing hydrogen in fuel cells bringing hydrogen to the fore-front again (41).

Butanol

The current shift to using ethanol as a fuel additive is an important progression towards the utilization of renewable fuels. The use of butanol as a fuel additive has been of great interest because of its advantages over ethanol. Butanol has a low solubility in water. It is also hydrophobic and has complete solubility with gasoline at any ratio (168). Gasoline/butanol mixtures could be pumped in pipelines without further modification and this approach do not require a separate mixing station. Butanol also provides higher energy per unit mass than ethanol with a value closer to gasoline (86 %). The combustional energy of butanol is 16,000 BTU/lb whereas gasoline and ethanol yields are 18,600 BTU/lb and 11,600 BTU/lb, respectively (168). Since butanol's properties resemble those of gasoline, 100 % butanol could be used in automotive engines, even on older cars built in the early 1990's, without any modification (168).

The history of biological production of butanol dates back to its discovery by Pasteur in the mid 1800's. Industrial ABE fermentations were greatly employed from the 1910's to the late 1940's as a source of solvents and synthetic rubber (107). The emergence of the, at the time plentiful and cheap, petrochemical based solvent production in the 1940's led to the demise of ABE fermentations. Sixty years later, as the petroleum cost and reserves reached problematic levels, butanol fermentations are being explored again as a source of renewable energy.

CHAPTER 2
BACKGROUND ON HYDROGEN PRODUCTION

Current Hydrogen Production Methods

As mentioned before, hydrogen is an excellent fuel whose combustion only releases heat and water. This section will briefly summarize current technology in hydrogen production from both fossil fuel and renewable sources. I will also introduce biological sources and microbial biocatalysts available for both photosynthetic and fermentative hydrogen production.

Methane Steam Reforming

At present, hydrogen is produced by a process called steam reforming which utilizes the water-gas-shift reaction (Equation 2-1)

$$\begin{array}{ll} CH_4 + H_2O \rightarrow CO + 3H_2 & (700 - 1{,}100\ ^oC) \\ CO + H_2O \rightarrow CO_2 + H_2 & (130\ ^oC) \\ \hline CH_4 + 2H_2O \rightarrow CO_2 + 4H_2 & \end{array} \qquad (2\text{-}1)$$

When compared with other fossil fuels, methane, commonly known as natural gas, is currently the most favorable feedstock for hydrogen production because of its availability and its high hydrogen to carbon ratio, which minimizes the yield of CO_2 (152). The disadvantage of this method is that it uses a fossil fuel. In 2007, US imported 19.9 % of its natural gas needs which was about 4.8 % higher than in 2004 (65). Using this method for production of hydrogen for fuel production would require additional import of natural gas and would only increase this country's dependence on foreign energy imports.

Coal Gasification

United States has a abundant supply of coal with estimated reserves lasting for an additional 200 years at the current rate of use (42). The shift towards hydrogen production from coal will decrease energy import. The production of hydrogen from coal involves a process called gasification. This process comprises partial oxidation of coal with oxygen and steam in a

high temperature and pressure reactor (141). This process, like the steam reforming of natural gas, produces a mixture of carbon monoxide and hydrogen in which the CO can be used to make additional hydrogen. One concern with coal as a feedstock is that this process releases a significant amount of CO_2 due to its high carbon to hydrogen ratio compared to methane. Using current technology, the combustion of coal produces 19 kg of CO_2 per kg hydrogen produced compared to the combustion of natural gas that produces 10 kg of CO_2 per kg hydrogen produced (152). Coal also contains impurities that would be released into the environment such as sulfur oxides, nitrogen oxides, lead, and mercury. These concerns are being met with clean coal technologies that reduce plant emissions and increase plant thermal efficiencies. Further improvements in these technologies could enhance coal's future as a source of hydrogen. However, the collected toxic materials still need to be disposed in an environmentally safe manner. The cost of hydrogen production from coal is one of the lowest only if the demands for hydrogen are sufficient to construct a centralized plant and a large distribution system (152). In 2003, then President Bush announced that the United States would be the first to sponsor a $1 billion, 10-year demonstration project to create world's first coal-based, zero-emission electricity and hydrogen plant. This technology is expected to accelerate the commercialization of hydrogen fuel by 2020 (42).

Hydrogen from H_2O

Hydrogen could be generated by splitting water into its two elemental components: hydrogen and oxygen, with input of energy. This process, termed electrolysis, involves passing an electric current through water. The water molecule dissociates producing hydrogen at the cathode and oxygen at the anode. The electrolysis efficiency ranges from 75-80 % with the remainder of the energy lost as heat (152). Increasing the operating temperatures could increase the efficiency to 85-90 %; however, certain challenges such as electrode and proton exchange

membrane stabilities must be overcome. Currently, the cost of the energy input into the system outweighs the value of the hydrogen evolved (152). This technology could be coupled with the electricity produced from nuclear and renewable resources as discussed below for H_2 production.

Nuclear power could also serve as the source of energy for hydrogen production reactions. The heat produced from the nuclear fission reaction could be coupled to steam reforming and gasification processes of natural gas and coal, respectively. As a heating source, this would reduce the CO_2 emission from natural gas steam reforming by 40 %. The electricity produced by nuclear power could be used in electrolysis of water although the efficiency of electrolysis makes it uneconomical (210). At high temperatures thermal-chemical water splitting reactions can be used to catalyze the dissociation of water. One example of this is the sulfur-iodine cycle (39) (Equation 2-2):

$$\begin{array}{ll} I_2 + SO_2 + 2\ H_2O \rightarrow 2\ HI + H_2SO_4 & (120\ ^oC) \\ H_2SO_4 \rightarrow SO_2 + H_2O + \frac{1}{2}\ O_2 & (830\ ^oC - 900\ ^oC) \\ 2\ HI \rightarrow I_2 + H_2 & (300\ ^oC - 400\ ^oC) \\ \hline H_2O \rightarrow H_2 + \frac{1}{2}\ O_2 & \end{array} \qquad (2\text{-}2)$$

As with all nuclear technologies, there are also disadvantages of high capital cost and nuclear waste storage and disposal (152).

The use of renewable energy is the ultimate goal in sustainable hydrogen production. Wind energy is often viewed as an excellent source for renewable hydrogen production in a mid-term time span (152). Wind energy is pollution-free and requires no feed. The electricity produced from the wind turbines could be used to electrolyze water. In order for this technology to be economical, there needs to be a reduction in the cost of electricity produced by the wind powered turbines, a reduction in the cost of the electrolyzers, and optimization in hydrogen storage systems (152). The cost of electricity produced by wind could be attributed to the cost

and efficiency of the wind turbines. Location plays an important role in site selection and cost. The site must have powerful wind throughout the year, be located near existing distribution networks, and be economically competitive for land use. The variability of wind intensity may affect electricity output, thus affecting the sustainability of electricity and hydrogen production. This problem could be solved with a backup power grid, which supplies electricity when wind power is less than sufficient; however, this adds additional capital cost. Other disadvantages of wind power are the high noise generated by the turbines, impact on local bird life, visual esthetic of the landscape, and interferences to electromagnetic signals (152).

Solar energy could also be used for hydrogen production. One method of producing "solar-hydrogen" utilizes photovoltaic cells that capture solar energy and convert it to electricity. This electricity could again be used to produce hydrogen by electrolysis. Currently, the cost of electricity from a photovoltaic cell module is 6 to 10 times that of electricity from coal or natural gas (152). Significant cost reduction is required if solar energy is to be used for electricity and hydrogen production.

Another method of hydrogen production from solar energy that is being researched utilizes photoelectrochemical cells for the direct production of hydrogen from water without using an intermediate electrical current. This requires a submersed solid inorganic oxide electrode catalyst that is capable of splitting the water molecule directly when light energy is absorbed. Potential candidate materials are $SrTiO_3$, $KTaO_3$, SnO_2, and Fe_2O_3. Stability and catalytic efficiencies require further optimizations (126, 152). As with wind power, this renewable energy is not without its own problems. Solar output changes both daily and seasonally. Backup systems must be set up to supply energy when solar energy is not sufficient or absent to meet demands. This requires about four to six times more solar modules than needed during peak

operations. The surplus energy produced is stored for hydrogen production during less favorable conditions. Land considerations are similar to that of wind power: the site must have intense year-round sunlight, be located near existing distribution networks, and be economically competitive for land use. Other concerns with solar energy are the possible release of toxic materials such as cadmium in the production and disposal of photovoltaic cells (152).

Moving beyond inorganic catalysts, biocatalyst such as cyanobacteria and algae could evolve hydrogen by using solar energy coupled with photosynthesis. This process is presented in greater detail in a later section.

Biomass Conversion to Hydrogen

In association with solar energy, photons could be captured by biological processes to produce biomass via photosynthesis. Biomass could then be processed thermochemically by gasification/pyrolysis processes followed by steam reforming similar to hydrogen production from coal (10). Biomass conversion is renewable and non-polluting. Any CO_2 released from this process is fixed by recent photosynthesis; thus, zero net CO_2 is produced within this short time frame. However, this does not account for the CO_2 produced from the needed heating processes such as the burning of fossil fuels and this can be mitigated by the use of biomass. There are two general types of biomass that could be used: primary biomass and biomass residue (152). Primary biomass includes energy crops such as switchgrass, poplar, and willow. These are dedicated plants grown for energy production. Biomass residues include agricultural and municipal waste. The problems currently associated with biomass gasification/pyrolysis include variable efficiencies, tar production, and catalyst erosion (10, 152). In addition to gasification/pyrolysis of biomass, biological processes utilizing microbes could also yield hydrogen directly by fermentation (20).

Microbial Hydrogen Production

History

Hydrogen production by photosynthetic cyanobacterium *Anabaena* was first reported by Jackson and Ellms in 1896 (102). Hydrogen was later found, in 1901, to be also produced from light-independent anaerobic fermentation from formic acid (86, 157). In 1931, Stephenson and Strickland identified the enzyme responsible for reversible hydrogen production from enteric bacteria which they termed hydrogenase (186, 187). In 1949, Gest and Kamen demonstrated that hydrogen evolution by photosynthetic bacterium *Rhodospirillum rubrum* was dependent on nitrogen fixation, which was later determined to be from the nitrogenase reaction (71). In 1942, Gaffron observed that green alga *Scenedesmus obliquus*, in the presence of light, could use H_2 as an electron donor for CO_2 fixation in a process he named photoreduction (92, 136). Gaffron and Rubin also reported that *S. obliquus* could release molecular H_2 and CO_2 in the dark after adaptation in a nitrogen atmosphere (70). To prevent photoreduction and CO_2 fixation from occurring when the algae were exposed to light, they trapped the CO_2 released by the algae to produce a CO_2-free environment. Under these conditions, *S. obliquus* continually produced hydrogen in the presence of light at a 10-fold higher rate compared to the cultures without CO_2 trapping. Using electron-transport inhibitors, Gaffron concluded that the algae tested produced hydrogen via a non-cyclic electron flow through photosystems II and I to hydrogenase (189, 190). Arnon and Tagawa identified ferredoxin as the electron donor for hydrogenase, thereby linking photosynthesis to hydrogen production (192). *In vitro* experiments conducted by Benemann and others demonstrated hydrogen evolution by spinach chloroplasts mixed with *Clostridium kluyveri* hydrogenase and ferredoxin (21). It has been well established that microbes produce hydrogen by either photosynthetic or fermentative processes (9, 82). Photobiological hydrogen production utilizes H_2O as a source of electrons for the reduction of protons whereas

fermentative hydrogen production by algae obtains its reducing power from carbon storage compounds.

Photosynthetic Hydrogen Production

Members from both eukaryotes and prokaryotes carry out photobiological hydrogen production. Of the prokaryotes, cyanobacteria and photosynthetic bacteria carry out oxygenic photosynthesis and anoxygenic photosynthesis, respectively, utilizing either hydrogenase or nitrogenase as the terminal enzyme. In these processes, light provides the energy for both hydrogenase and nitrogenase based H_2 production (165). Eukaryotic hydrogen production is restricted to green algae and hydrogenase. In oxygenic photosynthesis, cyanobacteria and algae utilize chlorophyll as light harvesting pigments and water as the source of electrons (189, 190). Anoxygenic photosynthesis differs in that photosynthetic bacteria utilize bacteriochlorophylls as the light-harvesting pigments and either inorganic or organic compounds serve as the reductant for hydrogen production (151).

The underlying process of photosynthesis is well understood. Oxygenic photosynthesis revolves around the two photochemical reaction centers: Photosystems (PS) I and II (the classical Z scheme; Figure 2-1). These photosystems are located within the thylakoid of chloroplast or the membranes of cyanobacteria. Splitting of water is mediated by the excitation of an electron at PS II P_{680} reaction center or light harvesting complex (LHC-II) by the absorption of a photon. The electron passes through the membrane via electron carriers generating membrane potentials transferring electron to reaction center P_{700} (LHC-I) of PS I. P_{700} then absorbs another photon and the energized electron passes though additional membrane-bound carriers to soluble ferredoxin (Fd). Reduced Fd is the electron donor for Fd- nicotinamide adenine dinucleotide phosphate ($NADP^+$) oxidoreductase that produces reduced nicotinamide

adenine dinucleotide phosphate (NADPH) for CO_2 fixation (169). Under anaerobic conditions, the reduced Fd is also the electron donor for hydrogenase mediated hydrogen production.

There are two types of photobiological hydrogen production from water in green algae: direct and indirect biophotolysis. Direct biophotolysis involves both PS II and PS I simultaneously and electrons from water are transferred directly to hydrogenase for hydrogen production. The problem with direct biophotolysis is that the O_2 evolved by PS II inactivates hydrogenase, the H_2 producing enzyme. Indirect biophotolysis occurs in two stages. In the first stage, NADPH is produced from reduced Fd. NADPH and adenosine-5'-triphosphate (ATP) are used to fix CO_2 to carbohydrates. In the second stage, PS II activity is reduced to the level of respiration either by low light or by sulfur depletion, and the carbohydrates produced during photosynthesis stage are metabolized producing NAD(P)H. Electrons from NAD(P)H feed into quinone-Cytb_6f complex, then to PS I which leads to the reduction of Fd with the absorption of a photon (Figure 2-1). Reduced Fd then transfers its electrons to hydrogenase for hydrogen production. The advantage of indirect biophotolysis is that it temporally separates the production of O_2 and H_2 and eliminates hydrogenase inactivation by O_2. Another advantage is that the gas mixture produced in the second stage is composed of CO_2 and H_2, which is far less dangerous to handle compared to the explosive mixture O_2 and H_2 from direct biophotolysis (165). In addition, in indirect biophotolysis, H_2 production can proceed until all the stored carbohydrates have been converted to H_2 due to the stability of hydrogenase. In a similar experiment using cyanobacteria, Mitsui and his coworkers temporally separated carbohydrate production in the light and conversion to H_2 in the dark through nitrogenase (140). This light-dark cycle can be repeated several times.

Hydrogenase- and nitrogenase- based hydrogen production systems. The enzymes mediating the conversion of protons and electrons to molecular hydrogen are hydrogenase and nitrogenase. Hydrogenase is present in both eukaryotic and prokaryotic microorganisms whereas nitrogenase, an ATP-dependent enzyme, is restricted to bacterial and archaeal systems. These enzymes from different organisms range from moderately to extremely oxygen sensitive which causes a problem for oxygenic photosynthesis. The oxygen-sensitivity of hydrogenase is overcome by *Scenedesmus* by producing the enzyme only during dark anaerobic conditions (70). This allows *Scenedesmus* to temporally separate hydrogen production from photosynthesis; however, upon introduction of light, hydrogen production decreases dramatically within a short period of time due to inactivation of hydrogenase. Sustainability of H_2 production is increased by depriving the alga *Chlamydomonas reinhardtii* of sulfur-containing compounds (223). The deprivation of inorganic sulfur decreases oxygenic photosynthesis (PS II) without affecting PS I or the rate of cellular respiration. The absolute rate of photosynthesis mediated O_2 production decreases below the rate of respiration 24 to 30 hours (hrs) after S-depletion creating an anaerobic environment that is suitable for sustained hydrogen production (137).

Even with the use of cyclical sulfur availability, the algal culture is limited to producing hydrogen only during periods of sulfur deprivation. Ideally, a commercially viable photo-hydrogen producing system should simultaneously and continuously operate PS II and hydrogenase (direct biophotolysis). Much time and effort have been invested in producing an oxygen-stable hydrogenase with little success (40, 46). The Department of Energy (DOE) Hydrogen R&D Program does not believe that there is at present a plausible approach to overcome the O_2 inhibition of hydrogenase in a direct biophotolysis process and does not recommend further effort to pursue this area of research (22). Other research in this area

includes reducing the number of light harvesting pigments or antenna size per photosystem to increase photosynthetic efficiency. Individual algal cells exhibit maximal rate of photosynthesis at low light intensity of only 10 to 20 % of sunlight. Higher light intensities are not utilized due to the slow electron transfer rate between PS II and PS I resulting in an energy loss as heat or fluorescence (27, 29, 143). By combining the shading effects of the culture and the individual cell's efficiency, it was calculated that up to two-third of the light absorbed is wasted due to the light saturation effect (22). Current commercial algal production systems with *Spirulina* operate only at 1 % of total solar energy conversion. The goal of the DOE is to reach 10 % solar conversion efficiency (22).

The principal role of nitrogenase in the cell is to reduce molecular nitrogen to ammonia. Nitrogenase also produces molecular hydrogen with different stoichiometric yields along with NH_3 depending on the metal within the active center (63, 165) (Equation 2-3):

Molybdenum nitrogenase:	$N_2 + 8\ H^+ + 8\ e^- \rightarrow 2\ NH_3 + 1\ H_2$	(2-3)
Vanadium nitrogenase:	$N_2 + 12\ H^+ + 12\ e^- \rightarrow 2\ NH_3 + 3\ H_2$	
Iron nitrogenase:	$N_2 + 21\ H^+ + 21\ e^- \rightarrow 2\ NH_3 + 7.5\ H_2$	

Nitrogenases are classified by the metals found in the active site such as molybdenum, vanadium, or iron. Although V- and Fe- nitrogenases are found in the N_2-fixing bacteria, their concentration in the cell is significantly low compared to Mo-nitrogenase, even when these alternate nitrogenases are maximally induced. Only the structure of molybdenum nitrogenase has been solved; however, amino acid sequences reveal similarities between the other forms (116, 176).

In the absence of N_2, H_2 is the only product of nitrogenase. These reactions are energy intensive requiring 2 moles ATP per mole electron transferred (63). Unlike hydrogenase hydrogen production by nitrogenase is thermodynamically favorable due to the of hydrolysis of

ATP. With nitrogenase, hydrogen production continues at hydrogen pressures of up to at least 50 atmospheres (180). Hydrogen production by N_2-fixing bacteria is also associated with a hydrogen uptake hydrogenase reoxidizing H_2 with a net decrease in yield. Mutations in uptake hydrogenase are found to increase hydrogen yields (110).

Nitrogenases also exhibit varying levels of O_2 sensitivity. Through evolution, various organisms developed different mechanisms of separating oxygen from O_2 sensitive nitrogenase. In cyanobacteria, such as *Anabaena*, under nitrogen-limitation conditions, a fraction (~8-12 %) of the filament differentiates into a morphological state known as heterocyst which contains nitrogenase. Heterocysts lack the oxygen-evolving PS II and receive nutrients and reductant from adjoining vegetative cells (74). Protection mechanisms have also been discovered in nonheterocystous filamentous cyanobacteria such as *Trichodesmium* (23). In this organism, the nitrogenase is localized in subsets of consecutively arranged cells in each filament, which accounts for about 15-20 % of all the cells. Unlike heterocysts, these cells also contain PS II components. During times of increased nitrogen fixation, PS II components were found to be down regulated and vice versa. This allows *Trichodesmium* to spatially and temporally segregate nitrogen fixation and hydrogen evolution from oxygenic photosynthesis.

Fermentative Hydrogen Production

According to Gray and Gest (76), all prokaryotes that produce hydrogen belong to four groups: strict anaerobic heterotrophs that do not contain a cytochrome system (*Clostridium*), heterotrophic facultative anaerobes that contain cytochromes and use formate to produce hydrogen (*E. coli*), strict anaerobes with a cytochrome system (*Desulfovibrio*), and photosynthetic bacteria with light-dependent evolution of hydrogen (*Rhodospirillum*). They suggested the first group of organisms produce hydrogen as a way to dispose of electrons coupled to energy yielding oxidation of carbohydrates. Hydrogen production from the second

group was proposed to promote energy-yielding oxidations by removing the end-product formate. Group three organisms are believed to possess both mechanisms for hydrogen production (146). The only group three organism known is *Desulfovibrio* sp. (16). Group four organisms use light as the energy source for hydrogen production; however, unlike cyanobacteria and algae, electrons come from organic or inorganic substrates instead of water. The first three groups of bacteria use hydrogenase for hydrogen production while the primary enzyme of photosynthetic bacteria for hydrogen production is nitrogenase. Beyond prokaryotes, strict anaerobic protozoa also posses hydrogen producing capabilities within the hydrogenosome. Hydrogenosomal hydrogen production is mechanistically similar to that of group one organisms.

Strict anaerobes such as *Clostridium* sp. lack a cytochrome system for oxidative phosphorylation so all ATP generation must be from substrate level phosphorylation during fermentation. During glycolysis, glucose is oxidized to pyruvate producing ATP and reduced nicotinamide adenine dinucleotide (NADH). Pyruvate is further oxidized by pyruvate-ferredoxin oxidoreductase (PFOR) into acetyl-CoA, CO_2, and the electrons are transferred to Fd. Reduced Fd provides electrons for hydrogen production through a soluble [Fe]-hydrogenase. Initially, it was believed that NADH produced by 3-P-glyceraldehyde dehydrogenase during glycolysis is also used to reduce Fd by a putative NADH-ferredoxin oxidoreductase (NFOR) as described by Thauer *et al.* (82, 146, 215). Competing routes of NADH oxidation are the reduction of acetyl-CoA to ethanol, reduction of pyruvate to lactate, and conversion of acetyl-CoA to butyryl-CoA with an ATP yielding formation of butyrate catalyzed by phosphotransbutyrylase and butyrate kinase. Lactate or ethanol production does not yield ATP. ATP could also be generated from acetyl-CoA by phosphotransacetylase (PTA) and acetate kinase in the production of acetate. The maximum theoretical yield of 4 moles H_2 per mole glucose can be achieved in bacteria if acetate

is the sole fermentation product and all the NADH produced during glycolysis is converted to H_2. The yield is only 2 moles H_2 per glucose if butyrate is the sole end product. The observed yield is typically between 40-50 % (~1.5-2.0 H_2/glucose) of the theoretical maximum (4 H_2/glucose) for wild type *Clostridium* producing both acetate and butyrate as major fermentation products (146). This suggests that NADH is not a preferred reductant for H_2 production in *Clostridium*, although an NADH dependent H_2 production was demonstrated in cell extracts. My own studies also confirmed the existence of an NADH-dependent H_2 evolution activity in *C. acetobutylicum*. This reaction had a requirement for acetyl-CoA. However, an NADH-ferredoxin oxidoreductase was never isolated after several attempts by various investigators, including myself.

Recently, Thauer *et al.* discovered that the clostridial NADH-dependant ferredoxin reduction activity is actually a coupled reaction with crotonyl-CoA reduction by butyryl-CoA dehydrogenase/ETF (electron transfer flavoprotein) complex, thus, requiring butyrate producing pathway for NFOR activity (124). This explanation accounts for the lower observed hydrogen yield and also the need for acetyl-CoA in cell extract. Strict anaerobic protozoan hydrogen production is mechanistically similar to that of *Clostridium*. Protozoan hydrogen production is compartmentalized within a specialized energy producing organelle called the hydrogenosome. In this organelle, pyruvate, which was derived from glucose, is metabolized to acetyl-CoA, CO_2, and H_2 by PFOR and hydrogenase in the same manner as clostridia. However, protozoa such as *Trichomonas* have an NADH-dehydrogenase that is homologous to mitochondrial complex I capable of reducing low potential electron acceptors such as ferredoxin (94).

Heterotrophic facultative anaerobes such as *E. coli* produce hydrogen using the formate hydrogen-lyase (FHL). FHL complex consists of two enzymes, formate dehydrogenase (FDH-

H), [NiFe]-hydrogenase isoenzyme 3 (HYD3), and electron carriers connecting the two. FDH-H converts formate to CO_2, $2H^+$ and $2e^-$. The electrons are transferred to HYD3 for hydrogen production (28). Theoretically, *E. coli* could produce 2 moles H_2 per mole glucose through glycolysis, pyruvate formate-lyase and FHL; however, the observed net H_2 yields are only about 60 % of the theoretical maximum (146) suggesting that some of the formate or H_2 is consumed by other reactions in the cell. Another facultative anaerobe with higher hydrogen yield is *Enterobacter aerogenes*. Mutations leading to decreased α-acetolactate synthase activity have been shown to increase H_2 yield from 0.8 H_2/glucose to 1.8 H_2/glucose when compared to wild-type strain HU101 (101). Ogino and coworkers compared different strains of *Clostridium butyricum* to *E. aerogenes* and found that *E. aerogenes* is not sensitive to oxygen, has a broad range of substrate utilization, and has comparable hydrogen yields with *C. butyricum. E. aerogenes* also grows in mineral salts medium and does not require expensive reducing agents in growth medium which lowers the cost of hydrogen production (153).

According to an economic analysis submitted to the National Renewable Energy Laboratory, production of hydrogen by fermentation is expected to be cost effective if the organism could produce a yield of 10 moles H_2 per mole of glucose (64). This takes into account capital cost of plant, plant production rate, cost of substrates, and H_2 market value. Theoretically, up to 12 moles H_2 could be produced from a mole of glucose by complete oxidation (Equation 2-4)

$$C_6H_{12}O_6 + 6\ H_2O \quad \rightarrow \quad 12\ H_2 + \ 6\ CO_2 \qquad (2\text{-}4)$$

Only an *in vitro* enzymatic reaction was reported to produce this higher yield although low rates and the high cost of the enzymes makes this method impractical for large-scale application (219, 220, 233). None of the whole cell based H_2 production methods could reach this minimum

requirement of 10 H_2 per glucose for cost effective hydrogen production due to physiological and thermodynamic barriers. Strict anaerobes have the ability to couple NADH to H_2 production but lack the capability to fully oxidize acetyl-CoA to CO_2 due to an incomplete tricarboxylic acid (TCA) cycle. Most of the carbons and associated reductants are lost as fermentation products. As for facultative anaerobes, formate appears to be the sole substrate for hydrogen production. Although these organisms do have a complete TCA cycle, the inability to convert NADH directly or indirectly to H_2, lowers the yield to only 2 H_2/glucose.

In order to approach the goal of 10 H_2/glucose, a hybrid hydrogen producing system would be required, combining the pathways of facultative and strict anaerobic organisms. *E. coli* produces 10 NAD(P)H from glucose during aerobic conditions from the following reactions: 2 NADH from 3-P-glyceraldehyde dehydrogenase; 2 NADH from pyruvate dehydrogenase; 2 NADH from α-ketoglutarate dehydrogenase; 2 NADH from malate dehydrogenase; and 2 NADPH from isocitrate dehydrogenase. Transcriptional regulation of TCA cycle genes is effected by the ArcAB and FNR systems. During anaerobic conditions, a membrane bound ArcB senses the redox state, perhaps from increased concentrations of reduced electron carriers from NADH dehydrogenase to quinones and activates ArcA by phosphorylation (215). ArcA-P is a global regulator that represses transcription of the genes for many TCA cycle enzymes. FNR is also activated under anaerobic conditions and regulates *arcA* transcription (183). The role of FNR is to induce genes encoding anaerobic respiration proteins and repress some of the aerobic genes (215). Unlike the two-component regulatory system of ArcAB, FNR is activated by the reduction of a bound [Fe-S] cluster, causing a conformational change in the protein (215). If an electron sink that could actively convert electrons from NADH to hydrogen is active in the cell, the NADH/NAD^+ ratio will be kept low allowing the TCA cycle to be active even under

anaerobic conditions. In this case, the electron sink would be NADH-dependant hydrogen production pathway, such as the one from *Trichomonas*, transferred to the facultative anaerobe *E. coli*.

The thermodynamics of hydrogenase could hinder the NADH-dependent hydrogen pathway in *E. coli*. The enzyme hydrogenase catalyzes a simple reaction (Equation 2-5):

$$2\ H^+ + 2\ e^- \leftrightarrow H_2 \qquad (2\text{-}5)$$

The E'_o for H_2 oxidation is -420 mV and that for the clostridial ferredoxin (source of electrons for hydrogenase) is about -390 mV. The equilibrium constant for the above reaction is close to 1 so hydrogenase is said to be "reversible" (195). In order for hydrogen to be produced from NADH, the NADH/NAD^+ ratio must be increased to higher levels to lower the E_o' of the NAD^+/NADH couple from -320 mV to that of Fd and H_2. This could conflict with the activation of the above described anaerobic TCA cycle. Since the hydrogenase reaction is reversible, hydrogen production is subjected to product inhibition at increasing hydrogen levels. This requires continual removal of the produced hydrogen to maintain high rates of H_2 production, leading to a dilute stream of H_2 mixed with other gases.

Hydrogenase Biochemistry

There are three classes of hydrogenases: [Fe], [NiFe], and metal-free hydrogenase. Each of these is characterized by a distinctive functional core, which is conserved within each class. [Fe] and [NiFe]-hydrogenase structures have been solved by x-ray crystallography (90, 159, 207). The active sites of these two classes of hydrogenases show some similarities in their structural framework and chemistry, which support the idea of convergent evolution. Based on amino acid sequence analysis, the third class of metal-free hydrogenases lacks any resemblance

to the two metal containing classes. Even though they are classified as metal-free, these hydrogenases do contain heme clusters (207).

[NiFe]-hydrogenase

[NiFe]-hydrogenases are generally αβ-heterodimers and many of them are associated with membranes and H_2 uptake. The large α-subunit is about 60 kDa and contains the [NiFe] active site. The small β-subunit, about 30 kDa, holds the [Fe-S] clusters. Using sequence analysis, [NiFe]-hydrogenases were separated into four different groups (207, 222). Group one [NiFe]-hydrogenases are membrane bound respiratory enzymes that link the oxidation of H_2 to the reduction of electron acceptors such as O_2, NO_3^-, SO_4^{2-}, fumarate, or CO_2. Examples include *Wolinella succinogenes* (59) and *E. coli* HYD2 isoenzyme (28) reducing fumarate or inorganic oxidants, *Ralstonia eutropha* (24) reducing O_2, and methanogenic archaeon *Methanosarcina mazei* (95) reducing CO_2 from H_2. Group two represents cytoplasmic H_2 sensors and the cyanobacterial uptake hydrogenases such as in *Anabaena variabilis* (85). H_2 signaling hydrogenases, found in *Rhodobacter capsulatus* (66) and *Bradyrhizobium japonicum* (26), are involved in hydrogenase gene regulation in response to H_2. Group three enzymes are bi-directional heteromultimeric cytoplasmic [NiFe]-hydrogenases. In this group, the dimeric hydrogenase is associated with other subunits that are capable of binding cofactors such as F_{420} (*Methanococcus voltae* (38)), NAD^+ (*R. eutropha* (177)), or $NADP^+$ (*Pyrococcus furiosus* (130)). Group 4 are hydrogen evolving membrane-associated hydrogenases. *E. coli* HYD3 along with many archaeal hydrogenases such as the ones from *Methanosarcina barkeri* and *P. furiosus* belong to this group. These enzymes are energy-conserving, meaning that they reduce protons in order to dispose of excess reducing equivalents produced by anaerobic oxidation of low potential C1 compounds with associated proton gradient generation (208).

[Fe]-hydrogenase

[Fe]-hydrogenases are the main interest of this study since these enzymes are cytoplasmic and couple ferredoxin to H_2 evolution. [Fe]-hydrogenases are mainly monomeric proteins containing the H-cluster active site. The H-cluster consists of a binuclear [Fe] center bound by a [4Fe-4S] cluster. This H-cluster is coordinated by a non-protein dithiolate bridging ligand, CN^- ligand, and CO ligand. The composition of the dithiolate linkage is not known experimentally but has been proposed to be either $SCH_2CH_2CH_2S$ (PDT) or SCH_2NHCH_2S (DTN) (160).

[Fe]-hydrogenases are found in anaerobic bacteria such as *Clostridium* sp. and sulfate reducers and in lower eukaryotes such as *Trichomonas vaginalis* and green algae. [Fe]-hydrogenases, the predominant form of hydrogenase found in eukaryotes, are only found in either hydrogenosomes or chloroplasts. The smallest [Fe]-hydrogenases are found in green algae *Scenedesmus obliquus, Chlamydomonas reinhardtii,* and *C. fusca*. These hydrogenases are about 45-48 kDa in size and only contain the H-cluster (84). Clostridial [Fe]-hydrogenases, in addition to the H-cluster, contain three other domains: a [2Fe-2S] ferredoxin-like domain, a [4Fe-4S] cluster fold, and a 2[4Fe-4S] domain (150, 159).

Biosynthesis of the [Fe] active site is not known. The [Fe]-hydrogenase from *C. pasteurianum* has been crystallized and its structure was solved (159). The corresponding gene was cloned and was functionally expressed in a cyanobacterium *Synechococcus* PCC7942 that also produces a [Fe]-hydrogenase indicating the flexibility of the activation enzymes (8). *C. acetobutylicum* was also found to heterologously express algal [Fe]-hydrogenase from *C. reinhardtii* and *S. obliquus* with high specific activities (72). However, the cyanobacterial hydrogenase was not functionally expressed in a non-[Fe]-hydrogenase producing organism such as *E. coli* (8). In the organisms investigated, the genes coding for the structural genes and the accessory genes are not clustered. Recently, Posewitz *et al*. identified three novel proteins,

HydEF and HydG, that are required for the assembly of an active [Fe]-hydrogenase in *C. reinhardtii* (164). Through sequence homology, these enzymes were suggested to be members of radical S-adenosylmethionine (SAM) proteins. These proteins were purified and characterized from *Thermatoga maritima* (171). HydE and HydG were able to reductively cleave SAM when reduced by dithionite confirming that they are radical SAM enzymes. The characterization of HydF revealed its ability to hydrolyze GTP (37). Using known models, such as the radical dependent sulfur insertion of LipA and BioB in the biosynthesis of lipoic acid and biotin, Peter *et al.* proposed a H-cluster biosynthesis mechanism involving the HydEFG proteins (160). They suggested that HydE and HydG form the dithiolate ligand to a [2Fe-2S] cluster from either amino acid or glycolytic intermediates. The role of HydF could be the translocation and insertion of the [2Fe-2S] cluster into the apohydrogenase. The incorporation of genes encoding these proteins along with [Fe]-hydrogenase from *C. reinhardtii* into a non-[Fe]-hydrogenase producing organism such as *E. coli* supported small (but variable) amount of active hydrogenase (164). Upon purification, recombinant [Fe]-hydrogenases from various organisms coexpressed with *C. acetobutylicum* HydEFG in *E. coli* yielded active enzymes with low specific activities (113). These results suggest that HydEFG are the minimally required accessory proteins for [Fe]-hydrogenase activation. However, just after the establishment of the required maturation accessory proteins for [Fe]-hydrogenase, Inoue *et al.* expressed a [Fe]-hydrogenase gene from a symbiotic anaerobic protozoan, *Pseudotrichonympha grassii*, found in the digestive hindgut of the termite *Coptotermes formosanus* without the accessory genes and purified a active recombinant [Fe]-hydrogenase from *E. coli* (99). Purified recombinant *P. grassii* [Fe]-hydrogenase produced in *E. coli* without added accessory genes was about 30 times more active than recombinant clostridial [Fe]-hydrogenase with HydEFG also purified from *E. coli* (99, 113).

These results suggest that although the HydEFG proteins are required to activate [Fe]-hydrogenase, a [Fe]-hydrogenase can be produced in an active form in *E. coli* using only the native proteins to activate the enzyme.

NADH-Dependent Hydrogen Producing Pathway

There are two demonstrated NADH-dependent H_2 production reactions; a clostridial pathway and a hydrogenosomal pathway. NADH-dependent production of H_2 was demonstrated using crude extracts of *C. kluyveri* as well as other clostridia with acetyl-CoA as an activator (108, 197). It was believed that NADH is oxidized by NADH-ferredoxin oxidoreductase (NFOR) which reduces ferredoxin (108, 163). Reduced ferredoxin transfers electrons to [Fe]-hydrogenase for H_2 production. However, recently, the same group that first detected NADH to H_2 activity in *C. kluyveri* extracts, purified the key enzyme responsible for the NADH-dependent reduction of ferredoxin (124). Their results show that the initially discovered NFOR activity was a coupled side reaction of crotonyl-CoA reduction by butyryl-CoA dehydrogenase/electron transfer flavoprotein (Bcd/Etf) complex (Figure 2-2) (Equation 2-6).

$$\begin{array}{ll} NADH + Fd_{ox} \rightarrow NAD^+ + Fd_{red} & \Delta G_o = +4.15 \text{ kcal mol}^{-1} \\ NADH + \text{crotonyl-CoA} \rightarrow NAD^+ + \text{butyryl-CoA} & \Delta G_o = -14.31 \text{ kcal mol}^{-1} \\ \hline 2\ NADH + \text{crotonyl-CoA} + Fd_{ox} \rightarrow 2\ NAD^+ + \text{butyryl-CoA} + Fd_{red} & \Delta G_o = -10.16 \text{ kcal mol}^{-1} \end{array} \quad (2\text{-}6)$$

Using the E_1 (-60 mV) and E_2 (-430 mV) redox potential of *Acidaminococcus fermentans* flavodoxin (83, 121, 124, 224), NADH (-320 mV) dependent reduction of ferredoxin (-410 mV) appears to be thermodynamically favorable when coupled to crotonyl-CoA reduction (-10 mV) where electrons from the E_2 state ($FADH/FADH_2$) were transferred to ferredoxin and E_1 state (FAD/FADH) was transferred to crotonyl-CoA. Acetyl-CoA, required in the initial studies, turns out to be a precursor of the substrate crotonyl-CoA and not an activator. Diez-Gonzalez *et al.* also partially purified Bcd from *C. acetobutylicum* and determined that crotonyl-CoA reduction

could also use electron donors from reduced dyes such as 3-(4,5-dimethylthiazol-2-yl)-2,5-diphenyltetrazolium bromide (MTT) (E_o'= -110 mV), 2,6-dichlorophenolindophenol (DCPIP) (E_o'= +217 mV), and methyl viologen (MV) (E_o'= -440 mV) where MV based activity was 18-fold higher than observed with MTT (55). This recent information clearly shows that a clostridial NADH-dependent system may not be prudent for the construction of a biocatalyst for hydrogen production, using NADH as the reductant, since for every H_2 produced, a molecule of butyryl-CoA will also produced. This loss of carbon and energy will significantly lower the H_2 per glucose yield and the overall process will be uneconomical.

The alternative NADH to H_2 pathway starts with NFOR, a hydrogenosomal enzyme in anaerobic protozoan. *T. vaginalis* NFOR is a heterodimer consisting of a small (NdhE) and a large (NdhF) subunit and these proteins have high homology to mitochondrial 24-kDa and 51-kDa subunits of NADH-dehydrogenase (NDH) of respiratory complex I (94). Unlike other known respiratory NDH enzymes, the anaerobically produced *T. vaginalis* NDH has a unique capability for reduction of low potential electron acceptors such as its native [2Fe-2S] ferredoxin (E_o'= -347 mV) and MV (E_o'= -440 mV) (94). This difference in electron acceptors is expected to reside in the structural components of the *T. vaginalis* NDH, such as FMN, [Fe-S] clusters, etc. In this study, I purified the NDH heterodimer, as well as the individual subunits and biochemically characterized them to elucidate the mechanism by which the recombinant enzyme utilizes low potential electron carriers as substrate.

It has been previously demonstrated that chemically reduced viologen dyes can couple to hydrogenase for hydrogen production both *in vivo* and *in vitro* (17, 81, 117, 174). Since *T. vaginalis* NDH has been demonstrated to readily reduce methyl viologen (E_o'= -440 mV) (94), which has a lower redox potential than hydrogen (E_o'= -420 mV), the reduced MV produced *in*

vivo by *T. vaginalis* NDH (expressed in *E. coli*) can potentially couple NADH oxidation to hydrogen production (Figure 2-3). This pathway has the potential to increase hydrogen yield beyond the theoretical 2 mol per mol glucose in *E. coli* and other facultative anaerobes.

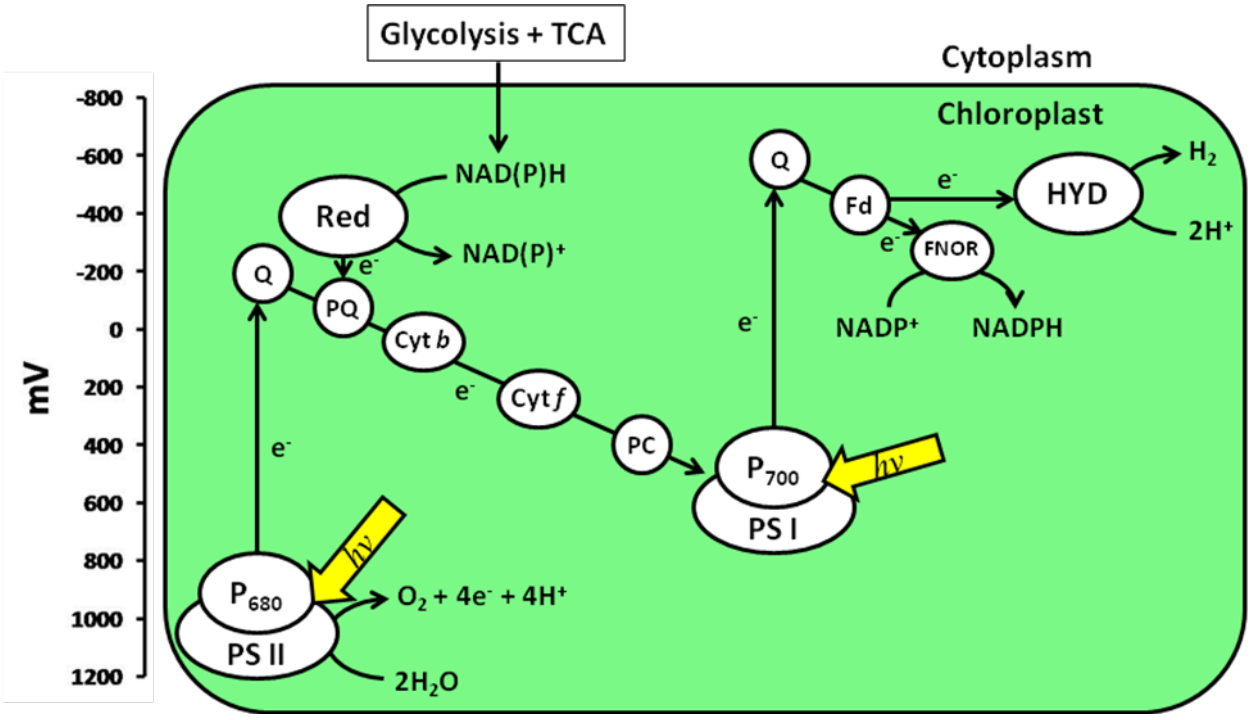

Figure 2-1. Photosynthetic electron transport pathways for hydrogen production in green algae. Electrons may originate from photo-oxidation of water at PS II or at the plastoquinone pool from the oxidation of endogenous substrates such as glycogen and starch. Reduced Fd from PS I could transfer electrons to hydrogenase for hydrogen production, or to FNOR to generate NADPH for CO_2 fixation. TCA, Tricarboxylic acid cycle; P_{680}, photoreaction center of PS II; Q, primary electron acceptor of photosystems; PQ, plastoquinone; Cyt, cytochrome; PC, plastocyanin; Fd, ferredoxin; Red, NAD(P)H quinone oxidoreductase; HYD, hydrogenase; FNOR, ferredoxin-$NADP^+$ oxidoreductase [Adapted from Melis, A., and T. Happe. 2001. Hydrogen production. Green algae as a source of energy. Plant Physiol 127:740-748 (Page 743, Figure 2)]

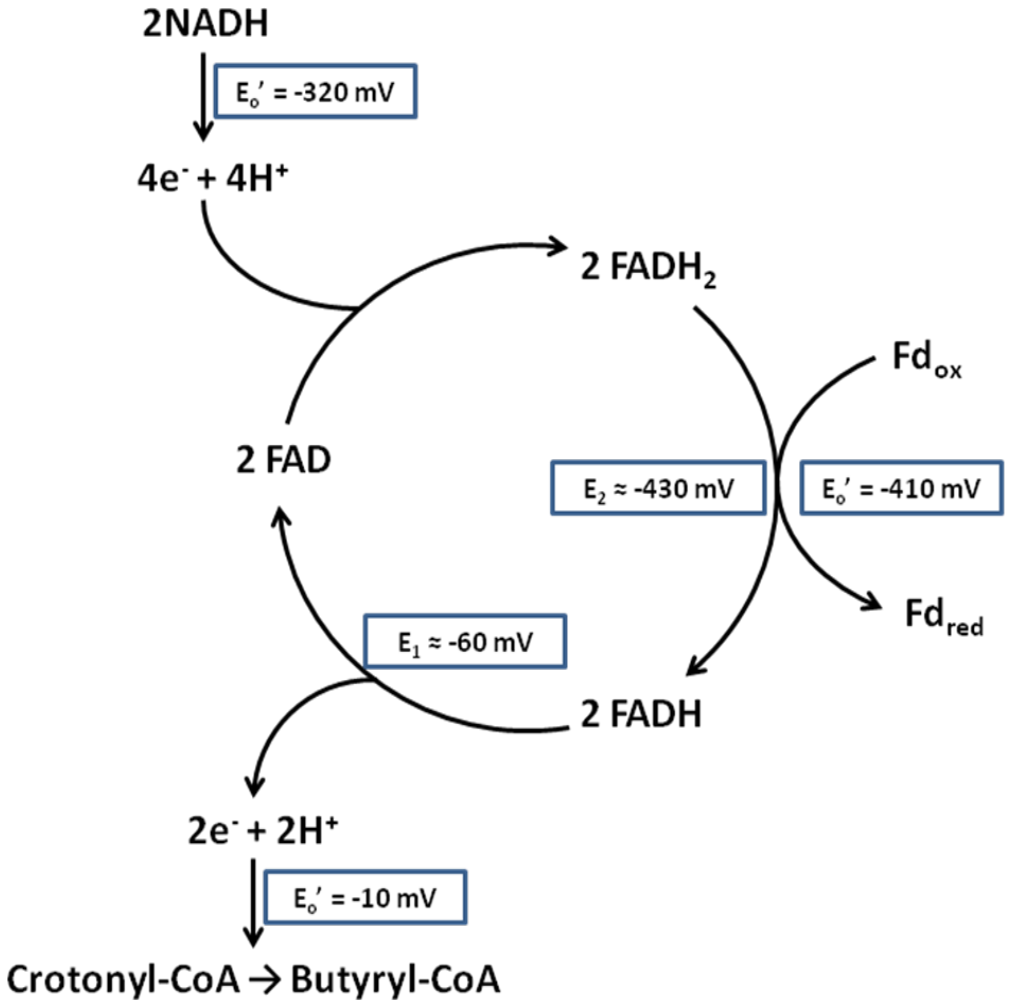

Figure 2-2. NADH-dependent reduction of ferredoxin by *C. kluyveri* Bcd/EtfBA (clostridial NFOR) coupled to crotonyl-CoA to butyryl-CoA reaction. The E_1 and E_2 redox potential of FADH and $FADH_2$ was an estimate based on *Acidaminococcus fermentans* flavodoxin which had similar properties to electron transfer flavoproteins (124). The energetics of this ferredoxin reduction is thermodynamically favorable by coupling crotonyl-CoA reduction (Equation 2-6). [Adapted from Li, F., J. Hinderberger, H. Seedorf, J. Zhang, W. Buckel, and R. K. Thauer. 2008. Coupled ferredoxin and crotonyl coenzyme A (CoA) reduction with NADH catalyzed by the butyryl-CoA dehydrogenase/etf complex from *Clostridium kluyveri*. J Bacteriol 190:843-850. (Page 848, Figure 3]

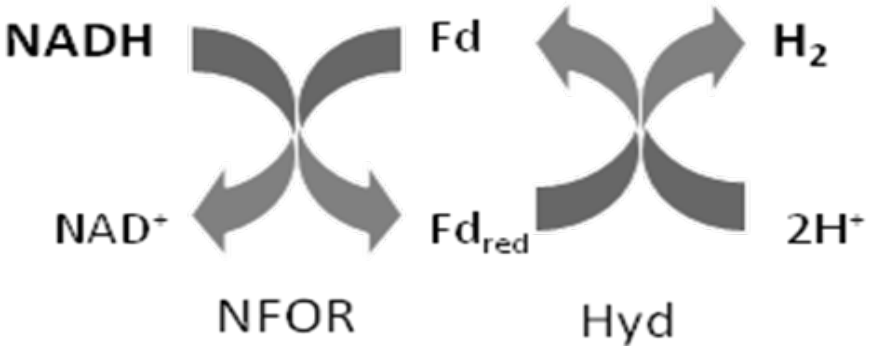

Figure 2-3. NADH-dependent hydrogen producing pathway. NADH is oxidized by NADH-ferredoxin oxidoreductase (NFOR) which reduces ferredoxin (Fd). Reduced Fd is the electron donor for hydrogenase (Hyd) for H_2 production.

CHAPTER 3
BACKGROUND ON BUTANOL PRODUCTION

Although H_2 is a more desired transportation fuel, other next generation fuels such as butanol may become a reality before the H_2 economy is realized. As stated before, butanol has several advantages over ethanol as a transportation fuel. Butanol fermentation has a long history and modification of microbial biocatalysts for butanol production is being attempted by several laboratories around the world. In this section, the current status of butanol fermentation is presented.

Fossil Fuel-Based Butanol Production

Currently, the majority of butanol is produced by the conversion of petroleum-based hydrocarbon to butanol by a process called hydroformylation followed by hydrogenation. Hydroformylation is defined as the addition of a formyl group to a double bond of a hydrocarbon by reaction with a mixture of carbon monoxide and hydrogen in the presence of a catalyst. For butanol production, the formyl group is added to the double bond of propylene producing butyraldehyde (194). Butyraldehyde is reduced to butanol by a hydrogenation reaction (200). This process yields both n-butanol and isobutanol, which is separated by distillation (148).

Microbial Butanol Production

History

Microbial butanol fermentation was first described by Pasteur in 1861 (107). In 1905, Schardinger discovered that butanol fermentation included the co-production of acetone (107). At the beginning of the 20th century, with an increase in the automotive industry, a shortage in natural rubber for the fabrication of tires sparked an interest in butanol fermentation for the production of synthetic rubber from butadiene (68, 69). In 1910, an English firm, Strange and Graham Ltd., was on a venture for the production of synthetic rubber. They recruited the work of

Weizmann and Perkins of Manchester University, UK and later Fernbach and Schoen of Pasteur Institute, France. In 1911, Fernbach isolated a bacillus culture that was able to produce butanol from potato starch but not from corn (68, 69, 107). Weizmann left Strange and Graham Ltd. in 1912 to continue his research at Manchester University. By 1914, Weizmann isolated strain BY that was more robust in butanol production than Fernbach's bacillus and used many different sources of starch such as from corn (107). This strain was later renamed as *C. acetobutylicum*. At the time, *C. acetobutylicum* gained global attention due to its ability to produce acetone, which is used as a solvent for cordite production. During World War I, cordite was used as the main constituent in explosives and gun powder which consists of 58 % nitroglycerine, 37 % guncotton, and 5 % vaseline (198). With high demands for cordite and promising results for the production of acetone by the Weizmann process, England constructed a plant for the production of acetone at the Royal Naval Cordite Factory at Poole in Dorest and adapted six distilleries in Great Britain for the production of acetone using the Weizmann process (107). A shortage of grain due to war efforts forced Great Britain to move the fermentation process to plants in Canada. In 1917, upon the United States' entry into World War I, United States decided to produce acetone in the Midwest corn belt at Terre Haute, Indiana where substrates are readily available (107). The fermentation production was continued until November 1918 when all plants were closed due to the end of the war.

Butanol, the other product of *C. acetobutylicum* fermentation was stored until after the end of the war. At that time, the automotive industry was rapidly expanding and was in need of a quick drying lacquer. E. I. du Pont de Nemours & Co. developed a nitrocellulose lacquer which required butanol and butyl-acetate as solvents. With the increase in demand for butanol instead of acetone, the plants at Terre Haute reopened under the newly formed Commercial Solvent

Corporation (CSC) of Maryland in 1920, which operated under the U.S. license for the Weizmann process patent issued in 1919. To meet rapidly growing demands, CSC acquired another plant in Peoria, IL (68, 107).

In the 1930s, a new method using petroleum to produce synthetic solvents posed a threat to the butanol fermentation industry. In efforts to improve the fermentation processes, research was initially dedicated to the isolation of a strain, which could use higher concentrations of starch with limited results. Research efforts were then shifted to the fermentation of carbohydrates such as readily available molasses, which at the time, cost less than starch. CSC strain number 8, later known as *C. saccharoacetobutylicum*, was able to ferment up to 6.5 % sugars producing up to 2 % total solvents that lowered the distillation cost by half (68, 107).

The start of World War II once again catapulted the demands for acetone for munitions. Plants were built in a number of countries around the world including Japan, India, Australia, China, USSR, and South Africa. By the end of the war in 1945, about two-thirds of the butanol in the United States and one-tenth of acetone were produced by fermentation (107). However, a rapidly growing petro-chemical industry in the 1950s, in addition to an increase in molasses usage as cattle feed made butanol-acetone fermentation no longer cost-effective; thus, by 1960 almost all butanol-acetone fermentation ceased in the United States and Great Britain (107).

Butanol Fermentation

Unlike hydrogen production, microbial butanol production is more restricted to few members of the clostridia class, *Clostridiaceae* family, and more specifically the genus *Clostridium*; however, some members of the *Lachnospiraceae* family such as *Butyrivibrio fibrisolvens* contain most of the butanol biochemical pathway, producing butyric acid. Members of the *Clostridium* genus are anaerobic, Gram-positive, spore-forming, rod-shaped bacteria. Of the clostridia, *C. acetobutylicum*, *C. beijerinckii*, *C. saccharobutylicum*, and *C.*

saccharoperbutylacetonicum are primary solvent producers (60, 120). The most studied clostridia is *C. acetobutylicum* which was the strain originally isolated by Weizmann in 1914 (107). *C. acetobutylicum* possesses a 210 kb megaplasmid, pSol1, which was originally named for its ability to produce solvents (48). Strains lacking pSol1 are unable to produce solvents (48). During normal growth, *C. acetobutylicum* undergoes two defined growth phases: acidogenesis and solventogenesis (78). *C. acetobutylicum* during exponential growth exhibits acidogenesis where the major fermentation products are acetate, butyrate, hydrogen, and carbon dioxide. At the onset of stationary phase triggered by a drop in pH, *C. acetobutylicum* shifts to solventogenesis where it takes up the acids produced during acidogenesis and produces solvents such as acetone, butanol, and ethanol (ABE) (78). Depending on the fermentation conditions, wild type *C. acetobutylicum* produces from 5.5 to 11.0 g L^{-1} butanol (87, 88, 120, 145, 234). The typical molar ratio of acetone : butanol : ethanol in the fermentation broth is about 3:6:1, respectively (166). Mutations up-regulating butanol dehydrogenase and/or down-regulating *solR* (repressor of the *sol* operon) and acid production genes have led to concentrations up to 17.8 g L^{-1} butanol (87, 88, 120, 145, 234). Hyper-butanol producing mutant *C. beijerinckii* BA101 can produce over 20 g L^{-1} butanol and 33 g L^{-1} total solvents in batch fermentations (44, 120, 166). When compared with wild-type parent, *C. beijerinckii* NCIMB 8052, transcriptional analysis of mutant strain *C. beijerinckii* BA101 revealed a decrease in sporulation efficiency and PTS sugar transport and an increase in several metabolic genes encoding butanol production (179).

The metabolic pathway for butanol production has been well studied (5, 48, 62, 68, 78, 107, 142, 145) (Figure 3-1). Under exponential growth conditions and acidogenesis, *C. acetobutylicum* consumes glucose via glycolysis to produce 2 pyruvate and 2 NADH (215).

Pyruvate is then converted to acetyl-CoA and CO_2 by pyruvate-ferredoxin oxidoreductase (PFOR) which is coupled to ferredoxin reduction and hydrogen production (215). Acetyl-CoA could be converted to acetate for ATP production (phosphotransacetylase, *pta* and acetate kinase, *ack*) (33) or two acetyl-CoA can be condensed into one acetoacetyl-CoA by thiolase (*thiA* and *thiB*) (217). Acetoacetyl-CoA is reduced by hydroxybutyryl-CoA dehydrogenase (*hbd*) coupled to NADH oxidation to produce hydroxybutyryl-CoA (32, 229). Hydroxybutyryl-CoA is then converted to crotonyl-CoA via a dehydration reaction catalyzed by crotonase (*crt*) (32, 213). Butyryl-CoA dehydrogenase (*bcd*) and electron transfer flavoprotein (*etfBA*) complex catalyzes the conversion of crotonyl-CoA to butyryl-CoA coupled to ferredoxin reduction using two NADH (32, 124). Analogues of Bcd that are capable of catalyzing the same reaction have been identified as crotonyl-CoA reductase (*ccrA* and *ccrB*) in some *Streptomyces* species. Crotonyl-CoA reductase converts crotonyl-CoA to butyryl-CoA coupled to NADPH oxidation. A coenzyme-A phosphotransbutyrylase converts butyryl-CoA to butyryl-phosphate (*ptb*) and butyrate kinase (*buk*) transforms butyryl-phosphate to butyrate and ATP (5, 215).

The shift to stationary phase triggers an 1,200-fold up regulation of the *sol* operon located on pSol1 megaplasmid (5, 61, 145). The *sol* operon has two promoters. The first promoter controls genes encoding an alcohol-aldehyde dehydrogenase (*aad*) and coenzyme-A transferase (*ctfA* and *ctfB*). The second promoter transcribes acetoacetate decarboxylase (*adc*) downstream of the first promoter on the complimentary strand. CtfAB transfers the CoA from acetoacetyl-CoA to either acetate or butyrate producing acetoacetate and acetyl-CoA or butyryl-CoA, respectively. Adc decarboxylates acetoacetate to produce acetone and CO_2. Aad catalyzes two reactions: the first is the reduction of acetyl-CoA to acetaldehyde and ethanol. The second

reaction reduces butyryl-CoA to butyraldehyde and 1-butanol (67, 144). Each reaction is coupled to the oxidation of NADH.

Molecular Organization of Butanol Production Pathway

C. acetobutylicum has two thiolase homologues; the first gene, *thlA* (CAC2873), is located on the chromosome and the second gene, *thlB* (CA_P0078) is located on the pSol1 megaplasmid. Northern blot analysis revealed high levels of *thlA* transcripts during acidogenesis and decreasing levels to minimal expression about 3 to 7 hrs after induction of solventogenesis (217). There is a σ70 consensus sequence upstream of *thlA* controlling the transcription of a 1.4kb monocistronic message. Genetic organization of *thlB* suggests that it forms an operon with two other genes, *thlC* and a possible regulator *thlR* (Figure 3-2). Transcriptional analysis of *thlB* showed very low expression relative to *thlA* during both acidogenesis and solventogenesis. This study also determined that *thlA* is the main gene encoding thiolase in all phases, and the physiological function of *thlB* is yet to be identified (217).

In *C. acetobutylicum*, *crt*, *bcd*, *etfB*, *etfA*, and *hbd* genes (CAC2712, CAC2711, CAC2710, CAC2709, and CAC2708 respectively) are arranged in a single polycistronic butyryl-CoA synthesis (BCS) operon (32, 142) (Figure 3-2). The BCS operon was expressed in *E. coli* and an increase in Crt and Hbd activity was detected in the crude extract; however, no Bcd/EtfBA activity was detected at that time. The same operon over-expressed from a plasmid in *C. acetobutylicum* had about a 2-fold increase in activity for all three enzymes including the Bcd/EtfBA complex which by far has the lowest activity indicating that it could be the rate limiting step of the butanol fermentation pathway (32).

The last reaction of the pathway converts butyryl-CoA into butanol. *C. acetobutylicum* is the first bacterium identified with two bifunctionally active Fe- aldehyde-alcohol dehydrogenases that are capable of catalyzing this reaction (67). The first of this type, *aad*

(*adhE1*, CA_P0162), was identified originally as a part of the *sol* operon (144). Aad has 74 % similarity and 56 % identity with *E. coli* AdhE. The expression of *aad* and the *sol* operon coincides with the start of solventogenesis (5, 61, 145). The second gene product, AdhE2 (*adhE2*, CA_P0035), is 77 % similar and 58 % identical to *E. coli* AdhE. The *adhE2* gene is expressed only in alcohologenic cultures and not in solventogenic culture (67). *C. acetobutylicum* also has two adjacent independently transcribed chromosomally located Zn-butanol dehydrogenases genes (*bdhA*-CAC2399 and *bdhB*-CAC2398) and their expression coincides with solventogenesis (5, 62, 161, 162, 212). The *bdhB* is induced prior to the induction of the *sol* operon and was found to have a 2.3 fold higher expression than *aad* (5, 161). It is proposed that *aad* and *bdhB* are the two major alcohol dehydrogenase genes responsible for butanol production (62).

Advances in Metabolic Engineering of Bacteria for Butanol Production

For over 50 years, from the 1910's to the 1960's, *C. acetobutylicum* was used in industrial ABE fermentation (107). Since then, there has not been much advancement in strain development for increasing butanol yield; instead, most studies are concentrated on butanol extraction and purification (120). Even though simple genetic tools are available for *C. acetobutylicum*, *e.g.* plasmid vectors, transformation protocols, and gene knockouts, the anaerobic physiology of this organism makes it difficult to work with for cost effective fuel production. *Clostridium* requires a relatively rich growth medium with an abundant supply of nitrogen and reducing agents which add to production costs (12, 120, 153, 166). Solvent producing clostridia utilize less than 25 % of carbon from glucose for butanol production. The rest of the carbon is used for the co-production of acetone, ethanol, and residual acids. The combustional energy from acetone, butanol, and ethanol is about 12,500 BTU/lb, 16,000 BTU/lb, and 11,500 BTU/lb, respectively. Thus, co-production of acetone and ethanol leads to a loss of

carbon to lesser energy containing molecules. Ideally, butanol should be the sole fermentation product of this process. For over 20 years, much work has been done towards the construction of a *Clostridium* for homo-butanol production by mutating competing pathways but with only limited success.

Towards the goal of generating a homo-butanol producing organism, it may be easier to recombinantly express the butanol production pathway in other commonly used microbes. Genes in the butanol production pathway have been cloned and expressed to produce active proteins in other microorganisms such as *S. cerevisiae* and *E. coli* (12, 100, 185). In these experiments, Steen *et al.* cloned the BCS operon and *aad2* from *C. beijerinckii*, *atoB* (thiolase) from *E. coli*, and *ccrA* from *Streptomyces collinus* into *S. cerevisiae* resulting in the production of about 2.5 mg L^{-1} (0.034 mM or 0.00025 %) butanol (185).

To date, there are only two published reports on butanol producing *E. coli* (12, 100). Atsumi *et al.* was the first to demonstrate the production of butanol in *E. coli* using the clostridial pathway (12). Atsumi *et al.* cloned the same genes as Steen *et al.* and functionally expressed them in various *E. coli* mutants deficient in native fermentation pathways. Atsumi *et al.* identified three possible rate limiting steps: thiolase, butyryl-CoA dehydrogenase, and the aldehyde-alcohol dehydrogenase reactions. Using their parent strain, which has a wild-type fermentation profile, with the entire butanol pathway genes expressed from plasmids, they compared the productivity of *E. coli* thiolase, *atoB*, and *C. acetobutylicum thlA* under different growth conditions. Strains with over-expressed *atoB* produced about 4 times more butanol (70 mg L^{-1}; 0.94 mM butanol) than with *thlA* (18 mg L^{-1}; 0.24 mM butanol) alone under O_2-limiting conditions. Atsumi *et al.* then tested the effect of butyryl-CoA dehydrogenase by replacing *C. acetobutylicum bcd-etfBA* with *Megasphaera elsdenii bcd-etfBA* or *S. coelicolor ccr*. An *E. coli*

mutant lacking native fermentative pathways (Δ*adhE* Δ*ldhA* Δ*frdBC* Δ*fnr* Δ*pta*) bearing *C. acetobutylicum bcd-etfBA* produced more butanol (~155 mg L^{-1}; 2.09 mM) than the ones with *M. elsdenii bcd-etfBA* (~18 mg L^{-1}; 0.24 mM) or *S. coelicolor ccr* (~2 mg L^{-1}; 0.03 mM) under O_2-limiting conditions. An *E. coli* fermentation defective mutant expressing *atoB, C. acetobutylicum bcd-etfBA, crt, hbd,* and *aad2* was able to produce 552 mg L^{-1} (7.45 mM) butanol in rich medium with glycerol as a carbon source and 113 mg L^{-1} (1.52 mM) butanol in M9 minimal medium with glucose as a carbon source under O_2-limiting condition (12).

Inui *et al.*, cloned the BCS operon from *C. acetobutylicum* along with *thlA* and compared the difference in the two aldehyde-alcohol dehydrogenases – *aad1* and *adhE2* (100). *E. coli* strain JM109 (wild-type fermentation) was transformed with compatible plasmids expressing the above genes with either *aad1* or *adhE2*. In crude extract, they detected an increase in activity for all enzymes tested. Bcd/EtfBA activity still appeared to be the rate limiting process. AdhE2 had a 27-fold higher butyraldehyde dehydrogenase activity specific for butyryl-CoA as substrate than Aad1 for butyryl-CoA as substrate. Both enzymes preferentially reduced acetyl-CoA to ethanol rather than butyryl-CoA to butanol. Aad1 and AdhE2 had about a 14-fold and a 2-fold, respectively, higher specific activity using acetyl-CoA as substrate than butyryl-CoA as substrate. High density cultures of JM109 with BCS, thiolase, and *adhE2* genes (OD_{660nm} = 20; pH 6.5) in an anaerobic chamber with an atmosphere comprising of 95 % nitrogen and 5 % hydrogen, were able to produce up to 16 mM (1185 mg L^{-1}) butanol and 5 mM butyrate; whereas, *aad1* containing JM109 instead of *adhE2* only produced 3.5 mM (259 mg L^{-1}) butanol and 1 mM butyrate in 60 hrs at 30^{o}C (100). The fermentation balance was not presented; however, one can assume this strain also produced high concentrations of lactate, acetate,

ethanol, formate, and succinate since strain JM109 still contained all the native fermentation pathways.

Based on the pathway presented in Figure 3-1, the reduction of 2 acetyl-CoA to butanol will require 4-5 NAD(P)H depending on the enzyme used for the conversion of crotonyl-CoA to butyryl-CoA. Since *E. coli* can only produce 2 NADH per glucose under anaerobic conditions, it lacks the reducing equivalents needed for homo-butanol production anaerobically. This is also apparent in the work of Inui *et al.* where a high density culture co-produced both butanol and butyrate indicating the inability of the bacterium to operate the entire butanol pathway (100). The availability of hydrogen in the gas phase may be beneficial for butanol production because hydrogen is a known electron donor for fumarate reductase (119, 221). Since Bcd/EtfBA is a flavoprotein and reduces a C=C bond in a manner that is similar to fumarate reductase, hydrogen uptake may also supply the needed additional reducing power to aid the conversion of crotonyl-CoA to butyryl-CoA.

According to Knoshaug *et al.*, higher butanol concentration could inhibit growth (114). Butanol at a concentration of 1.0 % lowers the relative growth of the yeast studied to about 60 % and no growth was observed at 2.0 % butanol (114). *Lactobacillus* spp. were found to be more tolerant to butanol than yeast. The two strains tested, *L. delbrueckii* and *L. brevis*, had 60 % of the growth rate compared to the control without butanol at 2.0 % butanol in the medium. *L. brevis* had the highest butanol tolerance of all the strains tested having a 35 % growth rate at 3.0 % butanol compared to butanol-less control. *E. coli* butanol tolerance appears to be temperature dependent. *E. coli* strain W3110 has a 25 % and 75 % relative growth rate of the control cultures at 37^{o}C and 30^{o}C, respectively, in 1.0 % butanol (114). According to Atsumi *et al.*, *E. coli* can tolerate up to 1.5 % butanol, which is within the range of clostridial butanol tolerance (12).

Engineering *Escherichia coli* for Butanol Production

E. coli is one of the most studied organisms in the world. Nonpathogenic *E. coli* strains such as K12, C, and B strains are classified as a GRAS (Generally Regarded As Safe) organism and its physiology makes it an ideal model organism to study. *E. coli* is a Gram-negative, non-sporulating, facultative anaerobe and has the ability to utilize a vast array of carbon sources and can grow in minimal salts medium (135). *E. coli* has many industrial applications which include the production of insulin, amino acids, pyruvate, lactate, succinate, and ethanol (43, 75, 103, 104, 209, 228, 232).

E. coli fermentation products are a mixture of acids and ethanol (Figure 3-3) (215). Under anaerobic conditions, glucose is consumed and is converted to 2 moles phosphoenolpyruvate (PEP) and then to 2 moles pyruvate during glycolysis. One NADH is produced during the oxidation of glyceraldehyde-3-phosphate (G3P) to 1-3-bisphosphoglycerate by G3P dehydrogenase of the glycolysis pathway (2 per glucose). Pyruvate is converted to acetyl-CoA and formate by pyruvate formate-lyase (*pflB*) or reduced to lactate coupled to NADH oxidation by lactate dehydrogenase. Acetyl-CoA is further reduced to acetaldehyde and then to ethanol using 2 moles NADH by alcohol dehydrogenase (*adhE*). Acetyl-CoA is also converted to acetate by phosphotransferase (*pta*) and acetate kinase (*ack*) for the production of 1 ATP. Succinate is produced by the carboxylation of PEP to oxaloacetate. Oxaloacetate is reduced to malate by malate dehydrogenase consuming one NADH. Malate is dehydrated by fumarase to produce fumarate. Fumarate is then reduced by a membrane bound fumarate reductase (*frdABCD*) for succinate production. The standard mid-point potential for reduction of fumarate to succinate is +31 mV. Of all the reactions of anaerobic glycolysis and fermentation, the fumarate reductase is the only enzyme that is membrane-bound. NADH is not an electron donor

for fumarate reduction *in vitro*. This flavoprotein apparently utilizes electrons from an unknown source and not directly from NADH *in vivo* also (215).

As noted earlier, *E. coli* generates only 2 moles NADH per mole glucose under anaerobic condition from the G3P dehydrogenase activity. Kim *et al.* described a strain of *E. coli* with a mutation in dihydrolipoamide dehydrogenase (*lpdA*), the E3 component of pyruvate dehydrogenase (PDH), that alters the NADH sensitivity of PDH (111, 112). PDH, like PFL, catalyzes the conversion of pyruvate to acetyl-CoA; however, PDH releases CO_2 and couples the reaction with reduction of NAD^+ to NADH instead of producing formate. The inherent sensitivity of this enzyme to high NADH concentrations under anaerobic conditions inhibit PDH activity. Point mutation E354K in *lpdA* (*lpd101**) lowers NADH sensitivity of the PDH complex (112). The lower NADH sensitivity of the mutated form of the PDH increases PDH activity during anaerobic growth leading to an additional 2 NADHs per glucose (112). This critical mutation is required to produce a more reduced product such as butanol.

Another problem to address in engineering *E. coli* for butanol production is the activity of Bcd/EtfBA complex. The low activity of Bcd/EtfBA in recombinant *E. coli* is an inherent characteristic of this enzyme and not because of recombinant expression in *E. coli*. This reaction may also be the rate limiting reaction in clostridia (32). Prior attempts to increase the conversion of crotonyl-CoA to butyryl-CoA in *E. coli* included expressing *Streptomyces* CcrA and Bcd/EtfBA from other organisms without significant success (100, 185). *Streptomyces* CcrA uses NADPH instead of NADH. Lower levels of NADPH under anaerobic conditions make this reaction less favorable. To increase CcrA activity in *E. coli*, higher NADPH pool will be required. Overexpression of *E. coli* transhydrogenase, *udhA* (*sthA*) and *pntAB*, has been found to increase NADPH levels (109, 172, 214).

Bcd/EtfBA activity in *E. coli* could be increased by using succinate producing strains. As mentioned before, succinate is produced from the reductive branch of the anaerobic TCA cycle. Succinate is produced by the reduction of fumarate by fumarate reductase coupled to the oxidation of an unknown electron carrier. *E. coli* strain KJ104 (103) produces near theoretical yields of succinate producing up to 1.30 mol succinate per mol glucose. This high succinate production raises the possibility that an unknown electron-transport pathway was elevated in this strain to reduce fumarate by fumarate reductase, which is a flavoprotein with unique electron carriers like the Bcd/EtfBA complex. Perhaps this specific electron carrier could also function with the clostridial Bcd/EtfBA and the succinate production strain described by Jantama, *et al.* (103) carrying the butanol pathway and appropriate mutations to knock out succinate production could increase the activity of Bcd/EtfBA and butanol production.

This study will evaluate the potential of *E. coli* as a biocatalyst for butanol production. Since *E. coli* with an NADH-insensitive PDH can generate 4 NADH per glucose, this strain is an ideal choice for further engineering for butanol production. Towards this objective, recombinant *C. acetobutylicum* enzymes as well as *Streptomyces* CcrA in the butanol pathway will be expressed in *E. coli* to identify the enzymes (genes) that are minimally needed to catalyze the conversion of acetyl-CoA to butanol. Demonstration of the *in vitro* enzyme-catalyzed butanol production will provide the proof of principle that when produced in *E. coli* these enzymes can support production of butanol as a fermentation product. Furthermore, in this study, I will also attempt to optimize the carbon flux to butanol and identify the rate limiting steps in this pathway. An understanding of the recombinant butanol pathway in *E. coli* will serve as a foundation for engineering *E. coli* for homo-butanol production.

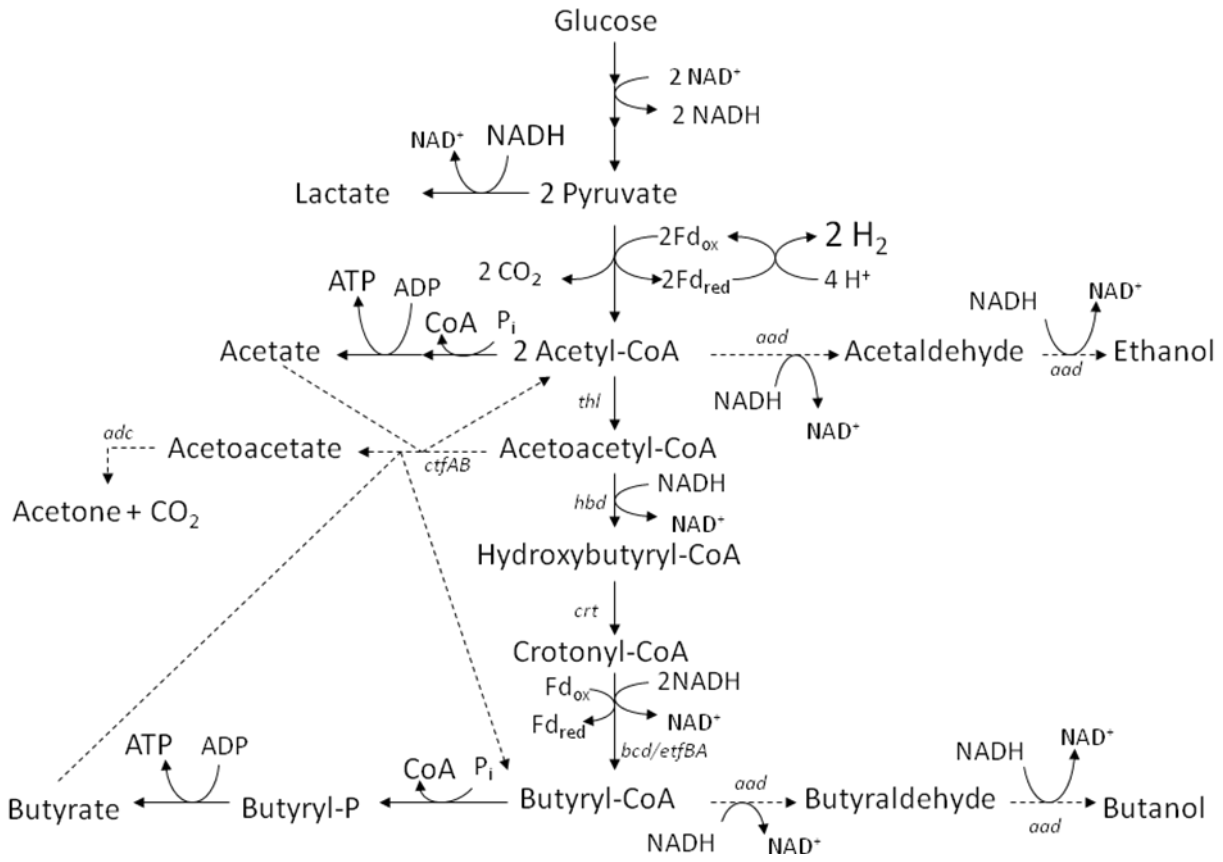

Figure 3-1. *C. acetobutylicum* fermentative pathway. Solid lines represent fermentative pathway during exponential growth (acidogenesis). Dashed lines represent the metabolic pathway during the onset of stationary phase (solventogenesis). During acidogenesis phase, *C. acetobutylicum* produces primarily acetate, butyrate, hydrogen, and carbon dioxide. Solventogenesis phase is a shift in cellular metabolism when cells take up acids and hydrogen produced during acidogenesis, followed by further reduction of the metabolites to produce acetone, butanol, and ethanol (ABE). *thl*, thiolase; *hbd*, hydroxybutyryl-CoA dehydrogenase; *crt*, crotonase; *bcd*, butyryl-CoA dehydrogenase; *etfBA*, electron transfer flavoprotein; *ctfAB*, coenzyme-A transferase; *adc*, acetoacetate decarboxylase; *aad*, alcohol-aldehyde dehydrogenase. [Adapted from Jones, D. T., and D. R. Woods. 1986. Acetone-butanol fermentation revisited. Microbiol Rev 50:484-524 (Page 494, Figure 1)]

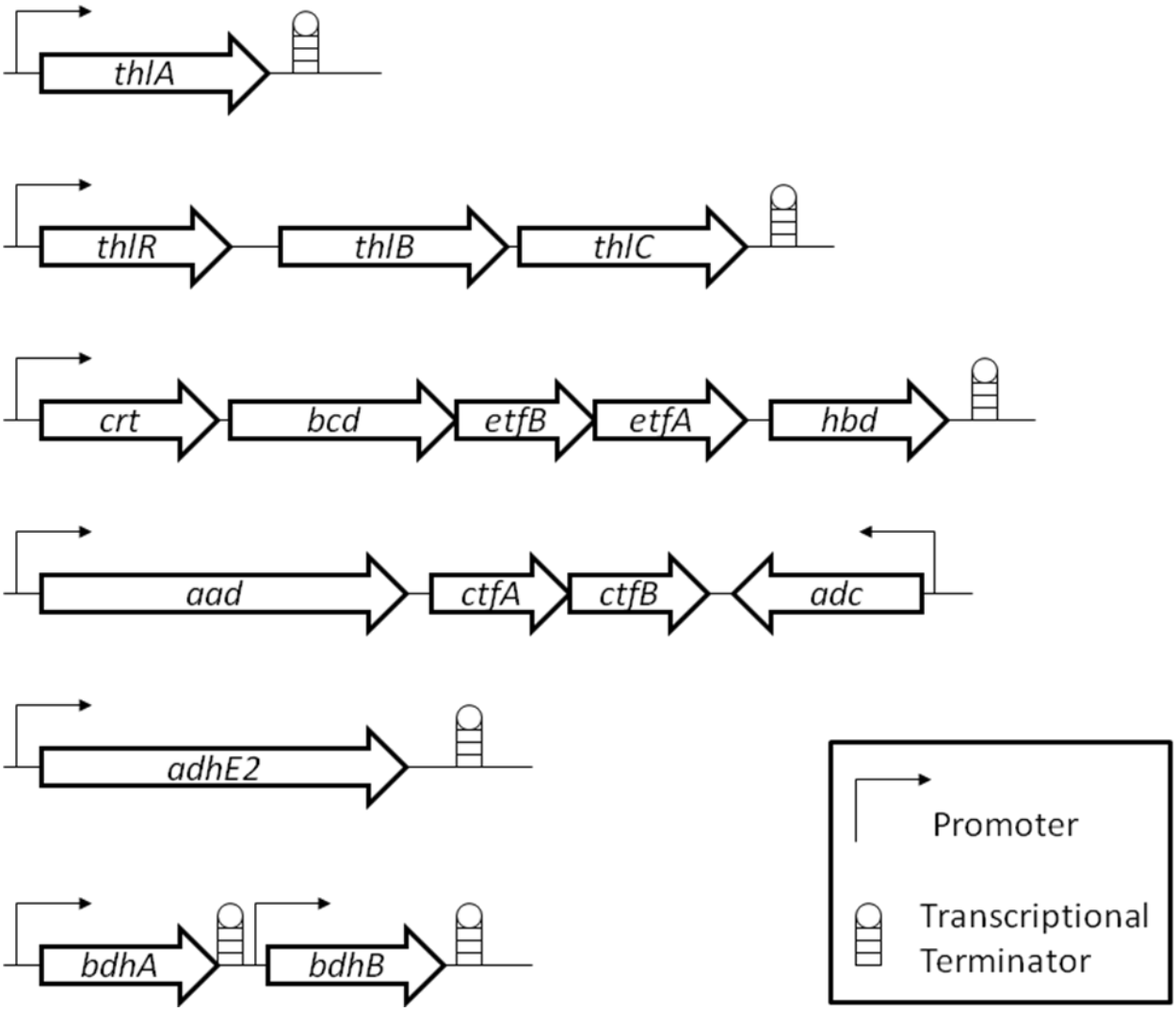

Figure 3-2. Molecular organization of genes encoding butanol/solvent pathway in *C. acetobutylicum*. *C. acetobutylicum* has two thiolases encoded by *thlA* and *thlB*. *thlA* is in a single gene operon whereas *thlB* is transcribed with two adjacent genes: *thlR* and *thlC*. The butyryl-CoA synthesis (BCS) operon consists of five genes, *crt* (crotonase), *bcd* (butyryl-CoA dehydrogenase), *etfB* (electron transfer flavoprotein subunit B), *etfA* (electron transfer flavoprotein subunit A), and *hbd* (hydroxybutyryl-CoA dehydrogenase), for the conversion of acetoacetyl-CoA to butyryl-CoA. The BCS operon is transcribed as a single polycistronic mRNA controlled by a promoter upstream of *crt*. The *sol* operons responsible for majority of solvent production have two promoters. The first promoter controls the transcription of *aad* (aldehyde-alcohol dehydrogenase), *ctfA* (coenzyme A transferase), and *ctfB*. The second promoter transcribes *adc* (acetoacetate decarboxylase) on the complimentary strand. *C. acetobutylicum* has an additional aldehyde-alcohol dehydrogenase (*aad2*) transcribed in its own operon. In addition to the aldehyde-alcohol dehydrogenase, *C. acetobutylicum* has two butanol dehydrogenases, *bdhA* and *bdhB*, which are transcribed independently in tandem.

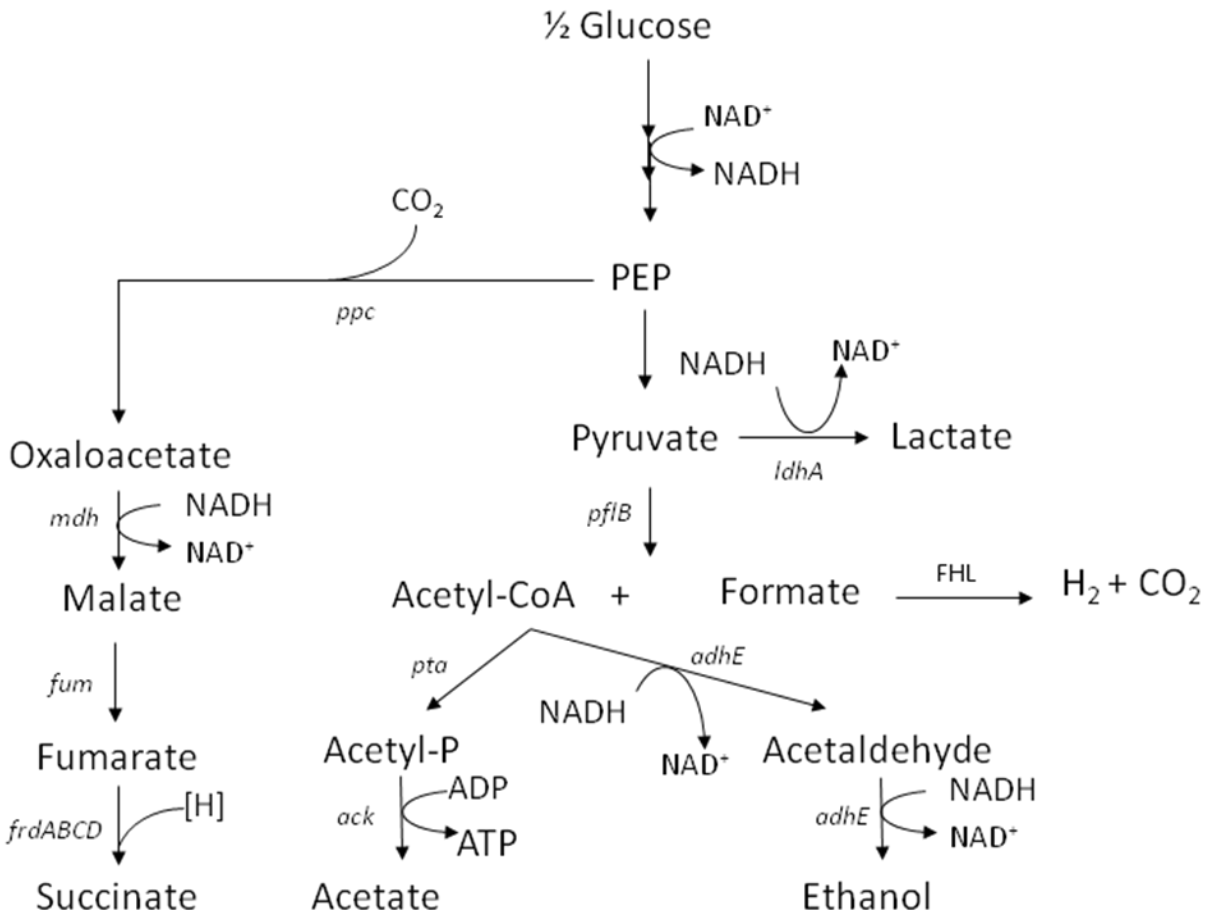

Figure 3-3. *E. coli* mixed acid fermentation. Under anaerobic conditions, glucose is converted to PEP and then to pyruvate. Pyruvate could be reduced to produce lactate or could be converted to acetyl-CoA and formate. Formate could be broken down to hydrogen and carbon dioxide. Acetyl-CoA could either be reduced to produce ethanol or be converted to acetate for ATP production. Succinate is produced from the carboxylation of PEP followed by further reduction. *ldhA*, lactate dehydrogenase; *pflB*, pyruvate formate-lyase; FHL, formate hydrogen-lyase; *adhE*, alcohol dehydrogenase; *pta*, phosphotransacetylase; *ack*, acetate kinase; *ppc*, PEP carboxylase; *mdh*, malate dehydrogenase; *fum*, fumarase; *frdABCD*, fumarate reductase.

CHAPTER 4
MATERIALS AND METHODS

General Methods

Materials

Biochemicals were purchased from Sigma-Aldrich (St. Louis, MO) and Fisher Scientific (Pittsburg, PA). Phusion DNA polymerase, DNA restriction endonuclease, T4 DNA ligase, and Klenow were purchased from New England Biolabs, Inc (Ipswich, MA). Oligonucletides were synthesized by Invitrogen (Carlsbad, CA). Plasmid extraction kit and DNA gel-extraction kit were purchased from Qiagen Inc (Germantown, MD) or Bio-Rad Laboratories, Inc. (Hercules, CA).

Bacterial strains, Bacteriophages, Plasmids, and Primers Used

The bacterial strains, bacteriophages and plasmids used in this study are listed in Table 4-1. All primers used in this study are listed in Table 4-2.

Media and Growth Conditions

Luria broth was prepared as described previously (158). Glucose-mineral salts medium contained 10 g glucose, 6.25 g Na_2HPO_4, 0.75 g KH_2PO_4, 2.0 g NaCl, 10 mg $FeSO_4 \bullet 7H_2O$, 10 mg $Na_2MoO_4 \bullet 2H_2O$, 0.2 g $MgSO_4 \bullet 7H_2O$, and 1.0 g $(NH_4)_2SO_4$ in 1 L of deionized water. Glucose, $MgSO_4 \bullet 7H_2O$, and $(NH_4)_2SO_4$ were added after autoclaving basal salts solution. Solid medium was prepared by the addition of 15 g L^{-1} agar into liquid medium. Antibiotics used for selection were added to medium after autoclaving. Typical antibiotics and concentrations used in this study were ampicillin (100 mg L^{-1}), kanamycin (50 mg L^{-1}), chloramphenicol (15 mg L^{-1}), tetracycline (15 mg L^{-1}), and spectinomycin (100 mg L^{-1}).

Fermentation

Batch fermentations without pH control were carried out in a 13 x 100 mm screw-cap tubes filled to the top with appropriate medium. An inoculum was grown aerobically for about 16 hrs at 37^{o}C in a rotator (80 rpm) and was inoculated into the tubes at a concentration of 1 % (v/v). Microaerobic batch fermentation was carried out in 13 x 100 mm screw cap tubes (9 ml capacity); however, the tube contained 4-7 ml of appropriate medium depending on the desired oxygen concentration. The microaerobic culture tubes were incubated in a rotator (80 rpm) at 37^{o}C. pH-controlled fermentations were conducted at 37^{o}C in 500 ml fleaker vessels containing 250 ml of the corresponding medium along with a custom-made pH-stat. pH was controlled with 0.5 N KOH (96).

DNA Extraction and Purification

Plasmid DNA was extracted with Qiagen QIAprep Spin Miniprep Kits. DNA extracted from agarose after electrophoresis was purified by either Qiagen QIAquick Gel Extraction Kits or Bio-Rad Freeze 'N Squeeze spin columns followed by ethanol precipitation as previously described (14). PCR-DNA purification was done with Qiagen QIAquick PCR Purification Kits. Genomic DNA was extracted with a modified protocol as described by Ausubel *et al.* (14). Two ml of an overnight culture grown at 37^{o}C aerobically was pelleted and resuspended in 567 µl of P1 buffer with the addition of RNase from QIAprep Spin Miniprep Kit instead of TE buffer, followed by the addition of 50 µl 10 % sodium dodecyl sulfate (SDS). The cell lysate/SDS solution was mixed by inversion and then incubated at 60^{o}C for 5 minutes to increase cell lysis. 120 µl of 5 M NaCl was then added, mixed by inversion, followed by 1 minute incubation at 60^{o}C. Then, 80 µl of cetyl trimethylammonium bromide (CTAB)/NaCl solution (14) preheated to 60^{o}C was added, mixed thoroughly by inversion, and incubated at 60^{o}C for 5 more minutes. The lysate was extracted with Tris-saturated phenol, pH 8.0, followed by phenol:chloroform:

isoamyl alcohol (25:24:1) extraction. DNA was then precipitated with 0.7 volume isopropyl alcohol, pelleted by centrifugation, and washed with 600 µl of 70 % ethanol. DNA was pelleted again and the ethanol was carefully decanted. The DNA pellet was allowed to dry briefly at 42^{o}C and then dissolved in 100 µl TE buffer. Genomic DNA was incubation at 50^{o}C to completely dissolve the DNA as needed.

Polymerase Chain Reaction (PCR)

Polymerase Chain Reaction (PCR) was performed using Phusion High-Fidelity DNA Polymerase (NEB). A 50 µl reaction typically contained 1x High Fidelity (HF) buffer, 200 µM each of the four dNTPs, 0.4 µM of each forward and reverse primer, and 0.5 units of Phusion polymerase. Denaturing temperature was set at 98^{o}C (20 sec), annealing temperatures were set at 5^{o}C below the lowest primer T_m (15 sec), and elongation was at 72^{o}C (30 sec per 1 kb).

DNA Modification

Digestion conditions and ligation were as modified from manufacturers' recommendations. Typically, a 20 µl digestion reaction consisted of 0.5 µg DNA, 1x buffer, 1 µl BSA (1 mg ml^{-1}), and 0.5 µl restriction endonuclease. 10 units or 100 units of T4 ligase was typically used per "sticky" end or blunt end ligation reaction, respectively, at 16^{o}C for at least 12 hrs.

Transformation

Chemical transformation was carried out as described previously with minor modification (133). Cells were cultured in a 125 ml flask containing 5 ml Luria-Bertani (LB) medium and a 1.0 % inoculum of an overnight, culture at 37^{o}C for about 1.5 hrs or until the $OD_{420nm} = 0.2$. Cells were harvested and resuspended in 0.2 ml of cold 0.1 M $CaCl_2$. About 0.5 µg of plasmid DNA was then added to the cell suspension. The cell and DNA mixture was incubated on ice for 15 minutes and heat-shocked for 1 minute at 42^{o}C. After heat-shock, the cell/DNA mixture was immediately transferred to ice for additional 10 minutes. Two ml of LB was added to the

reaction mixture and this was incubated for 1 hour at 37^{o}C. Electroporation was conducted as recommended by Bio-Rad Laboratories (MicroPulser electroporation apparatus operating instructions and applications guide).

Transduction

Gene transfer mediated by bacteriophage P1 mediated transduction was performed as described by Miller (138).

Gene Deletions

Method used for gene deletion in *E. coli* was as described by Datsenko *et al.* (51). Using plasmid pKD4 as template, PCR primers with 50 bases homologous to the gene of interest were designed to amplify FRT:kanamycin resistance cassette (kan^{R}):FRT. The resulting PCR product, gene':FRT:kan^{R}:FRT:'gene, was electroporated into strain BW25113 containing plasmid pKD46 which encodes an arabinose inducible Red recombinase. Transformants harboring deletion of the targeted gene were selected for kanamycin resistance located within the deleted gene. PCR was used to confirm the deletion. P1 phage transduction was used to transfer the deleted gene to other strains of interest. The kanamycin cassette was removed by transforming in a temperature sensitive plasmid, pCP20, harboring yeast FLP recombinase gene leaving an 84 bp insert of a single FRT sequence at the site of deletion.

Construction of Plasmid pET15b Based T7 Expression Plasmids

Protein over-expression was mediated by plasmid pET15b based T7 expression system. Primers were designed to PCR amplify the gene of interest with 5' extension of CAT<u>ATG</u> on the forward primer and GGATCC on the reverse primer corresponding to the NdeI and BamHI endonuclease recognition sites, respectively. The underlined <u>ATG</u> correspond to an overlapping translation start initiation codon of the gene of interest. XhoI recognition sequence (CTCGAG) was substituted for NdeI or BamHI site if these recognition sequences appeared within the gene

of interest (see Table 4-2 for complete list of primer sequences). PCR products and plasmid pET15b (Novogen) were digested with the respective enzymes, ligated, and transformed into *E. coli* strain TOP10. Transformants were selected as ampicillin resistant colonies. Plasmid was extracted and the presence of insert was confirmed by PCR with gene specific primers. Plasmids with appropriate insert DNA were transformed into Rosetta (λDE3) bearing plasmid pRARE encoding rare *E. coli* codon tRNAs for recombinant expression of heterologous proteins in *E. coli*. Proteins were expressed as N-terminal His_6-thrombin recognition site protein fusions.

Protein Production Using pET15b Based T7 Expression

A few colonies of freshly transformed Rosetta strain bearing pET15b derived plasmid were inoculated into 20 ml of LB-amp (250 ml flask) and incubated at 37^{o}C (200 rpm) shaking for about 15 hrs. Fifteen ml of this culture was transferred to 1.0 L LB-amp medium in a 2.8 L Fernbach flask. This culture was incubated for 2 hrs at 37^{o}C (250 rpm) or until OD_{420nm} reached ~ 0.60. Arabinose was added to a final concentration of 1.5 % and incubation was continued at room temperature with the same shaking rate for an additional 4 hrs. Cells were harvested by centrifugation and washed twice with 40 ml of cold 50 mM KPO_4 buffer pH 7.5 with 0.1 M NaCl (Buffer A). The cells were collected, and stored at -20^{o}C until use.

His-tagged Protein Purification

Frozen cells were thawed on ice in 10 ml of Buffer A. All purification steps were performed at 4^{o}C or on ice. The cells were disrupted by passing through a French pressure cell operating at 20,000 psi. 100 units of DNaseI was added to reduce viscosity and the lysate was incubated on ice for 10 minutes. The lysate was centrifuged at 30,000 x g for 45 min. The supernatant was filtered using a 0.2 μm syringe filter. The filtered crude extract was then loaded on a 1 ml HiTrap Chelating column (GE) (1 ml min^{-1} flow rate) that was pre-washed with Ni^{+2} (0.1 M $NiCl_2$ in Buffer A) followed by 20 volumes of Buffer A to remove excess nickel. The

protein-bound column was washed with 5 volumes of Buffer A followed by 10 volumes of Buffer A with 50 mM imidazole. The His-tagged protein was eluted with Buffer A containing 150 mM imidazole at a flow rate of 0.5 ml min^{-1} and 1 ml fractions were collected. Fractions with the highest protein concentration determined by Bradford assay (14) were separated by sodium dodecyl sulfate polyacrylamide gel electrophoresis (SDS-PAGE) to determine purity. Highest purity fractions were combined and digested with 50-100 units of thrombin to remove the His-tag while being dialyzed in 4 L Buffer A with 0.5 mM DTT for 16 hrs. The dialyzed protein and thrombin mixture were separated on HiPrep 26/60 Sephacryl S-200 HR (GE) gel filtration column (pre-equilibrated with Buffer A containing 0.5 mM DTT) with a flow rate of 0.5 ml min^{-1} and 3.75 ml fractions were collected. Fractions with the highest purity as determined by SDS-PAGE were combined. Glycerol was added to the purified protein to a final concentration of 20 %, flash frozen in liquid nitrogen, and stored at -75^{o}C until use.

Analytical Methods

Protein concentration was determined using Coomassie blue (Bradford reagent) or bicinchoninic acid (BCA) assays (14, 34, 182) with bovine serum albumin as standard. SDS-PAGE utilized 12.5 % gels as per Laemmli (118). The protein standards used in SDS-PAGE (Bio-Rad Laboratories, Hercules, CA) were aprotinin (6.5 kDa), lysozyme (14.4 kDa), trypsin inhibitor (21.5 kDa), carbonic anhydrase (31.0 kDa), ovalbumin (45.0 kDa), serum albumin (66.2 kDa), phosphorylase b (97.4 kDa), β-galactosidase (116.3 kDa), and myosin (200 kDa). Protein standards used to calibrate Hi Prep Sephacryl S-200 HR column used for gel filtration (Sigma Chemical Co., St. Louis, MO) were bovine carbonic anhydrase (29.0 kDa), ovalbumin (45.0 kDa), bovine serum albumin (66.0 kDa), and yeast alcohol dehydrogenase (150 kDa). Non-heme iron was determined as described by Harvey *et al.* (89), and sulfur was determined using the method described by Cline (45). Organic acids and sugars were analyzed by high-

performance liquid chromatography (HPLC, Hewlett Packard 1090 series II chromatograph equipped with refractive index and UV detectors) with a Bio-Rad Aminex HPX-87H ion exclusion column. Hydrogen gas was measured by gas chromatography (Gow Mac series 580, GOW-MAC Instrument Co., Bethlehem, PA) using a thermal conductivity detector and a stainless steel column (1.8 m × 3.2 mm) packed with molecular sieve 5 Å, using N_2 as the carrier gas. Optical density of the cultures grown in 13 x 100 mm tubes were measured with a Bausch & Lomb Spectronic 20 at 420 nm. Analytical spectrophotometric measurements were performed in a Beckman DU 640 spectrophotometer.

Methods for Hydrogen Production

Construction of Tandem T7 Expression of *ndhE* and *ndhF* Subunits

T. vaginalis ndhE and *ndhF* DNA were received from Dr. Hrdy at Charles University, Czech Republic. *T. vaginalis ndhE* and *ndhF* were each cloned into pET15b as previously described producing pET15b-*ndhE* and pET15b-*ndhF* plasmids (Figure 4-1) (56). The entire T7 expression operon from pET15b-*ndhF* including T7 promoter and T7 terminator was PCR amplified using primers "pET15b-T7 F (HindIII)" and "pET15b-T7 R (HindIII)" and the purified PCR product was digested and cloned into the HindIII site on pET15b-*ndhE* (pPMD38) producing pET15b-*ndhE*-*ndhF* (pPMD40). The resulting plasmid was digested with XhoI to confirm the orientation of the insert. The plasmid pPMD40 has the two genes, *ndhE* and *ndhF*, encoding the two subunits of NDH expressed in tandem by independent T7 promoters.

Construction of Tandem *trc* Promoter Controlled Expression of *ndhE* and *ndhF*

T. vaginalis ndhE and *ndhF* were cloned into plasmid pTrc99a as described above in the construction of plasmid pPMD40 with independent T7 promoters. Genes encoding *ndhE* and *ndhF* were independently cloned into the NcoI and BamHI sites in pTrc99a using PCR primers "*ndhE* F (NcoI)" / "*ndhE* R (BamHI) and "*ndhF* F (NcoI)" / "*ndhF* R (BamHI)", respectively.

Using pTrc99a-*ndhF* as template, *ndhF* including the *trc* promoter was PCR amplified with primers "pTrc99a F (XbaI-*trc*)" / "*ndhF* R (HindIII)" and the resulting product was cloned into XbaI and HindIII site of pTrc99a-*ndhE* producing pTrc99a-*ndhEF*. Plasmid pTrc99a-*ndhEF* harbors two independently expressed *trc* promoters and a rho-independent terminator (*rrnB*) downstream of the last gene, *ndhF*.

NADH-Dehydrogenase (NDH) Enzymatic Activity

NDH activity was determined spectrophotometrically using NADH as the electron donor and various artificial electron acceptors. Standard reaction mixture consisted of K-phosphate buffer (50 mM, pH 7.5), NADH (1 mM), and benzyl viologen (1 mM). Reaction mixture in a 13×100 mm tube was sealed with a serum stopper, and the gas phase was replaced by evacuation and refill with N_2. Enough sodium dithionite was added to the reaction mixture to titrate out the residual O_2. Reaction was initiated by the addition of enzyme, and BV reduction was monitored continuously at 600 nm at room temperature. Although the small amount of added dithionite will reduce both the Fe-S cluster and flavin in the protein, the presence of excess BV in the reaction mixture is expected to reoxidize these cofactors and not interfere with the assay. Under these conditions, the small amount of added dithionite did not affect the kinetics of BV reduction. With ferricyanide as electron acceptor, assays were under aerobic condition. Concentrations of BV, methyl viologen, and K-ferricyanide were 1.00 mM in the experiments leading to determination of K_m of NADH. Molar extinction coefficients used for BV and MV are 7,800 and 6,300, respectively, at 600 nm with 1.00 cm path length. Ferricyanide-dependent NDH activity was determined in the same buffer as the BV assay (410 nm; extinction coefficient of 1,020 M^{-1} cm^{-1}). Ferredoxin-dependent NDH activity was determined in the same buffer with 0.10 mM NADH and 40 μM *C. acetobutylicum* ferredoxin by following the oxidation of reduced NADH at 340 nm. One unit of enzyme activity is defined as 1 μmol substrate oxidized min^{-1}.

Clostridium Ferredoxin Purification

C. acetobutylicum strain 824 (NRRL B-23491) obtained from USDA-ARS (Peoria, IL) was cultured in Reinforced Clostridial Medium (Oxoid, Cambridge, UK) without the agar in 12 L carboys for 16 hrs at 37^{o}C. Ferredoxin was isolated from the cells as described previously for *C. pasteurianum* ferredoxin (167, 178). Protein concentration was determined from the molar extinction coefficient of 30,600 cm^{-1} at 390 nm, a value reported for *C. pasteurianum* ferredoxin (167).

(Electron Paramagnetic Resonance) EPR Measurements

EPR experiments were performed by Dr. Angerhofer, Department of Chemistry, University of Florida. Cw-EPR spectra of the NDH complex at cryogenic temperatures were determined using a commercial EPR spectrometer (Bruker Elexsys E580) equipped with an Oxford Instruments ESR900 helium-flow cryostat and the standard TE102 mode rectangular cavity (Bruker ER4102ST). EPR samples were placed in a Wilmad 3×4 (ID×OD)-mm quartz tubes (CFQ), prefrozen in liquid nitrogen, before insertion into the precooled cryostat.

Selection of Methyl Viologen (MV) Resistant *E. coli*

MV resistant *E. coli* was selected by serial transfers with increasing concentrations of MV. Ten ml of LB supplemented with 10 μM MV in a 125 ml Erlenmeyer flask was inoculated with 1.0 % of an overnight culture of *E. coli* strain PMD45 grown in LB at 37^{o}C. The culture with MV was incubated for 16 hrs at 37^{o}C with shaking (250 rpm). This culture was sequentially transferred to 10 ml fresh LB medium with 100 μM MV at a 1.0 % inoculum level and each transfer was incubated for 16 hrs. After which, it was used as an inoculum for 10 ml LB with 1.0 mM MV. As needed, a culture at an OD_{420nm} of 0.6 was diluted and plated on LB agar plates supplemented with 1.0 mM MV and incubated aerobically overnight at 37^{o}C. Colonies that formed were selected, streaked on the same solid medium supplemented with glucose and were

incubated at 37°C in an anaerobic jar. After 48 hrs, colonies that were resistant to 1 mM MV under anaerobic growth conditions were replicated onto the same solid medium and incubated aerobically for 8 hrs. Over 95 % of the colonies that were resistant to MV anaerobically were killed by the switch to an oxygenic atmosphere. Colonies that survived were selected and anaerobic/aerobic cycle was repeated two more times until a more stable *E. coli* strain was recovered that was resistant to 1 mM MV and could survive the transition from anaerobic to aerobic conditions.

Detection of Hydrogen Production

Overnight cultures were used as a 1.0 % inoculum for 1 ml LB with 0.3 % glucose supplemented with the appropriate antibiotics and electron acceptors in a 12 x 75 mm heavy wall tube sealed with a rubber stopper. Electron acceptors tested were 1.0 mM of each MV, BV, and DCPIP. The tubes were degassed and filled with N_2 and incubated at 37°C. Hydrogen production was determined after injecting 50 or 100 µl gas sample with a Hamilton gas tight syringe into a gas chromatograph.

Electrochemical Potential

The electrochemical potential of a redox couple was calculated using the Nernst equation (Equation 4-1):

$$E = E_o' + \frac{R\,T}{n\,F}\,ln\left(\frac{[\text{Oxidized}]}{[\text{Reduced}]}\right) \qquad (4\text{-}1)$$

Where E = concentration dependent redox potential (V); E_o' = midpoint standard redox potential (V) (Table 4-3); R = 8.314 J K^{-1} mol^{-1} (ideal gas constant); T = temperature (K); *F* = 96,500 Coulombs mol^{-1} (Faraday constant); *n* = number of e^-. The Nernst equation has been simplified by calculating the constants listed at standard temperature (298°K) and converting natural log (*ln*) to $\log_{10}$ as follows (Equation 4-2):

$$E = E_o' + \frac{0.0592\ V}{n} \log \left(\frac{[Oxidized]}{[Reduced]} \right) \quad (4\text{-}2)$$

Free energy was calculated using a derivation of Gibbs free energy (Equation 4-3):

$$\Delta G = -nF\Delta E \quad (4\text{-}3)$$

Where ΔG is the change in free energy (J mol^{-1}) and ΔE is the change in redox potential ($E_{product} - E_{reactant}$; V). Joules can be converted to calories using the conversion factor 1 cal = 4.18 J.

Cloning of [Fe]-Hydrogenase Isolated from Termite Gut

[Fe]-hydrogenase genes from the symbionts present in the digestive tract of *Reticulitermes flavipes* were received from Dr. Mike Scharf, Department of Entomology and Nematology, University of Florida. The ORFs were fully sequenced and the putative gene was identified after BLAST alignment as [Fe]-hydrogenases. Protein alignments were performed with ClustalG ver. 1.5. The gene encoding the [Fe]-hydrogenase most similar to the published enzyme from *P. grassii* (99) was subcloned into pET15b and pTrc99a using PCR primers "*gutHyd* F (NdeI)"/"*gutHyd* R (BamHI)" and "*gutHyd* F (NcoI)"/"*gutHyd* R (BamHI)", respectively. *gutHyd* including the *trc* promoter was subcloned into NdeI and PflMI sites of pTrc99a-*ndhEF* using PCR primers "*gutHyd trc* F (NdeI)"/"*gutHyd* R (PflMI)" resulting in plasmid pTrc99a-*ndhEF-gutHyd*.

Methods for Butanol Production

Construction of Plasmid pET15b Derivatives for the Expression of Enzymes in the Butanol Pathway

All butanol genes were amplified from *C. acetobutylicum* American Type Culture Collection (ATCC) 824D genomic DNA obtained from ATCC using the respective PCR primers listed in Table 4-2. The gene *ccrA* was PCR amplified from *Streptomyces avermitilis* ATCC

31267D-5 genomic DNA obtained from ATCC. Amplified PCR products were cloned into plasmid pET15b for expression and purification of His-tagged fusion proteins. *E. coli* strain Rosetta (λDE3) bearing the appropriate plasmid pET15b-derivatives were induced with arabinose, and protein was purified as described in the section on NDH.

Enzyme Assays for Butanol Pathway

The enzymes that constitute the butanol pathway were produced in recombinant *E. coli* and purified. Specific activities of these enzymes was determined spectrophotometrically using NAD(P)H as the electron donor and the appropriate CoA derived intermediates or aldehydes as acceptors. All assays were performed in 1 ml of 50 mM K-PO_4 buffer pH 7.5 and 0.1 mM NAD(P)H at room temperature. Enzyme kinetics were determined by measuring NAD(P)H oxidation (molar extinction coefficient of 6,220 M^{-1} cm^{-1} at 340 nm). Thiolase (0.5-1.0 µg of ThlA or ThlB) activity was determined by using 0.1 mM acetyl-CoA as substrate in a coupled reaction with NADH oxidation by Hbd (6µg) (217). Hbd (0.1-0.2 µg) activity was determined using 0.2 mM acetoacetyl-CoA as substrate (32, 47, 229). Crt (2-5 ng) activity was determined using 0.1 mM hydroxybutyryl-CoA as substrate in a coupled reaction with NADPH oxidation by CcrA (2 µg) (32). Bcd-EtfBA (10 µg Bcd-complex) and CcrA (0.2-2.0 µg) activity were determined by measuring oxidation of NADH or NADPH, respectively, using 0.1 mM crotonyl-CoA as substrate. Aldehyde-alcohol dehydrogenase (10 µg of Aad or AdhE2) activity was determined by measuring the oxidation of NADH using 0.1 mM butyryl-CoA and 2.5 mM butyraldehyde, respectively (67, 144).

***In Vitro* Butanol Production**

Based on the specific activates of the recombinant enzymes, 1 unit (µmol min^{-1}) of each purified enzyme in the butanol pathway from acetyl-CoA up to butyryl-CoA (ThlA, Hbd, Crt, and CcrA) was added to 0.5 ml assay buffer containing a final concentration of 50 mM K-PO_4

pH 7.6, 5 mM acetyl-CoA, 10 mM NADH, and 10 mM NADPH. The reaction mixture was incubated at 37^{o}C for 30 minutes after which a 100 µl sample was removed for analysis. One unit of AdhE2 and 10 mM NADH were then added and incubated for an additional 30 minutes at 37^{o}C. H_2SO_4 was added to final concentration of 0.1 M to stop the reaction and to hydrolyze the CoA releasing free acids. The final mixture and the starting and intermediate sample were analyzed by HPLC for butanol and other intermediates.

Enzyme Assay from Crude Extract

E. coli strain JM107 bearing the plasmid(s) pCBEHTCB and/or pAA were grown and the enzymes were induced with IPTG as described above for T7-based expression of the same genes. Induced cells were disrupted in the same manner as described for T7-based protein production. The cell lysate was clarified by ultracentrifugation at 100,000 x g for 1 hr to minimize membrane-bound NADH dehydrogenase activity. Enzyme assays were performed as described above.

Plasmid Construction for Butanol Production

Construction of pButanol: Genes from *C. acetobutylicum* butanol production pathway were cloned into plasmid pTrc99a (Figure 4-2). The BCS operon was PCR amplified using "*crt* F (NcoI)" and "*hbd* R (BamHI)" primers producing PCR product that has a NcoI site extension on the 5' and a BamHI site attached to the 3' end. The gene encoding AdhE2 was amplified with "*adhE2* F (BamHI)" and "*adhE2* R (XhoI)" primers producing a PCR product that has a BamHI site extension on the 5' and XhoI site attached to the 3' end. The *adhE2* PCR product also includes the native 18 bp region upstream of the gene that contains the Shine-Dalgarno (SD) sequence. The gene encoding ThlA was amplified with "*thlA* SD F (XhoI)" and "*thlA* R (HindIII)" producing a PCR product that has a XhoI site extended on the 5' and a HindIII site attached to the 3' end. Since *thlA* does not have a good *E. coli* SD sequence immediately

upstream of the gene, a 16 bp region was added through primer "*thlA* SD F (XhoI)" that contains an optimized *E. coli* SD sequence in addition to the XhoI site. The resulting PCR products were digested with the respective enzymes and ligated all together into the NcoI and HindIII site of pTrc99a resulting in the plasmid pButanol. Plasmid pButanol contains all the genes necessary for production of butanol expressed as a single synthetic polycistronic operon controlled by IPTG inducible *trc* promoter.

Construction of pButyrate: To construct a plasmid for the production of butyrate, *adhE2* was removed from pButanol and replaced with a FRT:Kan^R:FRT cassette (Figure 4-3). Primers "pKD4 F (BamHI)" and "pKD4 R (XhoI)" were used to PCR amplify the FRT:Kan^R:FRT cassette with the addition of BamHI and XhoI sites on the 5' and 3'ends, respectively. The resulting PCR product was cloned into the BamHI and XhoI restriction sites of pButanol replacing the *adhE2* gene. The resulting plasmid, pButyrate, has the BCS operon expressed from an IPTG inducible *trc* promoter. The *thlA* gene is still expected to be expressed by the plasmid from the kan^R cassette.

Construction of pTrc99a derived plasmids: The vector pTrc99a was used to express various individual steps of butanol pathway (Figure 4-4) (6). The first gene, *adhE2*, was amplified from pButanol with PCR primers "*adhE2* F (NcoI)" and "*adhE2* R (XmaI)" to produce a PCR product with NcoI site on the 5' and XmaI sites on the 3', respectively. The *adhE2* PCR product was cloned into NcoI and XmaI site within the pTrc99a multiple cloning site resulting in pTrc99a-*adhE2*. *E. coli* thiolase gene, *atoB*, was amplified from *E. coli* W3110 genomic DNA with primers "*atoB* F (KpnI)" and "*atoB* R (HindIII)" to produce a product that includes 11 bp upstream of *atoB* containing its native SD sequence and KpnI and HindIII sites at the 5' and 3' ends, respectively. This PCR product was cloned into KpnI and HindIII site in pTrc99a resulting

in pTrc99a-*atoB*. The plasmid pTrc99a-*atoB* was then used as template for PCR using "pTrc99a F (XmaI)" and "*atoB* R (HindIII)" to amplify *atoB* with the *trc* promoter and XmaI and HindIII sites at the 5' and 3' ends, respectively. The *atoB* with its own *trc* promoter was then cloned into the XmaI and HindIII sites of pTrc99a to produce pAA, where both genes were expressed independently by tandem *trc* promoters. The gene c*crA2* was PCR amplified from *S. avermitilis* genomic DNA using primers "*ccrA2* F (NcoI)" and "*ccrA2* R (XbaI)" to produce a PCR product with NcoI and XbaI sites at the 5' and 3' ends, respectively. *E. coli* soluble transhydrogenase gene, *udhA*, was amplified from W3110 genomic DNA with primers "*udhA* F (XbaI)" and "*udhA* R (HindIII)" to produce a PCR product with XbaI and HindIII sites at the 5' and 3' ends, respectively. The primer "*udhA* F (XbaI)" also replaced *udhA* upstream region with a more optimal SD sequence for improved translation. PCR products of *ccrA2* and *udhA* were digested with the respective endonucleases and were all ligated into NcoI and HindIII site of pTrc99a resulting in pTrc99a-*ccrA2*-*udhA* plasmid where *ccrA2* and *udhA* were expressed as a single polycistronic synthetic operon.

Consolidation of pTrc99a derived plasmids into a single low copy number plasmid: Large plasmids with high copy number replication systems tend to result in reduced plasmid stability and/or retention. Therefore the *trc* operons constructed previously we cloned into a low copy number plasmid vector (pACYC184) to improve stability (Figure 4-5). The BCS operon including *trc* promoter from pButanol was amplified using "pTrc99a F (EagI)" and "*hbd* R (BamHI)" primers and cloned into EagI and BamHI endonuclease restriction sites on pACYC184, producing pCBEH. Using pTrc99a-*ccrA2*-*udhA* as template, PCR primers "pTrc99a F (BamHI)" and "*udhA* R (XbaI)" were used to amplify the P_{trc}-*ccrA2*-*udhA* operon and the PCR product was cloned into BamHI and XbaI endonuclease sites on pCBEH to make

pCBEHCU. Using pTrc99a-AA as template, PCR primers "pTrc99a F (Bsu36I)" and "*atoB* R (EagI)" were used to amplify the *lacI*^{q}-P$_{trc}$-*adhE2*-P$_{trc}$-*udhA* operon and the PCR product was cloned into Bsu36I and EagI endonuclease sites on pCBEHCU to make pAACBEHCU. The plasmid pAACBEHCU contains all the genes required to produce butanol from acetyl-CoA on a low-copy plasmid with p15a origin of replication. Genes with lower specific activities (*adhE2*, *atoB*, *bcd/etfBA*, and *ccrA2*) were expressed independently by individual *trc* promoters.

Another plasmid, pCBEHTCB, was constructed in a similar manner. A three gene synthetic operon was constructed with *thlA*, *ccrA*, and *bdhB*. The three genes, *thlA*, *ccrA*, and *bdhB*, were PCR amplified with primer sets "*thlA* F (NcoI)"/"*thlA* R (XhoI)", "*ccrA* F (XhoI)"/"*ccrA* R (SexAI)", and "*bdhB* F (SexAI)/"*bdhB* R (SbfI)", respectively. The resulting PCR products were digested with their respective enzymes and ligated all together into the NcoI and SbfI site of plasmid pTrc99a resulting in plasmid pTCB in a similar manner as Figure 4-2. The whole operon including the *trc* promoter was PCR amplified from plasmid pTCB using primers "pTrc99a F (BamHI)"/"*bdhB* R (ClaI)" and cloned into the BamHI and ClaI restriction sites of pCBEH resulting in pCBEHTCB.

E. coli Strain Construction for Butanol/Butyrate Production

Strain KJ104 (*E. coli* ATCC 8739 Δ*ldhA* Δ(*focA-pflB*) Δ*adhE* Δ*ackA* Δ*mgsA* Δ*poxB* Δ*tdcDE* Δ*citF*), a microbial biocatalyst developed for succinate production (103), was used as the starting strain for engineering a butanol-producing strain To eliminate succinate production, a deletion in *frdBC* was introduced into strain KJ104 to disrupt fumarate reductase activity. The resulting strain, PMD71, cannot grow anaerobically due to the inability to oxidize NADH generated during glycolysis.

Integration of plasmid pAACBEHCU into *E. coli* chromosome: Even though the butanol genes were on a low-copy plasmid, the large size (15,550 bp) and repeat *trc* promoter

sequences could lower plasmid stability. To stabilize the genes, the entire plasmid was integrated into *E. coli* chromosome via single recombination. The plasmid pAACBEHCU was digested with BstBI, which removed p15a origin of replication and the chloramphenicol resistance gene (*Cm*). The linearized DNA was then treated with Klenow fragment to fill in the 5' overhang left over from BstBI digestion to produce blunt ends. The spectinomycin resistance gene (spc^R) from pAW016 was PCR amplified using primers "*spc* F" and "*spc* R". The resulting PCR product was ligated to the linearized pAACBEHCU to produce a circular DNA that has no origin of replication. The resulting DNA was electroporated into BW25113/pKD46 expressing red recombinase. Genomic DNA was extracted from colonies that were resistant to spectinomycin (100 μg ml^{-1}), and PCR was performed using genomic DNA as template and appropriate primers to confirm the integration of *adhE2-atoB*, *crt-hbd*, and *ccrA2-udhA*. PCR using primers "*adhE-atoB* F" and "*adhE-atoB* R", "*crt-hbd* F" and "*crt-hbd* R", and "*ccrA2-udhA* F" and "*ccrA2-udhA* R" produced fragments of 3,487 bp, 4,042 bp, and 2,195 bp respectively, confirming the presence of the butanol genes in the chromosome. The colony with all three correct size PCR products was noted to have chromosomal insertion of pAACBEHCU (but^+) and the genes were transduced to strain PMD50 and PMD71 resulting in PMD70 and PMD72, respectively. The site for chromosomal integration is yet to be determined; however, possible recombination sites were *atoB*, *udhA*, and $lacI^q$ since these *E. coli* genes were present in the circular DNA used for integration.

Chromosomal insertion of BCS operon at *pflB*: PCR using primers "*focA* F (HindIII)" and "*pflA* R (XmaI)" were used to amplify *pflB* including 389 bp and 643 bp upstream and downstream DNA, respectively, with the addition of HindIII and XmaI sites to the primers (Figure 4-6). The 3.4kb PCR product was cloned into HindIII and XmaI sites of pUC19. The

resulting plasmid, pUC19-'*focA-pflA*', was used as template for outward PCR using primers "*focA* out (Blunt)" and "*pflA* out (XhoI)" producing a 3704 bp PCR product with a blunt 3' end near the end of *focA* and XhoI site at the 3' end near the start of *pflA*. Primers labeled with "Blunt" had a 5' phosphorylation modification during synthesis. At the same time, pButyrate was used as template for PCR using primers "*crt* F (Blunt)" and "pKD4 R (XhoI)" to produce a 6214 bp PCR product of the promoterless BCS operon upstream of a kanamycin cassette. The two PCR products, BCS-kan and pUC19-'*focA-pflA*' outward PCR, were then digested with XhoI and ligated together to produce the final plasmid pUC19-Δ*pflB*-BCS-kan^R. Plasmid pUC19-Δ*pflB*-BCS-kan^R was then doubly digested with NruI and Acc65I producing 7171 bp and 2729 bp DNA fragments. The larger fragment was gel purified with Qiagen Gel Extraction Kit and the purified DNA was electroporated into BW25113/pKD46 as described in Datsenko *et al.* (51). The digested DNA fragment had 312 bp and 643 bp region of homology to the upstream and downstream regions of *pflB* respectively. Colonies that were resistant to kanamycin were selected and grown anaerobically for 24 hrs at 37^{o}C. HPLC was used to analyze fermentation products. Cultures with lactate as a major fermentation product with little or no formate, acetate and ethanol were noted to have a BCS operon replacing *pflB*. The ATG start codon of the first gene, *crt*, replaced the ATG of *pflB*; thus the BCS operon should now be transcriptionally regulated by all of *pflB*'s seven promoters (173). Genomic DNA was extracted and PCR was performed with primers "*crt-hbd* F" and "*crt-hbd* R" (4042 bp) to confirm chromosomal insertion. P1 phage was used to transfer Δ*pflB*-BCS-kan^R to strain PMD72 resulting in strain PMD74.

Production of butyrate: PCR was performed using pKD4 as template and "*spc-adhE2* F (pKD4 F)" and "*spc-adhE2* R (pKD4 R)" primers to amplify FRT:Kan^R:FRT cassette with 50 bp

up and downstream homologous to 5' of *spc*^{R} gene and 3' of *adhE2*. *E. coli* strain PMD52/pKD46 was electroporated with the derived linear PCR product and transformants were selected for kanamycin resistance and spectinomycin sensitivity. The resulting strain, PMD75, had a Δ (*adhE2-spc*^{R}) mutation.

Integration of an additional copy of *C. acetobutylicum bcd-etfBA* replacing *E. coli adhE*: An additional copy of *bcd/etfBA* was used to replace *E. coli adhE* in a similar manner as the BCS operon integration replacing *pflB*. *E. coli adhE* was PCR amplified from W3110 genomic DNA using "*adhE* F (SbfI)" and "*adhE* R (XmaI)" primers including 279 bp and 239 bp upstream and downstream of *adhE*, respectively. This DNA was cloned into SbfI and XmaI sites of pUC19. At the same time, the FRT:Kan^{R}:FRT cassette was also amplified from plasmid pKD4 with "pKD4 F (BamHI)" and "pKD4 R (XhoI)". This PCR product was digested with only *Bam*HI leaving the 3' end undigested (blunt) and was cloned into BamHI and ScaI (blunt) restriction sites on pTrc99a-*bcd-etfBA* introducing a kanamycin resistance cassette directly downstream of the *bcd-etfBA* operon. The *bcd-etfBA*-kan^{R} operon was amplified using "*bcd-etfBA*-kan F (homology)" and "*bcd-etfBA*-kan R (homology)" primers. Using pUC19-*adhE* as template, "pUC19-*adhE* F OUT" and "pUC19-*adhE* R OUT" primers, which bind directly upstream and downstream, respectively, of *adhE* were used to amplify outward away from *adhE*. These primers also include 20 bases 5' extensions of sequences homologous to "*bcd-etfBA*-kan F (homology)" and "*bcd-etfBA*-kan R (homology)" for homologues recombination cloning by CloneEZ^{TM} Kit (GenScript Corp) for seamless cloning without restriction enzyme and ligation. Cloning was performed as described by GenScript Corp. The resulting plasmid, pUC19-Δ*adhE-bcd-etfBA*-kan^{R}, had *bcd-etfBA*-kan^{R} flanked by 279 bp and 239 bp *E. coli adhE* up and downstream regions, respectively. The plasmid pUC19-Δ*adhE-bcd-etfBA*-kan^{R} was then

digested with SbfI and XmaI and the purified product was used for double recombination cross-over in BW25113/pKD46 expressing red recombinase. Colonies that were resistant to kanamycin were grown anaerobically in liquid media and were tested by HPLC for ethanol production deficient phenotype. P1 transduction was used to transfer Δ*adhE-bcd-etfBA*-kan^R into strain PMD75 resulting in strain PMD76.

Table 4-1. Bacterial strains, bacteriophages, and plasmids

Strains	Genotype	Notes
W3110	Wild-type	ATCC
TOP10	F^- *mcrA* Δ(*mrr-hsdRMS-mcrBC*) Φ80*lacZ*Δ*M15* Δ*lacX74 recA1 ara*Δ*139* Δ (*ara-leu*)*7697 galU galK rpsL* (Str^R) *endA1 nupG*	Invitrogen
JM107	*endA1 glnV44 thi-1 relA1 gyrA96* Δ(*lac-proAB*) [F' *traD36 proAB*$^+$ *lacI*^{q} *lacZ*Δ*M15*] *hsdR17*(R_K^- m_K^+) λ^-	Lab collection
JM109	*endA1 glnV44 thi-1 rel*A1 *gyrA96 recA1 mcrB*$^+$ Δ(*lac-proAB*) *e14-* [F' *traD36 proAB*$^+$ *lacI*^{q} *lacZ*Δ*M15*] *hsdR17*($r_K^-m_K^+$)	NEB
BL21 (λDE3)	F^- *ompT gal dcm lon hsdS*$_B$(r_B^- m_B^-) λ(DE3 [*lacI la*cUV5-T7 gene 1 *ind1 sam*7 *nin*5])	Lab collection
JM109 (λDE3)	JM109 λ(DE3 [*lacI la*cUV5-T7 gene 1 *ind1 sam*7 *nin*5])	Lab collection
Rosetta (λDE3)	BL21 (λDE3) / pRARE	Novagen
PMD40	W3110 Δ*ldhA*	
PMD42	W3110 Δ*ldhA* Δ(*focA-pflB*)	Anaerobic (-)
PMD43	W3110 Δ*ldhA* Δ*adhE*	Anaerobic (-)
PMD44	W3110 Δ*ldhA* Δ*adhE* Δ*frdBC*	PMD43 Δ*frdBC*
PMD45	W3110 Δ*ldhA* Δ*adhE* Δ*frdBC* Δ*mgsA*	PMD44 Δ*mgsA*
PMD46	W3110 Δ*ldhA* Δ(*focA-pflB*) *lpd101**	PMD42 *lpd101**
PMD47	W3110 Δ*ldhA* Δ(*focA-pflB*) *lpd101** Δ*mgsA*	PMD46 Δ*mgsA*
PMD48	W3110 Δ*ldhA* Δ(*focA-pflB*) *lpd101** Δ*mgsA* Δ*tcdE*	PMD47 Δ*tcdE*
PMD50	JM107 Δ*ldhA*	This study
PMD51	JM107 Δ*ldhA* Δ(*focA-pflB*)	Anaerobic (-)
PMD52	JM107 Δ*ldhA* Δ(*focA-pflB*) *lpd101**	
PMD53	JM107 Δ*ldhA* Δ(*focA-pflB*) *lpd101** Δ*tcdE*	Anaerobic (-)
PMD54	JM107 Δ*ldhA* Δ(*focA-pflB*) *lpd101** Δ*adhE*	Anaerobic (-)
KJ104	*E. coli* ATCC 8739 Δ*ldhA* Δ (*focA-pflB*) Δ*adhE* Δ*ackA* Δ*mgsA* Δ*poxB* Δ*tdcDE* Δ*citF*	(103) Succinate strain
PMD70	JM107 Δ*ldhA but*$^+$[*spc*^{R}-P_{trc}-*adhE2*-P_{trc}-*atoB*-P_{trc}-*crt-bcd-etfBA-hbd*-P_{trc}-*ccrA-udhA*]	PMD50 *but*$^+$
PMD71	KJ104 Δ*frdBC*	

Table 4-1. Continued

Strains	Genotype	Notes
PMD72	KJ104 Δ*frdBC but*$^{+}$[*spc*^{R}-P$_{trc}$-*adhE2*-P$_{trc}$-*atoB*-P$_{trc}$-*crt-bcd-etfBA-hbd*-P$_{trc}$-*ccrA-udhA*]	PMD71 *but*$^{+}$
PMD73	JM107 Δ*ldhA but*$^{+}$ Δ*pflB-crt-bcd-etfB-etfA-hbd*	PMD70 Δ*pflB*-BCS
PMD74	KJ104 Δ*frdBC but*$^{+}$ Δ*pflB-crt-bcd-etfB-etfA-hbd*	PMD72 Δ*pflB*-BCS
PMD75	KJ104 Δ*frdBC but*$^{+}$[Δ*adhE2-spc*^{R}] Δ*pflB-crt-bcd-etfB-etfA-hbd*	Butyrate strain
PMD76	KJ104 Δ*frdBC but*$^{+}$[Δ*adhE2-spc*^{R}] Δ*pflB-crt-bcd-etfB-etfA-hbd* Δ*adhE-bcd-etfB-etfA*	PMD75 Δ*adhE-bcd-etfB-etfA*
Bacteriophages	**Genotype**	**Notes**
P1	*clr*100 *dam* rev6	
Plasmid	**Genotype**	**Notes**[a]
pUC19	*bla*$^{+}$	
pET15b	P$_{T7}$	Novagen
pTrc99a	P$_{trc}$	Lab collection
pPMD38	pET15b-*ndhE* (P$_{T7}$-*ndhE*)	from *T. vaginalis*
pPMD39	pET15b-*ndhF* (P$_{T7}$-*ndhF*)	from *T. vaginalis*
pPMD40	pET15b-*ndhEF* (P$_{T7}$-*ndhE* P$_{T7}$-*ndhF*)	Figure 4-1
pTrc99a-*ndhEF*	P$_{trc}$-*ndhE* P$_{trc}$-*ndhF*	This study
pET15b-*gutHyd*	P$_{T7}$-*gutHyd*	Symbiont [Fe]-hydrogenase
pTrc99a-*gutHyd*	P$_{trc}$-*gutHyd*	This study
pTrc99a-*ndhEF-gutHyd*	P$_{trc}$-*ndhE* P$_{trc}$-*ndhF* P$_{trc}$-*gutHyd*	This study
pET15b-*adhE2*	P$_{T7}$-*adhE2*	*C. acetobutylicum*
pET15b-*aad*	P$_{T7}$-*aad*	*C. acetobutylicum*
pET15b-*thlA*	P$_{T7}$-*thlA*	*C. acetobutylicum*
pET15b-*thlB*	P$_{T7}$-*thlB*	*C. acetobutylicum*
pET15b-*hbd*	P$_{T7}$-*hbd*	*C. acetobutylicum*
pET15b-*crt*	P$_{T7}$-*crt*	*C. acetobutylicum*
pET15b-*bcd-etfBA*	P$_{T7}$-*bcd-etfBA*	*C. acetobutylicum*
pET15b-*bcd*	P$_{T7}$-*bcd*	*C. acetobutylicum*
pET15b-*etfB*	P$_{T7}$-*etfB*	*C. acetobutylicum*

Table 4-1. Continued

Plasmid	Genotype	Notes[a]
pET15b-*etfA*	P_{T7}-*etfA*	*C. acetobutylicum*
pET15b-*etfBA*	P_{T7}-*etfBA*	*C. acetobutylicum*
pET15b-*ccrA1*	P_{T7}-*ccrA1*	*S. avermitilis*
pET15b-*ccrA2*	P_{T7}-*ccrA2*	*S. avermitilis*
pET15b-*bdhA*	P_{T7}-*bdhA*	*C. acetobutylicum*
pET15b-*bdhB*	P_{T7}-*bdhB*	*C. acetobutylicum*
pButanol	P_{trc}-*crt-bcd-etfB-etfA-hbd-adhE2-thlA*	Figure 4-2
pButyrate	P_{trc}-*crt-bcd-etfB-etfA-hbd*-FRT:Kan^R:FRT-*thlA*	Figure 4-3
pTrc99a-*adhE2*	P_{trc}-*adhE2*	Figure 4-4
pTrc99a-*atoB*	P_{trc}- *atoB*	Figure 4-4
pTrc99a-*ccrA-udhA*	P_{trc}-*ccrA-udhA*	Figure 4-4
pAA	P_{trc}-*adhE2* P_{trc}-*atoB*	Figure 4-4
pCBEH	P_{trc}-*crt-bcd-etfB-etfA-hbd*	Figure 4-5
pCBEHCU	P_{trc}-*crt-bcd-etfB-etfA-hbd* P_{trc}-*ccrA-udhA*	Figure 4-5
pCBEHTCB	P_{trc}-*crt-bcd-etfB-etfA-hbd* P_{trc}-*thlA-ccrA-bdhB*	
pAACBEHCU	P_{trc}-*adhE2* P_{trc}-*atoB* P_{trc}-*crt-bcd-etfB-etfA-hbd* P_{trc}-*ccrA-udhA*	Figure 4-5
pUC19-'*focA-pflA*'	'*focA-pflB-pflA*'	Figure 4-6
pUC19-Δ*pflB*-BCS-kan^R	*'focA-crt-bcd-etfB-etfA-hbd-pflA'*	Figure 4-6
pUC19-*adhE*	$adhE^+$	
pUC19-Δ*adhE-bcd-etfBA*-kan^R	Δ*adhE-bcd-etfBA*-kan^R	

[a]The name of the organism in the Notes column indicates the source of the cloned DNA.

Table 4-2. List of PCR primers used in this study.

Primer Name	Vector/Note	Primer Sequence
ndhE F (XhoI)	pET15b	GGAGCCTCGAG**ATG**AACAAGAAGTCTGTTCT
ndhE R (BamHI)	pET15b	CGGCGGATCCTTATGGGAGTGGTCTTGGTG
ndhF F (XhoI)	pET15b	GCCGCTCGAG**ATG**CAGACAAAATTCCTTGA
ndhF R (BamHI)	pET15b	CGGCGATATCGGATCCTTACTCAGCGACGCAAGCC T
pET15b-T7 F (HindIII)	pET15b-*ndhF*	CGGCAAGCTTCCACGATGCGTCCGGCGTAG
pET15b-T7 R (HindIII)	pET15b-*ndhF*	GCCGAAGCTTTTGGTTATGCCGGTACTGCC
ndhE F (NcoI)	pTrc99a	GCGACCATGGAGA*AGGAG*ATATACC**ATG**AACAAG AAGTCTGTTCT
ndhE R (BamHI)	pTrc99a	CGGCGGATCCTTATGGGAGTGGTCTTGGTG
ndhF F (NcoI)	pTrc99a	GCGACCATGGAGA*AGGAG*ATATACC**ATG**CAGACA AAATTCCTTGA
ndhF R (BamHI)	pTrc99a	CGGCGATATCGGATCCTTACTCAGCGACGCAAGCC T
pTrc99a F (XbaI-*trc*)	pTrc99a-*ndhF*	CGGCGTCTAGACGACTGCACGGTGCACCAATG
ndhF R (HindIII)	pTrc99a-*ndhF*	CGCCGAAGCTTTTACTCAGCGACGCAAGCCT
gutHyd F (NdeI)	pET15b	GCAATAACAT**ATG**AAAATTGATTCTTCTTCGTT
gutHyd F (NcoI)	pTrc99a	GCAATAACC**ATG**GAAATTGATTCTTCTTCGTTTT
gutHyd R (BamHI)	pET15b, pTrc99a	GCAATAAGGATCCTTACTTGGTCTTTCGATTCG
gutHyd trc F (Ndel)	pTrc99a-*ndhEF*	GCAATAACAT**ATG**CGACTGCACGGTGCACCAAT
gutHyd R (PflMI)	pTrc99a-*ndhEF*	GCAATAACCATTCGATGGTTACTTGGTCTTTCGATT CG
adhE2 F (XhoI)	pET15B	GCAACTCGAG**ATG**AAAGTTACAAATCAAAA
adhE2 R (BamHI)	pET15B	GCAAGGATCCTTAAAATGATTTTATATAGA
adhE2 F (NdeI)	pET15B	GCAACAT**ATG**AAAGTCACAACAGTAAA
adhE2 R (XhoI)	pET15B	GCAACTCGAGGAAGGTTTAAGGTTGTTTTT
thlA F (XhoI)	pET15B	GCAACTCGAG**ATG**AAAGAAGTTGTAATAGC
thlA R (BamHI)	pET15B	GCAAGGATCCCTAGCACTTTTCTAGCAATA

Table 4-2. Continued

Primer Name	Vector/Note	Primer Sequence
thlB F (XhoI)	pET15B	GCAACTCGAG**ATG**AGAGATGTAGTAATAGT
thlB R (BamHI)	pET15B	GCAAGGATCCTTAGTCTCTTTCAACTACGA
hbd F (XhoI)	pET15B	GCAACTCGAG**ATG**AAAAAGGTATGTGTTAT
hbd R (BamHI)	pET15B; pCBEH	GCAAGGATCCTTATTTTGAATAATCGTAGA
crt F (XhoI)	pET15B	GCAACTCGAG**ATG**GAACTAAACAATGTCAT
crt R (BamHI)	pET15B	GCAAGGATCCCTATCTATTTTTGAAGCCTT
Bcd-etfBA F (XhoI)	pET15B	GCAACTCGAG**ATG**GATTTTAATTTAACAAG
Bcd-etfBA R (BamHI)	pET15B	GCAAGGATCCTTAATTATTAGCAGCTTTAA
Bcd R (BamHI)	pET15B	GCAAGGATCCTTATCTAAAAATTTTTCCTG
EtfB F (XhoI)	pET15B	GCAACTCGAG**ATG**AATATAGTTGTTTGTTT
EtfB R (BamHI)	pET15B	GCAAGGATCCTTAAATATAGTGTTCTTCTT
EtfA F (XhoI)	pET15B	GCAACTCGAG**ATG**AATAAAGCAGATTACAA
ccrA1 F (NdeI)	pET15B	GCAACAT**ATG**AAGGAAATCCTGGACGC
ccrA1 R (BamHI)	pET15B	GCAAGGATCCTCAGATGTTCCGGAAGCGGT
ccrA2 F (NdeI)	pET15B	GCAACAT**ATG**AAGGAAATCCTGGACGC
ccrA2 R (BamHI)	pET15B	GCAAGGATCCTCAGATGTTCCGGAAGCGGT
bdhA F (XhoI)	pET15B	GCAACTCGAG**ATG**CTAAGTTTTGATTATTC
bdhA R (BamHI)	pET15B	GCAAGGATCCTTAATAAGATTTTTTAAATA
bdhB F (XhoI)	pET15B	GCAACTCGAG**GTG**GTTGATTTCGAATATTC
bdhB R (BamHI)	pET15B	GCAAGGATCCTTACACAGATTTTTTGAATA
crt F (NcoI)	pButanol	GATTAGCC**ATG**GAACTAAACAATGTCAT
hbd R (BamHI)	pButanol	CGAATGGATCCTTATTTTGAATAATCGTAGA
adhE2 F (BamHI)	pButanol	TGCATTGGATCCATAAA*GGAG*TGTATATAA**ATG**
adhE2 R (XhoI)	pButanol	GGAAGTCTCGAGTTAAAATGATTTTATATAGA
thlA SD F (XhoI)	pButanol	GGAAGTCTCGAGT*AGGAGGAG*TAAAAC**ATG**AG
thlA R (HindIII)	pButanol	ATTGGTAAGCTTTTAGTCTCTTTCAACTACGA
pKD4 F (BamHI)	pButyrate	GCAATAGGATCCGTGTAGGCTGGAGCTGCTTC
pKD4 R (XhoI)	pButyrate; pUC19-Δ*pflB*-BCS-Kan	GCAATACTCGAGCATATGAATATCCTCCTTAG

Table 4-2. Continued

Primer Name	Vector/Note	Primer Sequence
focA F (HindIII)	pUC19	GCAATAAAGCTTGGTATGTCTGGCAGTATGGATGA GTTATT
pflA R (XmaI)	pUC19	GCAATAACCCGGGCAGCGTGCGGTGGTTGGAAA
focA out (Blunt)	pUC19-Δ*pflB*-BCS-Kan	GTAACACCTACCTTCTTAAGTGGATTT
pflA out (XhoI)	pUC19-Δ*pflB*-BCS-Kan	GCAATACTCGAGTTAGATTTGACTGAAATCGTACA GTA
crt F (Blunt)	pUC19-Δ*pflB*-BCS-Kan	**ATG**GAACTAAACAATGTCATCCTT
crt-hbd F	confirmation of gene insertion	GCAACGCAAGATTTGGTCAA
crt-hbd R	confirmation of gene insertion	GGTGCTTCTGCTACTTCTACA
adhE2-atoB F	confirmation of gene insertion	TGAGCCATCAATAGAACTTT
adhE2-atoB R	confirmation of gene insertion	TGCCAGCCCCAGCGTTTTAT
ccrA2-udhA F	confirmation of gene insertion	CAAGGACGAGACGGAGATGTT
ccrA2-udhA R	confirmation of gene insertion	TGTGGCTGTGCGGTCTGATA
adhE2 F (NcoI)	pTrc99a-*adhE2*	GCAAATGCC**ATG**GAAGTTACAAATCAAAAAGAA
adhE2 R (XmaI)	pTrc99a-*adhE2*	GCAATACCCGGGTTAAAATGATTTTATATAGA
atoB F (KpnI)	pTrc99a-*atoB*	GCAAAGGTACCTAAGAGGAGGAATATAAA**ATG**AA AAATTGT
atoB R (HindIII)	pTrc99a-*atoB*; pTrc99a-*adhE2-atoB*	GCAAAAAGCTTTTAATTCAACCGTTCAATCA
pTrc99a F (XmaI)	pTrc99a-*adhE2-atoB*	GCAATACCCGGGCGACTGCACGGTGCACCAATG
ccrA2 F (NcoI)	pTrc99a-*ccrA-udhA*	GCAATCC**ATG**GAGGAAATCCTGGACGCGATT
ccrA2 R (XbaI)	pTrc99a-*ccrA-udhA*	GCAATTCTAGATCAGATGTTCCGGAAGCGGT
udhA F (XbaI)	pTrc99a-*ccrA-udhA*	GCAATTCTAGAAATAATTTTGTTTAACTTTAAGA*AG GAG*ATATACC**ATG**CCACATTCCTACGATTA
udhA R (HindIII)	pTrc99a-*ccrA-udhA*	GCAATAAGCTTTTAAAACAGGCGGTTTAAAC
pTrc99a F (EagI)	pCBEH	GAATAGCGGCCGCGACTGCACGGTGCACCAAT
hbd R (BamHI)	pET15b; pCBEH	GCAAGGATCCTTATTTTGAATAATCGTAGA
pTrc99a F (BamHI)	pCBEHCU; pCBEHTCB	GCAATGGATCCCGACTGCACGGTGCACCAAT
udhA R (XbaI)	pCBEHCU	GCAACTCTAGATTAAAACAGGCGGTTTAAACCGT

Table 4-2. Continued

Primer Name	Vector/Note	Primer Sequence
thlA F (NcoI)	pTCB	GCAACC**ATG**GAAGAAGTTGTAATAGCTAGT
thlA R (XhoI)	pTCB	GCAACTCGAGCTAGCACTTTTCTAGCAATA
ccrA F (XhoI)	pTCB	GCAACTCGAG*AGAGGA*GGCAAACC**ATG**AAGGAAA TCCTGGACGC
ccrA R (SexAI)	pTCB	GCAAACCTGGTTCAGATGTTCCGGAAGCGGT
bdhB F (SexAI)	pTCB	GCAAAACCAGGTTATTAAG*GAGGA*AGAAATAT**AT G**GTTGATTTCGAATATTCAATACC
bdhB R (SbfI)	pTCB	GCAATGCCTGCAGGTTACACAGATTTTTTGAATA
bdhB R (ClaI)	pCBEHTCB	GCAATCATCGATTTACACAGATTTTTTGAATA
spc F	spectinomycin cassette	CTTTTCTACGGGGTCTGACGCT
spc R	spectinomycin cassette	GCAAGGAACAATTTCTTTCTATTTTC
adhE F (SbfI)	pUC19	GCAATACCTGCAGGTGGCGAAAAGCGATGCTGAA A
adhE R (XmaI)	pUC19	GCAATACCCGGGAGCGTCAGGCAGTGTTGTATCC
pUC19-*adhE* F OUT	pUC19-*adhE*	CTTGTTAAATTAAAATCCATAATGCTCTCCTGATAA TGTT
pUC19-*adhE* R OUT	pUC19-*adhE*	AAGGAGGATATTCATATGCTTCAGTAGCGCTGTCT GGCAA
bcd-etfBA-kan R (homology)	pTrc99a-*bcd-etfBA*	**ATG**GATTTTAATTTAACAAG
bcd-etfBA-kan F (homology)	pTrc99a-*bcd-etfBA*	AGCATATGAATATCCTCCTT
spc-adhE2 F (pKD4 F)	pKD4	ATGACCAATTTGATTAACGGAAAAATACCAAATCA AGCGATTCAAACATTAGTGTAGGCTGGAGCTGCTT C
spc-adhE2 R (pKD4 R)	pKD4	TTAAAATGATTTTATATAGATATCCTTAAGTTCACT TATAAGTGGATACCTCATATGAATATCCTCCTTAGT

Primers were listed with the respective plasmid vector the PCR product was cloned into unless otherwise noted. The underlined sequences represent the endonuclease recognition site indicated by the primer name. Bold sequence represents the ATG translation start site. Italicized sequences represent the Shine-Dalgarno sequence.

Table 4-3. Standard redox potential of electron donor / electron acceptor couple

Redox Couple	E_o' (V)	Reference
MV_{ox} / MV_{red}	-0.440	(128)
Flavodoxin$_{ox}$ / Flavodoxin$_{red}$ (*A. fermentans*)	-0.430	(83, 121, 124, 224)
CO_2 / Formate	-0.420	(128)
H^+ / H_2	-0.420	(128)
Ferredoxin$_{ox}$ / Ferredoxin$_{red}$ (*C. pasteurianum*)	-0.398	(196)
N1a$_{ox}$ / N1a$_{red}$ (*T. thermophilus* NDH)	-0.370	(175)
BV_{ox} / BV_{red}	-0.360	(128)
Ferredoxin$_{ox}$ / Ferredoxin$_{red}$ (*T. vaginalis*)	-0.347	(205, 206)
$NADP^+$ / NADPH	-0.324	(128)
NAD^+ / NADH	-0.320	(128)
Crotonyl-CoA / Butyryl-CoA	-0.010	(128)
Methylene Blue$_{ox}$ / Methylene Blue$_{red}$	+0.011	(128)
DCPIP$_{ox}$ / DCPIP$_{red}$	+0.217	(128)
$Fe(CN)_6^{-3}$ / $Fe(CN)_6^{-4}$	+0.360	(128)
O_2 / H_2O	+0.816	(128)

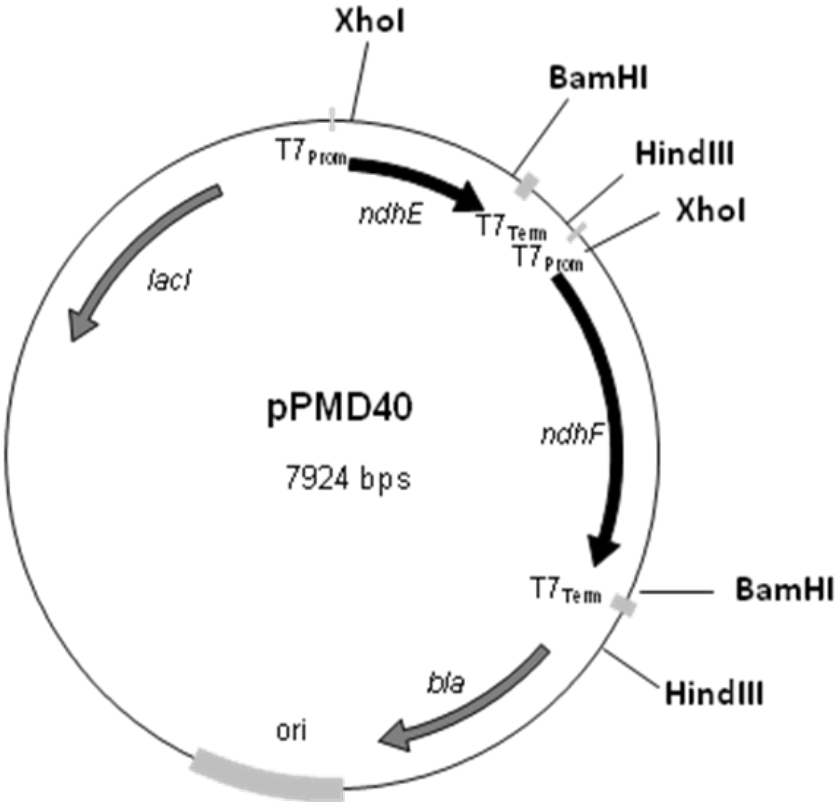

Figure 4-1. *T. vaginalis* NDH T7 expression plasmid.

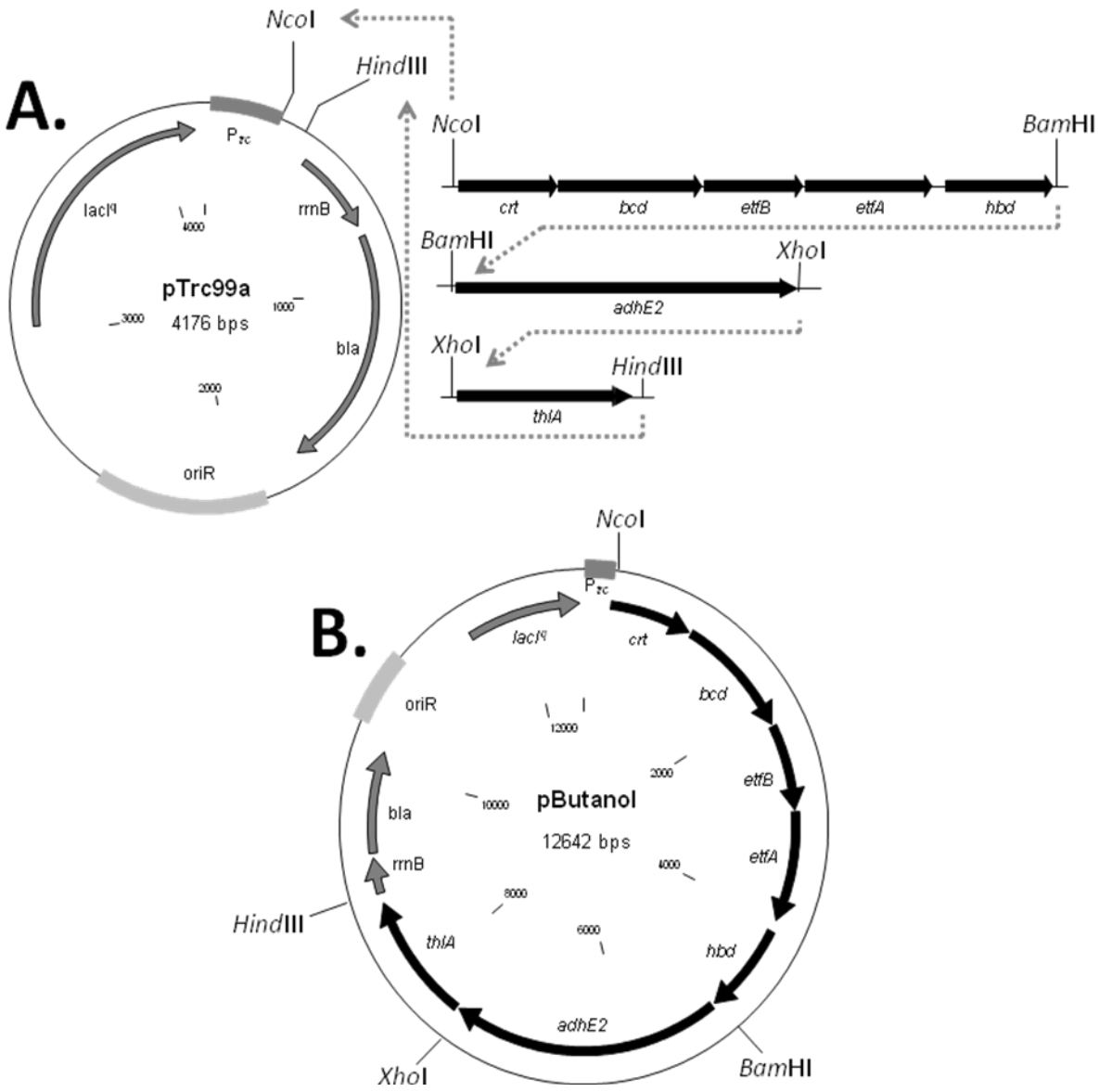

Figure 4-2. Construction of pButanol. A) PCR products used to clone *C. acetobutylicum* BCS operon. B) pButanol. pButanol contains all the genes necessary for production of butanol from acetyl-CoA expressed as a single synthetic polycistronic operon controlled by an IPTG inducible *trc* promoter.

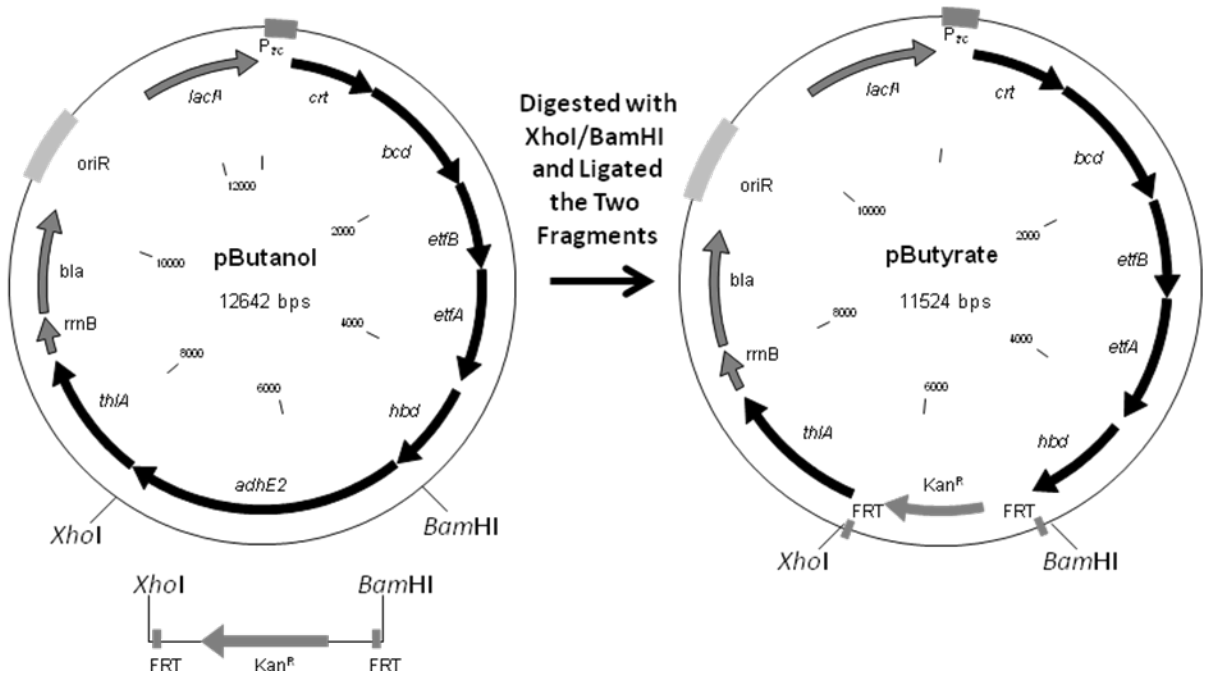

Figure 4-3. Construction of pButyrate. PCR was used to amplify the FRT:Kan^R:FRT cassette from pKD4 with the addition of BamHI and XhoI endonuclease site on the 5' and 3', respectively. The resulting PCR product was cloned into BamHI and XhoI restriction sites of pButanol replacing the *adhE2* gene. The resulting plasmid, pButyrate, has the genes necessary to produce up to butyryl-CoA from acetyl-CoA controlled by an IPTG inducible *trc* promoter.

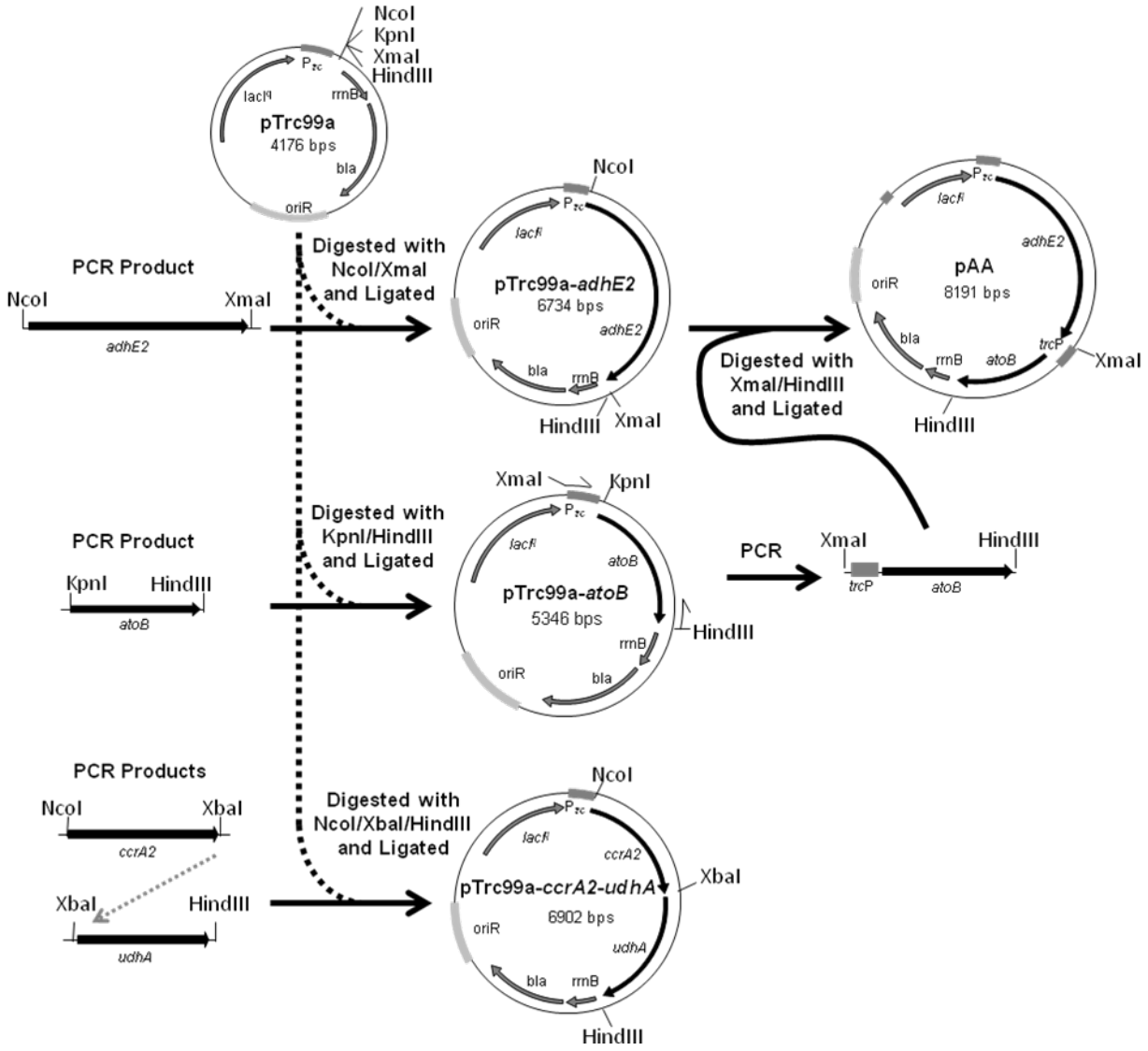

Figure 4-4. Construction of pTrc99a derived plasmids. *C. acetobutylicum adhE2*, *E. coli atoB*, *S. avermitilis ccrA2*, and *E. coli udhA* were cloned into plasmid pTrc99a and expressed from an IPTG inducible *trc* promoter. Clostridial *adhE* was cloned into NcoI and XmaI sites of pTrc99a producing pTrc99a-*adhE2*. *E. coli atoB* was cloned into the KpnI and HindIII sites to pTrc99a resulting in pTrc99a-*atoB*. Using pTrc99a-*atoB* as template, PCR was used to amplify *atoB* including the entire *trc* promoter with XmaI and HindIII on the 5' and 3', respectively. This PCR product was then cloned into XmaI and HindIII site of pTrc99a-*adhE2* producing pAA. The plasmid pAA contains *adhE* and *atoB* which are both independently expressed by tandem *trc* promoters. *S. avermitilis ccrA2*, and *E. coli udhA* were PCR amplified with addition of NcoI and XbaI, and XbaI and HindIII restriction sites respectively. The PCR products were digested with the respective endonucleases and cloned into NcoI and HindIII sites of pTrc99a resulting in pTrc99a-*ccrA2-udhA* which expressed both genes as a single synthetic operon controlled by *trc* promoter.

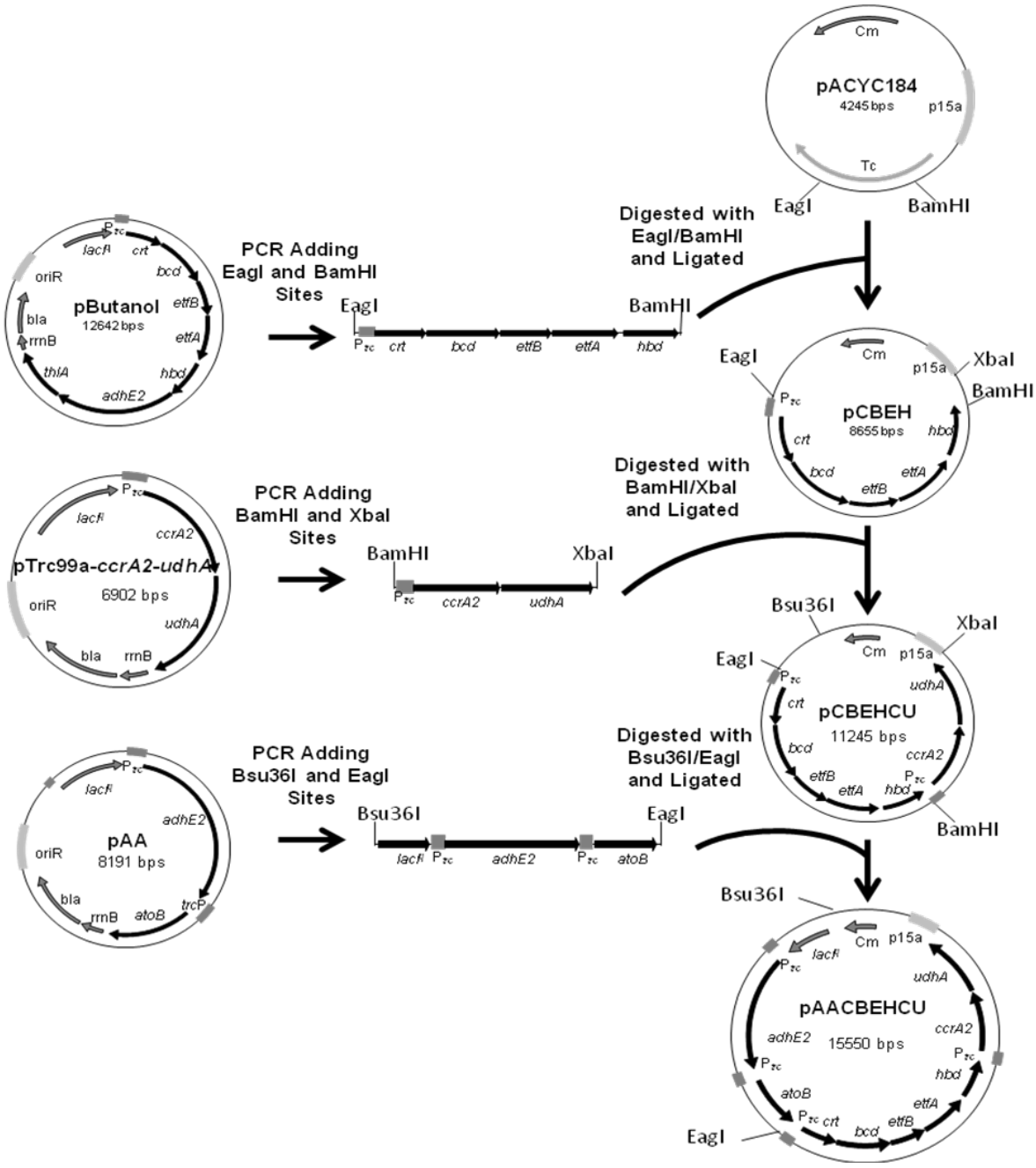

Figure 4-5. Consolidation of butanol pathway genes into a single low-copy vector pACYC184. The BCS operon including *trc* promoter from pButanol was cloned into EagI and BamHI endonuclease restriction sites on pACYC184 producing pCBEH. Using pTrc99a-*ccrA2-udhA* as template, the P_{trc}-*ccrA2-udhA* operon was PCR amplified with the addition of BamHI and XbaI restriction sites and was cloned into the respective endonuclease sites on pCBEH to make pCBEHCU. Using pTrc99a-AA as template, the *lacI*^{q}- P_{trc} -*adhE2*- P_{trc} -*udhA* PCR product with Bsu36I and EagI sites was cloned into the respective endonuclease sites on pCBEHCU to make the final resulting plasmid pAACBEHCU.

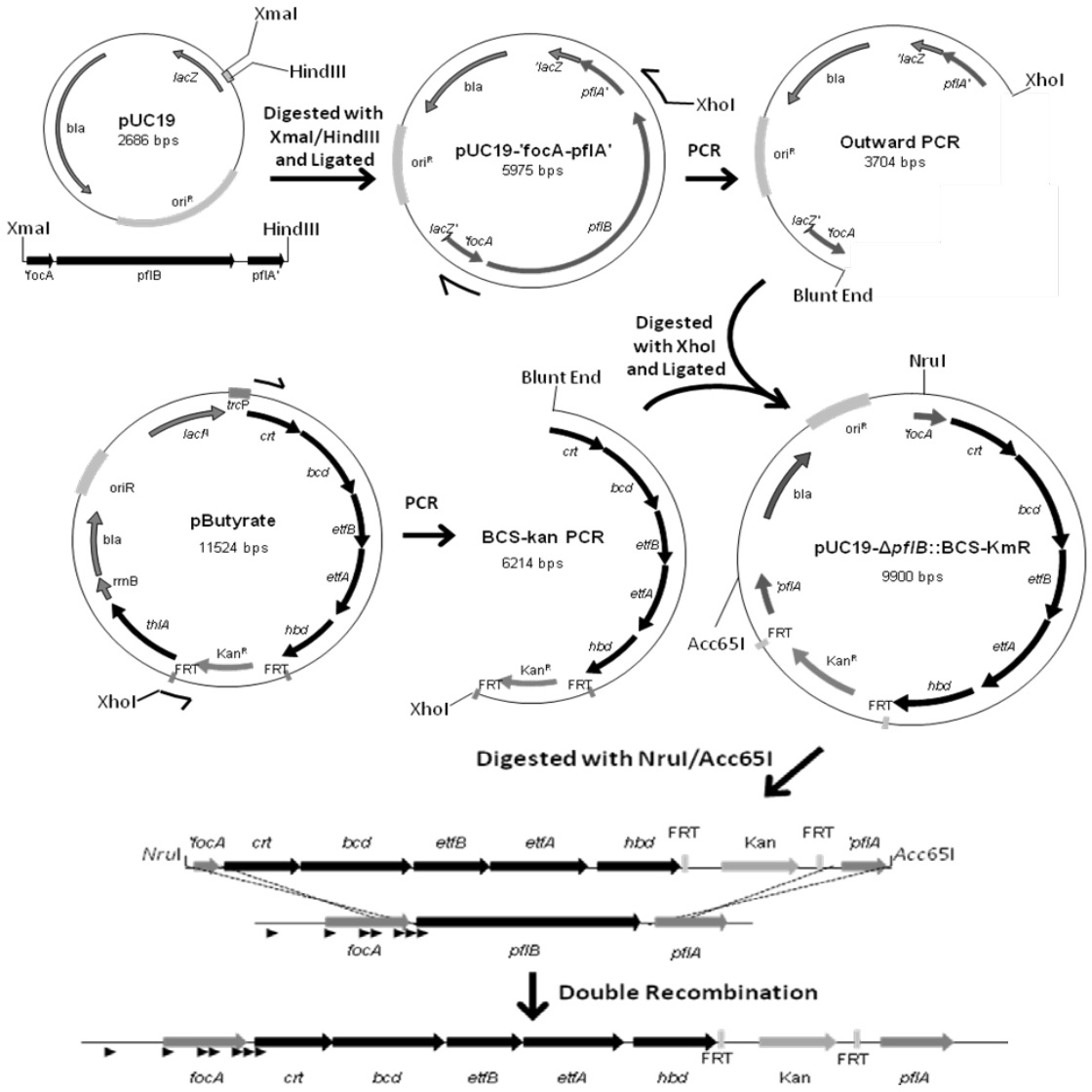

Figure 4-6. Chromosomal insertion of *C. acetobutylicum* BCS operon replacing *E. coli pflB*. *E. coli pflB* including 389 bp and 643 bp upstream and downstream, respectively, was PCR amplified with the addition of HindIII and XmaI restriction sites and was cloned into the respective sites within pUC19. The resulting plasmid, pUC19-'*focA-pflA*', was used as template for outward PCR amplifying everything except *pflB* with an addition of XhoI site near the 5' of *pflA*. PCR was used to amplify the BCS operon and a kanamycin gene cassette from pButyrate with the addition of XhoI site at the 3' end. The two PCR products were ligated together resulting in pUC19-Δ*pflB*-BCS-kan^R. The plasmid, pUC19-Δ*pflB*-BCS-kan^R, was then digested with NruI and Acc65I and the larger DNA fragment (7171 bp) with 312 bp and 643 bp region of homology to the upstream and downstream regions of *pflB* respectively was used to electroplorate into BW25113/pKD46 bearing red recombinase. Kanamycin was used to select for double recombination replacing *pflB* with the entire BCS operon which is now transcriptionally regulated by *pflB* seven promoters (►) upstream of *crt*.

CHAPTER 5
RESULTS AND DISSCUSSION

Biochemical Characterization of Recombinant NADH-Ferredoxin Oxidoreductase (NFOR; NDH) from *Trichomonas vaginalis*[1]

Expression and Purification of NDH

Converting all the energy in glucose to H_2 as a potential fuel using biological systems requires that the energy stored in NADH that is produced during oxidation of glucose carbon to CO_2 be transferred to an appropriate electron carriers such as ferredoxin that can support hydrogenase activity. There are two known NADH-dependent ferredoxin reductases, an NFOR from the hydrogenosomes and a crotonyl-CoA-dependent clostridial reaction. The hydrogenosomal NFOR was chosen as the primary enzyme in an attempt to engineer *E. coli* for higher H_2 yield. In contrast to the hydrogenosomal NFOR, the clostridial enzyme requires the production of crotonyl-CoA in the cell and the end products of glucose fermentation besides H_2 and CO_2 are butyrate and acetate. This reaction, although it could increase the H_2 yield per glucose to 2.7, which is higher than the theoretical maximum of *E. coli*, has no potential to elevate the H_2 yield/glucose to 10 due to loss of glucose carbon as butyrate and acetate. The hydrogenosomal NFOR has the demonstrated ability of transferring the reductant in NADH to ferredoxin (94).

NFOR is the key first step of the NADH dependent hydrogen production pathway in the hydrogenosomes of *T. vaginalis*. NDH from *T. vaginalis* is the only member of the NFOR class of proteins that is capable of oxidizing NADH coupled to the reduction of low potential electron carriers such as ferredoxin. The NDH from *Trichomonas* has not been produced in *E. coli*. As the first step in engineering *E. coli* for high yield H_2 production, the conditions needed for

[1] A portion of the Biochemical Characterization of NFOR (NDH) from *T. vaginalis* was published by Springer Science + Business Media and Copyright Clearance Center's Rightlink. See Appendix A for publication permissions.

production of *Trichomonas* hydrogenosomal NDH in *E. coli* in active form were established by this study. A plasmid that encodes the two subunits of the enzyme, pPMD40, was introduced into strain Rosetta (λDE3) or JM109 (λDE3) bearing plasmid pRARE and the transformants were induced with either IPTG or L-arabinose for production of NDH from tandem T7 promoters.

Expression with IPTG (50 μM) as an inducer supported significant amount of NDH protein synthesis; however, high recombinant protein production rate led to low specific activity of 2.4 U (mg protein)$^{-1}$ (Table 5-1). This value was less than 1 % of the activity of the native NDH isolated from *T. vaginalis* hydrogenosome. In order to produce the protein with specific activity close to that of the native protein, arabinose was used as an inducer for production of T7-polymerase from the *lac* promoter in λDE3. Arabinose is not a known inducer of *lac* promoter; however, a metabolic product of arabinose appears to induce the *lac* promoter at a lower level (147). The low level of induction led to an increase in specific activity to 582 U (mg protein)$^{-1}$ (Table 5-1), a value that is similar to native enzyme values possibly due to an increase in folding efficiencies and/or complete cofactor insertion (94). The protein migrated through the gel filtration column as a heterodimer with a molecular mass of 69,100 (Figure 5-1) and SDS-PAGE (Figure 5-2) revealed that the two subunits corresponding to NdhE (22 kDa) and NdhF (47 kDa).

Enzymatic Activities / Kinetics of NDH

The specific activity of the recombinant enzyme was highest with ferricyanide as the electron acceptor (Table 5-2) consistent with the behavior observed for the native enzyme described by Hrdy *et al.* (94). The specific activity of the enzyme with benzyl viologen as electron acceptor was comparable to that of the value with ferricyanide. The recombinant protein also reduced methyl viologen (about 65 % of the ferricyanide specific activity). The activity of the recombinant protein with methyl viologen as the electron acceptor was

significantly higher than that of the enzyme purified directly from the hydrogenosome. In addition, the enzyme also reduced clostridial ferredoxin. These results show that the recombinant NDH reduces low-potential electron acceptors such as methyl viologen (E_o' of -0.44 V) readily and heterologous ferredoxin.

NDH had an optimal pH of about 7.5 - 8.0 for activity (Figure 5-3). Apparent K_m for NADH for the recombinant enzyme was dependent on the electron acceptor and varied between 0.10 mM with BV and 0.31 mM with ferricyanide (Table 5-3). These values were significantly higher than the 0.021 mM (NADH) reported for the native enzyme with ferricyanide as the electron acceptor (94). The affinity of the recombinant protein to ferricyanide was significantly higher than that of the native protein purified from the hydrogenosome (K_m of 0.06 vs 0.29 mM) (94). The K_m for BV was about threefold higher than that of ferricyanide and the electron acceptor with the highest K_m was methyl viologen. The reaction rate was also highest with ferricyanide as the electron acceptor although the V_{max} with the other two acceptors was similar. These results show that the *T. vaginalis* hydrogenosome NDH produced in *E. coli* is capable of reducing electron acceptors with standard redox potentials that are significantly lower than that of NADH such as methyl viologen.

Iron / Sulfur Determination

The holoenzyme had a spectrum typical of Fe-S proteins with absorbance peaks at 326, 420, 463, and 551 nm (Figure 5-4). Upon reduction with dithionite, the peaks at 420 and 463 nm disappeared, and the absorbance at 551 nm was lower than the protein as purified. Oxidation of the reduced protein by air restored the original spectrum. A spectrum similar to that of the holoenzyme was also obtained with the small subunit NdhE alone that was purified separately (Figure 5-4). These spectra resemble the spectra of the corresponding flavoprotein subcomplex of respiratory NADH dehydrogenase complex I and the 25 kDa subunit of the same complex

from *Paracoccus denitrificans* (225, 226) and also a [2Fe-2S] clostridial hydrogenase N-terminal domain (13). The active NDH had 2.15 non-heme iron and 1.95 acid-labile sulfur atoms per heterodimer. The NdhE protein expressed and purified separately also had Fe and acid-labile sulfur at the same level. These results suggest that the holoenzyme contains a [2Fe-2S] cluster that is located in the small subunit.

The absence of Fe/S in the large subunit of NDH is unique since the NdhF homologs from respiratory chain complex I contain a [4Fe-4S] cluster (154, 225) and the cysteines implicated in liganding the tetranuclear [Fe-S] cluster in these proteins are conserved in the *Trichomonas* protein. The presence of only [2Fe-2S] cluster in the recombinant holoenzyme indicates that the NdhF component lacks the anticipated tetranuclear N3 cluster. In agreement with this, the NdhF protein expressed and purified separately also did not have any detectable Fe and labile S.

This lack of the tetranuclear [Fe-S] cluster in the large subunit could account for the about 15-fold higher K_m for NADH in the recombinant enzyme compared to the native enzyme. However, it is not known whether the native NDH contains the tetranuclear [Fe-S] cluster.

EPR Determination of Iron / Sulfur Clusters

In order to confirm that the binuclear Fe-S cluster was the only Fe-S cluster in the purified NDH, EPR spectra of the protein were obtained. The purified protein did not show an EPR spectrum but reduction with dithionite generated a spectrum that was rhombic in symmetry with g_{xyz} values corresponding to 1.917, 1.951, and 2.009 (Figure 5-5). Although NADH was a substrate for the enzyme, NADH failed to reduce it to an EPR-active form. An EPR signal corresponding to a tetranuclear [Fe-S] cluster N3 (g_{xyz}=1.87, 1.94, and 2.04) found in homologous 54 kDa proteins of the respiratory complex I (225) was not detected in this *Trichomonas* NDH purified from *E. coli*. The NdhE subunit by itself also produced an EPR spectrum that was similar to the holoenzyme upon reduction by dithionite (g_{xyz} = 1.92, 1.953,

and 2.008; Figure 5-6). These EPR spectra support the conclusion that the heterodimeric protein contains only the binuclear [Fe-S] cluster corresponding to N1a in the small subunit of NDH from respiratory complex. It is unlikely that an additional [Fe-S] cluster is present in the holoenzyme that is not reduced by dithionite to a paramagnetic state for detection by EPR since the visible spectrum of the holoenzyme in the 400-500 nm range was completely bleached by dithionite, indicating complete reduction of the [Fe-S] clusters in the protein (Figure 5-4). In addition, the Fe content of the purified protein was only 2 per heterodimer.

Potential Use of NDH for H_2 Production

The hydrogenosomal NADH dehydrogenase is the only known enzyme with a predicted physiological role of coupling NADH oxidation to H_2 evolution that has been purified and biochemically characterized (94). As a first step in our attempt to engineer *E. coli* for production of H_2 at a higher yield, we have developed methods for optimum expression of the protein in an active form in *E. coli*. The purified protein reduced ferredoxin, and it is likely that the NDH reduces ferredoxin *in vivo* also as an intermediate in H_2 evolution pathway. In metabolic engineering of *E. coli* for H_2 production, the other components of the hydrogenosome pathway, ferredoxin, and hydrogenase need to be cloned and expressed in *E. coli*. In the interim, the ability of the NDH to reduce viologen dyes leads to the possibility of using these intermediate electron carriers to couple the recombinant NDH with the native hydrogenase 3 isoenzyme of *E. coli* for H_2 evolution. *E. coli* whole cells as well as isolated membranes are known for their ability to utilize BV or MV as an intermediate electron carrier in coupling dithionite to HYD-3 for H_2 evolution (17, 81, 117, 174) and this reaction could replace the need for ferredoxin and hydrogenase from the hydrogenosome. The [NADH]/[NAD^+] ratio of anaerobic *E. coli* is also significantly higher than that of an aerobically growing *E. coli* (52) and this could lead to a reduction in the *in vivo* midpoint redox potential of the NADH/NAD^+ couple (less than the E_o' of

-0.32 V) to facilitate reduction of viologen dyes by NDH *in vivo*. However, this requires complete removal of O_2 from the fermenting *E. coli* since the reduced viologen dyes react with O_2 to generate superoxide radicals that are detrimental to the cell. An alternate possibility is to engineer the bacterium to be less sensitive to superoxide.

The tetranuclear N3 cluster that plays a critical role in electron transport to ubiquinone (35, 154, 175) in all homologs of the respiratory complex I is absent in the recombinant *T. vaginalis* NDH produced in *E. coli*. This is similar to the observed lack of the tetranuclear N3 cluster in the recombinant *Paracoccus denitrificans* NDH produced in *E. coli* (225). In contrast to the recombinant *T. vaginalis* NDH protein of this study, the recombinant *P. denitrificans* NDH protein also lacked FMN and NADH-dependent enzyme activity. Reconstitution of the recombinant *P. denitrificans* protein with FMN alone (without the N3 cluster but with N1a cluster) only produced about 25 % of the NADH-dependent ferricyanide reduction activity of a complex that was reconstituted with FMN, iron, and sulfur. This raises the possibility that a specific chaperone may be needed for insertion of the N3 cluster in heterologous NDH produced in *E. coli*. The absence of the N3 cluster in the recombinant *T. vaginalis* NDH is not due to high level of expression of the protein in *E. coli* as shown by the presence of N3 cluster in recombinant NuoF subunit of *E. coli* (204). However, it should be noted that the *T. vaginalis* protein produced in *E. coli*, although lacking the N3 cluster, did reduce several electron acceptors at rates that are comparable to the native enzyme isolated from the hydrogenosome (Table 5-2). The reported midpoint redox potential of FMN (-340 mV) in the respiratory complex I (154) may not suggest efficient electron flow from $FMNH_2$ to the N1a cluster of the recombinant *T. vaginalis* NDH. However, the higher [NADH]/[NAD^+] ratio of the anaerobic cell coupled with an increase in the ratio of [$FMNH_2$]/[FMN] may lower the redox potential

sufficiently to facilitate transfer of electrons to the [2Fe-2S] cluster at a midpoint potential of about -0.37 V. With the anticipated physiological role in NADH oxidation to H_2 production in a microbial biocatalyst such as recombinant *E. coli*, the tetranuclear cluster N3, if present in the flavoprotein of the NDH, would drain electrons from NADH to a more oxidized form (-0.25 V) that is not energetically favorable to H_2 production.

NADH-Dependent Hydrogen Production

Reduced Methyl Viologen Coupled to *E. coli* Hydrogenase-3 (HYD3) Isoenzyme

The ability of *T. vaginalis* NDH to reduce low potential electron carriers such as ferredoxin and viologen dyes could play an important role in NADH-dependent hydrogen production. Reduced viologen dyes are known for their ability to serve as intermediate electron carriers coupling dithionite to HYD-3 for H_2 evolution (17, 81, 117, 174); thus, in theory, NDH could couple NADH oxidation to H_2 production in *E. coli* with MV as an intermediate electron carrier.

The use of viologen dyes such as MV or BV could be problematic in growing cultures due to the reactivity of the dyes to oxygen generating superoxide radicals. To remedy this, *E. coli* strain PMD45 was serially transferred in medium with increasing MV concentrations under aerobic growth condition selecting for MV resistance. MV resistance under aerobic conditions often does not translate to MV resistance under anaerobic conditions, probably due to varying levels of expression of superoxide dismutase and catalase under those conditions (53). Strains that were resistant to 1 mM MV were transformed with pTrc99a-*ndhEF* and incubated anaerobically in the presences of 1 mM MV. Strains bearing plasmids encoding NDH were screened for increased ability to reduce MV identified by color change of growth media. Strains bearing *T. vaginalis* NDH reduced more MV than vector plasmid alone; however, there was no significant difference in H_2 evolution (Figure 5-7). Strains with NDH also grew to slightly higher OD probably due to the use of MV as an electron sink. Electron transfer from MV to

HYD3 may be the limiting step in these cultures or the concentration of reduced MV may not be sufficient to drive the reaction to H_2. The use of BV led to BV reduction that was higher than the upper limit of spectrophotometer since BV is a preferred substrate for NDH; however, this higher amount of reduced BV also failed to couple to H_2 production. In fact, BV led to a lower H_2 evolution with NDH than without indicating an electron sink in BV for formate oxidation. Since HYD3 is a membrane associated, multi-subunit complex, the accessibility of reduced viologen dyes to the HYD3 active site maybe a limiting factor in this coupled H_2 evolution reaction. A more accessible soluble [Fe]-hydrogenase may be required for NADH-dependent hydrogen production.

Reduced Methyl Viologen Coupled to [Fe]-Hydrogenase

It is known that the maturation of [Fe]-hydrogenase requires at least three accessory proteins – HydE, HydF, and HydG (37, 113, 164, 171). The genes encoding these proteins are conserved among [Fe]-hydrogenase bearing organisms. The expression of [Fe]-hydrogenase in recombinant bacteria that lack the genes encoding these accessory proteins such as *E. coli* yields inactive [Fe]-hydrogenase polypeptide. Even with over-expression of HydEFG in *E. coli,* the specific activity of [Fe]-hydrogenase was extremely low compared to hydrogenases from the native organism. *In vitro* hydrogen production from NADH using purified *C. acetobutylicum* [Fe]-hydrogenase, NDH, and MV, BV, or *C. acetobutylicum* ferredoxin yielded also extremely low hydrogen. The replacement of NDH and NADH with dithionite supported detectable levels of H_2 indicating that the hydrogenase was not irreversibly inactivated during the assay. Further examination of the two enzymes in this coupled reaction revealed that clostridial hydrogenase as well as many others had an optimal pH around 6.0 for H_2 evolution (1, 2, 58, 73, 93) and an optimal pH of 8 – 10 for H_2 oxidation/uptake (1, 2, 73, 93); whereas, *T. vaginalis* NDH optimal

pH was about 7.5 – 8.0 for NADH oxidation (Figure 5-3). The pH incompatibilities of the two systems may contribute to the very low H_2 evolution.

One possible substitution for clostridial [Fe]-hydrogenase could be a [Fe]-hydrogenase and ferredoxin from *T. vaginalis* that would reconstitute the native NADH-H_2 pathway in *E. coli*. An alternative set of components could be the proteins from another hydrogenosomal protozoan *Pseudotrichonympha grassii* from digestive hindgut of the termite *Coptotermes formosanus* (99). According to Inoue *et al.*, a non-hydrogen producing strain of *E. coli* expressing only the [Fe]-hydrogenase structural gene, *hydA*, from *P. grassii* (without the accessory maturation proteins) evolved hydrogen indicating that this hydrogenase can be activated by *E. coli* proteins. Purified recombinant *P. grassii* [Fe]-hydrogenase from *E. coli* was about 30 times more active than recombinant clostridial [Fe]-hydrogenase with HydEFG (99, 113). Furthermore, protozoan hydrogenase has an optimal pH of 8.0 that is compatible with *T. vaginalis* NDH.

Reticulitermes flavipes, is a native species of the State of Florida and is in the same family of subterranean termites, *Rhinotermitidae*, such as *C. formosanus*. Of the entire cDNA library of this termite gut symbiont, five genes in the expressed sequence tags (EST) were annotated as possible [Fe]-hydrogenase by Dr. Scharf and his colleagues who kindly provided these DNA for this study. One [Fe]-hydrogenase in particular had an E_{value} of 4×10^{-174} with 67 % identity and 81 % overall similarity to [Fe]-hydrogenase to *P. grassii* (Figure 5-8). This hydrogenase sequence also had high similarity to *T. vaginalis* HydA ($E_{value} = 1 \times 10^{-127}$) and to a lesser extent to *C. acetobutylicum* ($E_{value} = 3 \times 10^{-88}$). The high homology to *P. grassii* hydrogenase as well as others makes this hydrogenase a good candidate to further examine its potential to couple NADH oxidation to hydrogen evolution.

The ORF encoding the unknown symbiont [Fe]-hydrogenase without hydrogenosomal N-terminal signal peptide (first 28 amino acids), referred to here as *gutHyd*, was cloned into plasmid pET15b as well as plasmid pTrc99a for expression in T7 and non-T7 (*trc*) *E. coli* expression systems, respectively. The truncated gene *gutHyd* was designed in accordance to truncated *P. grassii* [Fe]-hydrogenase (09A82) described by Inoue *et al*. (99). Non-hydrogen-producing strains BL21 (λDE3) and PMD45 bearing pET15b-*gutHyd* and pTrc99a-*gutHyd*, respectively, failed to evolve H_2.

To rule out that the failure of these recombinant *E. coli* strains to produce hydrogen was due to inactive enzyme and not from the inability of the cell to supply reductant, *gutHyd,* under control of *trc* promoter, was subcloned from pTrc99a-*gutHyd* into pTrc99a-*ndhEF* resulting in plasmid pTrc99a-*ndhEF-gutHyd*. For expression, pTrc99a-*ndhEF-gutHyd* was transformed into PMD45. Strain PMD45 could not grow anaerobically due to the inability to reoxidize NADH. Plasmid with *ndhEF* and *gutHyd* did not restore anaerobic growth; however, this plasmid did increase slightly hydrogen production over strains carrying plasmid vector (Figure 5-9). The fermentation profile of the cultures indicated that the difference in H_2 evolution between the NDH/GutHyd and vector was probably due to the formate hydrogen-lyase (Figure 5-10).

Thermodynamic Barrier

PMD45 could not grow anaerobically because of its inability to oxidize NADH during fermentation. The expression of NDH and GutHyd did not alleviate the imbalance in redox state. Ideally, if the activities of NDH and GutHyd using MV as an intermediate electron carrier, created an alternate electron pathway, NADH produced during glycolysis would be oxidized to H_2 enabling growth to proceed. Its inability to do so maybe because of the thermodynamics of H_2 (-0.42 V) production from NADH (-0.32 V). The free energy for this reaction could be calculated using Equation 4-3. Using *n* equals 2 (number of electrons transferred from NADH to

$2H^+$ to make H_2), *F* (Faraday's constant) equals 96,500 C mol^{-1} and the standard redox potential E_o' of -0.42 V and -0.32 V for H_2 and NADH, respectively, the free energy for this reaction could be calculated as follows (Equation 5-1):

$$\Delta G = -(2)(96{,}500)(-0.42\ V - (-0.32\ V)) \quad (5\text{-}1)$$
$$\Delta G = +19300\ J\ mol^{-1} = +19.3\ kJ\ mol^{-1} = +4.62\ kcal\ mol^{-1}$$

The production of H_2 from NADH is an endothermic reaction requiring +4.62 kcal mol^{-1} of energy for the reaction to proceed. Internal ratios of $[NAD^+]/[NADH]$ could effect its redox potential. The internal $[NAD^+]/[NADH]$ ratio differs depending on availability of oxygen or external electron acceptors. Internal $[NAD^+]/[NADH]$ ratios had been previously determined to range between 10.6 aerobically and between 1.0 to 4.5 anaerobically where strains with a ratio of 1.00 carry mutations in global regulators such as ArcA and Fnr which is known to increase NADH levels (3, 122, 123). Internal potential (E) of $[NAD^+]/[NADH]$ in anaerobically growing cells could be calculated using the simplified Nernst equation previously described in Equation 4-2. Using wild-type *E. coli* strain DC271 anaerobic NAD^+/NADH ratio of 4.5 (122), the Nernst equation could be solved as follows (Equation 5-2):

$$E = -0.320\ V + (0.0596/2) \log(4.5) \quad (5\text{-}2)$$
$$E = -0.301\ V$$

With appropriate mutations in ArcA and Fnr, $[NAD^+]/[NADH]$ ratios had been demonstrated to reach a low as 1.0 (3, 123), bringing E to its midpoint potential of -0.32 V. A $[NAD^+]/[NADH]$ ratio of lower than 1.0 shifts the redox potential to a more negative value closer to that of H_2. For example, if the $[NAD^+]/[NADH]$ ratio was 0.1, then the redox potential shifts to -0.35 V and then the ΔG would lower to +3.23 kcal mol^{-1} from the +4.62 kcal mol^{-1} standard. In order for the reaction to be spontaneous, there must be a negative (-) ΔG value or more specifically, $E_{(NAD+/NADH)}$ must be more negative than $E_{(H+/H2)}$. To calculate the

$[NAD^+]/[NADH]$ ratio that is minimally required for a thermodynamic equilibrium reaction of NADH to H_2, the Nernst equation could be setup as follows (Equation 5-3):

$$E_o'_{(H+/H2)} > E_o'_{(NAD/NADH)} + 0.0296 \log([NAD^+]/[NADH]) \quad (5\text{-}3)$$

$$-0.420\ V > -0.320\ V + 0.0296 \log([NAD^+]/[NADH])$$

$$-3.378\ V > \log([NAD^+]/[NADH])$$

$$4.184 \times 10^{-4} > [NAD^+]/[NADH]$$

$$2390 > [NADH]/[NAD^+]$$

To reach an internal redox potential of -0.42V for the NAD^+/NADH couple, the same as the hydrogen electrode potential at pH 7.0, the NADH concentration in the cell should be at least 2,390 fold higher than the NAD^+ concentration. Of course, this ratio should be even higher for the reaction from NADH to H_2 to be thermodynamically favorable. Although MV was readily reduced by NDH *in vitro*, the reduced MV concentration of an anaerobic bacterial cell suspension was only 60 μM in the presence of 1 mM total MV added to the culture. It appears that NDH can only generate an *in vivo* ratio of $[MV_{red}]/[MV_{oxi}]$ of 0.06 using NADH as the electron donor and this ratio may not be high enough to drive the electrons to hydrogen. The 1 mM MV is at least 2-times higher than the NDH K_m value of 0.44 mM for this substrate (Table 5-3) and thus may not be limiting as a substrate. With the assumption that the external concentrations of oxidized and reduced MV represent the internal concentrations of these two, the calculated redox potential for the MV couple in this culture is -0.404 V. The intracellular ratio of reduced vs oxidized MV needs to be at least 5-times higher than the observed value for thermodynamically favorable coupling of reduced MV to H_2 production. This is in agreement with the ease with which MV that is reduced by dithionite donates electrons to HYD3 for H_2 evolution.

An alternate way of coupling NADH to H_2 production with the same components, NDH, MV and HYD3, would be to increase the internal redox potential of the H^+/H_2 couple by rapidly

removing the H_2 produced by the hydrogenase by sparging with N_2. Lowering the partial pressure of dissolved H_2 had been demonstrated to increase hydrogen production by lowering product inhibition (129, 132, 201). The amount of dissolved H_2 in aqueous solution saturates at about 1.4 mg L^{-1} (700 μM) at 37°C (18, 49). Given the $[H^+]$ at pH 7.0 is 1 x 10^{-7} or 0.1 μM, the redox potential of $[H^+]/[H_2]$ in water at pH 7.0 is -0.534 V with H_2 saturation. By lowering the dissolved $[H_2]$ at pH 7.0 or at pH 6.0 to 2.0 nM, or 200 nM, respectively, the redox potential will shift to -0.37 V, the reported redox potential of N1a cluster of NDH homologs. With these conditions, the use of recombinant NDH and MV may be favorable for H_2 production. This would indeed lead to a highly dilute H_2 gas stream and may not be an economical H_2 fermentation process.

The results presented in this section show that the hydrogenosomal NDH can couple to *E. coli* HYD3 with MV as an intermediate electron carrier but at a very low rate. Replacing the native HYD3 and MV with *Trichomonas* ferredoxin and [Fe]-hydrogenase may not be able to overcome some of the constraints discussed above. It is possible that in the *Trichomonas* hydrogenosome the various components of the NADH to H_2 pathway are compartmentalized and the H_2 is rapidly removed from the microenvironment of hydrogenosome to support this reaction. Such a compartmentalization of the components, substrates and products may not be achievable in a bacterial cell for cost-effective conversion of glucose to H_2 at high yield without energy input either in the form of electricity, sun light, etc.

Due to the constraints on H_2 production by dark fermentation discussed above, the potential of engineering *E. coli* for the production of the other alternate next generation biofuel, butanol was evaluated.

Production of 1-Butanol by Recombinant *E. coli*

Another potential next generation biofuel is butanol. Butanol is produced by several clostridia during later stages of growth and fermentation. However, due to the need to maintain redox balance, acetone and ethanol are also co-produced with butanol. In this section, I am presenting my studies aimed at transferring the genes encoding the enzymes that constitute the butanol pathway in *C. acetobutylicum* into *E. coli* to identify the critical rate-limiting steps in the butanol pathway towards producing butanol as the sole fermentation product. In addition, I also evaluated potential alternate choices in both enzymes and strains to overcome these rate-limiting steps.

In Vitro Production of Butanol from Acetyl-CoA Using Recombinant Proteins

E. coli, like *C. acetobutylicum*, has a natural ability to produce two moles acetyl-CoA from one mole glucose. In order to produce butanol in *E. coli*, the rest of the butanol fermentation pathway must be introduced from *C. acetobutylicum*. The first step is to assess if *E. coli* is capable of producing the enzymes in the clostridial butanol pathway in active form. To do so, all the enzymes that catalyze each reaction from acetyl-CoA to butanol were cloned into plasmid pET15b and expressed from T7 promoter in *E. coli*. The enzymes were purified to homogeneity and assayed for activity (Table 5-4).

Of the two clostridial thiolases, ThlA appears to have higher activity than ThlB when expressed in recombinant *E. coli*. Since it is believed that ThlA is the main thiolase in *C. acetobutylicum* for the condensation of acetyl-CoA (217), this is in agreement with the higher activity of ThlA. Recombinant Hbd had a significantly higher specific activity compared to ThlA and this is similar to Hbd purified from *C. beijerinckii* (47). Crt activity was determined to be the highest of all the enzymes of this pathway. The reduction of crotonyl-CoA to butyryl-CoA was catalyzed by Bcd/EtfBA complex in clostridial systems. Purified recombinant

Bcd/EtfBA enzyme complex had no detectable activity although Bcd activity in recombinant *E. coli* crude extract has been previously reported (12, 32, 100). It should be pointed that an active Bcd enzyme complex from *E. coli* has yet to be purified. To overcome this limitation, the *S. avermitilis* gene encoding CcrA was cloned and the protein was purified. The CcrA protein catalyzes the same reaction as Bcd/EtfBA except it uses NADPH instead of NADH (211). The specific activity of the recombinant CcrA was twice of the reported value of the native enzyme from *Streptomyces collinus* probably due to the difference in species (Table 5-4) (211). The last two steps of the pathway could be catalyzed by both Aad and AdhE2; however, only AdhE2 seems to have detectable activity for butyraldehyde to butanol. Fontaine *et al.* also purified an active recombinant AdhE2 from *E. coli* with similar activities (67).

Since all the predicted enzymes that catalyze the production of butanol from acetyl-CoA were produced in *E. coli* in an active form, the next step was to determine if these enzymes could constitute the butanol pathway *in vitro*. One unit (μmole min^{-1}) of each enzyme (ThlA, Hbd, Crt, CcrA, and AdhE2) in the presence of 5 mM acetyl-CoA, 10 mM NADH, and 10 mM NADPH catalyzed the sequential reactions from acetyl-CoA to butanol (Figure 5-11 and 5-12). The butanol concentration of 0.5 mM in this experiment represented about 20 % of the acetyl-CoA added as the starting substrate. In addition, other intermediates of the pathway were also detected, although at significantly lower levels.

This experiment clearly shows that the minimal set of enzymes needed for conversion of acetyl-CoA to butanol can be produced in *E. coli* in active form. It should be pointed out that the clostridial butyryl-CoA dehydrogenase (Bcd) complex was replaced in this *in vitro* pathway by the crotonyl-CoA reductase (CcrA) from *S. avermitilis* (Figure 5-12). Although both enzymes catalyze the reduction of crotonyl-CoA to butyryl-CoA, the clostridial Bcd has additional

substrate requirements in addition to NADH and crotonyl-CoA for catalysis. These are ferredoxin and soluble Fe-hydrogenase which would also need to be produced as active proteins in recombinant *E. coli*. As I presented in the previous section, production of active Fe-hydrogenase in *E. coli* is still a work in progress. Although Bcd complex utilized NADH as an electron donor *in vitro*, the actual electron donor *in vivo* is yet to be established. Coupling these enzymes with appropriate substrates, acetyl-CoA, NADH, and NADPH, is expected to support butanol biosynthesis *in vivo* in *E. coli*.

Plasmid Expression of Butanol Pathway

The detection of active recombinant enzymes that catalyzed the production of butanol from acetyl-CoA *in vitro* was instrumental for designing an *in vivo* butanol pathway. Assuming that enzyme activity was not lost during the purification process, if all the genes were expressed at a 1:1 ratio to each other, there will be severe bottlenecks in the later steps of the pathway (Figure 5-12). Higher levels of Bcd/EtfBA or CcrA and AdhE2 activities will be needed to increase flux through the pathway since these appear to be rate limiting steps. Also, higher thiolase activity may be needed to direct acetyl-CoA to this pathway and away from the alcohol dehydrogenase (ethanol production) activity of AdhE2 since no alcohol dehydrogenase that is specific for butyryl-CoA to butanol has been reported. All alcohol dehydrogenase enzymes that reduce butyryl-CoA also reduce acetyl-CoA to ethanol. During normal fermentative growth, NADPH-dependent CcrA cannot overcome this Bcd/EtfBA step due to a limitation of NADPH in the anaerobic *E. coli*. Previous attempts to utilize CcrA as a substitute for Bcd/EtfBA resulted in little to no butanol produced (12, 100).

The first plasmid constructed for butanol production, pButanol, had *crt*, *bcd*, *etfB*, *etfA*, *hbd*, *adhE2*, and *thlA* arranged in that respective order in a single operon controlled by an IPTG inducible *trc* promoter upstream of *crt*. Production of butanol by *E. coli* with pButanol plasmid

appeared to be strain dependent. Wild-type W3110 did not produce any detectable butanol. Since Inui *et al.* used JM109 for butanol production, strain JM107, a *recA*$^+$ parent strain of JM109, was tested for its ability to produce butanol with plasmid pButanol (100). JM107 bearing pButanol produced 0.20 ± 0.11 mM butanol with all fermentation pathways intact. Since all the genes were transcribed from a single promoter, differential translation efficiencies of the various genes in the multicistronic mRNA maybe the cause of low yields. A new expression system was constructed to optimize transcription.

To increase plasmid stability, all the genes were subcloned into a low copy vector pACYC184 with p15a origin of replication that is compatible with ColE1 plasmids. Instead of one *trc* promoter controlling transcription, the genes encoding enzymes with lower specific activities (*thlA*, *ccrA*, *bdhB*) were transcribed from their own tandem *trc* promoter. The gene *bdhB* was included in this construct instead of *adhE2* because previous reports indicated that it was functionally expressed in *E. coli* and BdhB had lower affinity to acetyl-CoA than AdhE2 (67, 144, 212). Strain JM107 bearing the new construct, pCBEHTCB, did not produce butanol. To determine the metabolic rate-limiting step in JM107 (pCBEHTCB), crude extract was tested for activity of each of the enzyme encoded in the plasmid (Table 5-5). Enzyme assays revealed the absence of BdhB activity and lower than expected CcrA and ThlA activities. Since butyrate was also not detected in JM107 (pCBEHTCB) fermentations, the rate-limiting reaction was probably the first step, ThlA activity. Higher thiolase activity may be needed to increase flux through the butanol pathway and away from ethanol production.

The plasmid pAA was constructed to increase AdhE2 and thiolase levels in the cell. Both *adhE2* and *E. coli* thiolase, *atoB*, were expressed from independent *trc* promoters. JM107 (pAA) produced significantly higher levels of both enzymes upon induction with IPTG especially for

AtoB (Table 5-6). The higher thiolase activity is expected to therefore increase carbon flux through butanol pathway, and away from the competing pathways to ethanol and acetic acid.

Based on this information, the plasmid pCBEHTCB was revised by removing the two genes with low or no activity (*thlA* and *bdhB*) and adding *udhA* (*sthA*) since previous studies had demonstrated an increase in NADPH level by over expression of this soluble trans-hydrogenase (172). JM107 bearing this construct, pCBEHCU, and pAA produced 0.21 ± 0.02 mM butanol and the crude extract had similar enzyme activities as detected in Table 5-5 and Table 5-6.

Low butanol yield could be attributed to the presence of intact native fermentation pathways in JM107 that divert carbon and reductant away from butanol pathway. To improve butanol yield, various native fermentation pathway enzymes were deleted in both W3110 and JM107 (Table 5-7). JM107 derivatives were inherently better at producing butanol than W3110 based strains. The highest butanol detected was 1.90 ± 0.06 mM from PMD50 (JM107Δ*ldhA*). PMD52 (JM107 Δ*ldhA* Δ*pflB* with *lpd101**) mutation reduced butanol production to 0.92 mM. Mutation in *lpd101** was expected to increase NADH yield to 4 per glucose; thus, theoretically increasing butanol yield by supplying all the required reducing equivalents. However, in the case of JM107, its incorporation in addition to a deletion in *pflB* reduced butanol production by 50 %. The highest value obtained thus far was still about half of the value reported by Atsumi *et al.* (12).

The observed strain-dependent variation in butanol yield led to an *E. coli* C based strain, in particular, an evolved strain developed for succinate production (103). Bcd/EtfBA activity in *E. coli* could perhaps be increased by using succinate producing strains. Succinate is produced by the reduction of fumarate by fumarate reductase coupled to the oxidation of an unknown electron carrier. *E. coli* strain KJ104 (103) produces near theoretical yields of succinate producing up to

1.30 mol succinate per mol glucose. This high succinate production raises the possibility that a unique electron-transport pathway was elevated to reduce fumarate reductase. Since fumarate reductase is a flavoprotein with its own unique electron carriers that reduces C=C bond in fumarate to succinate, it is possible that the same electron transport components feeding electrons to fumarate reductase could provide the needed reductant to Bcd complex, another flavoprotein that also reduces a C=C bond in crotonyl-CoA to butyryl-CoA. The succinate-production strain, KJ104, has either elevated this unique electron transport pathway to fumarate reductase or adapted other components of the cell to support high carbon flux through fumarate reductase. In this study, I tested if this high flux through fumarate reductase could be adapted to support carbon flux through the rate-limiting step at the Bcd complex in butanol production.

Chromosomal Insertion of Butanol Pathway into *E. coli*

Traditional directed evolution of *E. coli* which has been proved to be very successful at increasing fermentation yield (43, 103, 104, 111, 135, 227, 231, 235) could not be employed in this situation due to plasmid stability and plasmid retention. Chromosomal insertion of butanol pathway genes may be necessary for evolution of these strains for production of butanol. Plasmid pAACBEHCU was constructed by combining pCBEHCU and pAA into a single larger plasmid. The origin of replication and chloramphenicol resistance gene were replaced with spectinomycin resistance. Single recombination of the entire plasmid lacking the replicon was selected for by spectinomycin resistance and chromosomal insertion of *spc*^{R}-P$_{trc}$-*adhE2*-P$_{trc}$-*atoB*-P$_{trc}$-*crt-bcd-etfBA-hbd*-P$_{trc}$-*ccrA-udhA* and the strain was designated as *but*$^{+}$. Chromosomal insertion of the full plasmid was confirmed by PCR. The site for chromosomal integration is yet to be determined; however, possible recombination sites were *atoB, udhA,* and *lacI* since these were *E. coli* genes. JM107 Δ*ldhA* with *but*$^{+}$ (PMD70) insertion did not produce butanol or butyrate (Table 5-8). Succinate producer KJ104 withΔ *frdBC* and *but*$^{+}$ (PMD72) insert also

yielded similar results. The addition of pCBEHCU alone without pAA as a plasmid into these strains supported butanol production with yields of 0.30 ± 0.02 mM suggesting that this strain may have ample thiolase and butanol dehydrogenase activity and the rate-limiting reaction may be the reduction of crotonyl-CoA to butyryl-CoA. PMD70 bearing pButyrate (pButanol without *adhE2*) was able to produce 1.10 ± 0.05 mM butanol and 1.22 ± 0.02 mM butyrate. Since the strain without plasmid did not produce butyrate and the plasmid supplementation supported production of butyrate as well as butanol, the rate limited step may be Bcd/EtfBA and the genes expressed in trans from a low copy plasmid were able to overcome the low activity of the *but*$^+$ insert.

A second chromosomal insertion was made to remedy the poor butanol yield of *but*$^+$ strains. The BCS operon was inserted in the chromosome replacing *pflB* which places the entire operon under the control of *pflB* native promoters. By replacing/deleting *pflB* in addition to Δ*ldhA*, these strains are no longer capable of growing anaerobically. Micro-aerobic conditions that support PDH activity to produce acetyl-CoA were needed to assess the fermentation profiles. Strain PMD73 produced 0.16 mM butanol without plasmids (Table 5-9). PMD74 had a slightly higher flux through the pathway producing 0.31 mM butyrate and about 0.10 mM butanol. The inability of the cell to convert all butyrate to butanol could be because of an inadequate supply of NADH to complete the reduction of butyryl-CoA to butanol. Another possible reason could be an insufficient activity of AdhE2 which was part of the initial *but*$^+$ insert. The key to increasing butanol production is apparently to increase flux through the rate limiting Bcd/EtfBA reaction.

The most direct way to increase flux through Bcd/EtfBA was to initially focus on the production of butyrate not butanol since butanol production requires additional NADH that requires further engineering. The production of butyrate requires 2 reducing equivalents which

were readily supplied by glycolysis. In addition, increasing AdhE2 level may compete with thiolase for acetyl-CoA with production of ethanol as a co-product. Since PMD74 has the highest flux and the lowest co-production of other fermentation products, it will be used as the base strain for further genetic manipulations.

By deleting *adhE2* from the original *but*$^{+}$ insert, no butanol and only trace amounts of ethanol were produced. The new strains still lacked the ability to grow anaerobically and had no significant increase in butyrate production. pTrc99a based plasmids encoding enzymes of butyrate production pathway were inserted into these strains (Table 5-10). Plasmids pTrc99a-*atoB* and pTrc99a-*ccrA-udhA* had minimal effect on butyrate production. Plasmids pTrc99a-*bcd/etfBA* and pButyrate increased butyrate yield from 0.20 ± 0.07 mM butyrate to 3.08 ± 0.21 mM to 2.47 ± 0.10 mM butyrate, respectively. By increasing Bcd/EtfBA levels, the flux to butyrate correspondingly increased. The effect of Bcd/EtfBA analogue, CcrA, was insignificant on butyrate production probably due to low NADPH pools which negates any positive effect of CcrA's higher activity. These results confirm that Bcd/EtfBA activity needs to be elevated in order to increase butyrate production.

Additional Insertion of *bcd-etfBA* Transcriptionally Controlled by *E. coli adhE* Promoter

Low butyrate yields could be the result of inadequate activity of chromosomally expressed Bcd/EtfBA. To overcome the low activity, a third copy of *bcd-etfBA* was inserted into the chromosome replacing *E. coli adhE* similar to that of the previously described chromosomal insertion replacing *pflB*. Since *adhE* had higher promoter activity under anaerobic condition, the additional *adhE* promoter fusion is expected to increase overall Bcd/EtfBA activity in the cell.

The third *bcd-etfBA* insertion into *adhE* promoter led to an increase in butyrate production to 2.0 ± 0.50 mM under micro-aerobic fermentation condition. To further analyze these cultures, pH controlled fleaker fermentations were used to examine growth characteristics. Cultures of

PMD76 were inoculated into 1 % glucose minimal medium with an initial pH of 7.0 (Figure 5-13). pH controllers with set values of 7.0, 6.5, 6.0, and 5.0 were used to prevent pH from decreasing below the respective set values. Two different phases of growth were observed with cultures set to a minimum pH of 7.0 or 6.5. After the initial phase in which all four cultures grew at about the same level, the pH 7.0 and 6.5 cultures grew to a higher cell density. During the initial growth phase, pyruvate was accumulated by the cultures and it was consumed by the two cultures during the second phase of growth. The other two cultures with a set minimum pH of 5.0 and 6.0 continued to accumulate pyruvate and butyric acid. Accumulation of pyruvic acid by these cultures suggests that even with oxygen provided by mixing the cultures in air, acetyl-CoA that is required to drive the butyrate pathway is limiting in this *pfl* mutant. This requires reintroduction of PFL activity or increasing the PDH activity with the *lpd101** mutation to enhance the PDH activity of the anaerobic culture before attempting to overcome other rate-limiting steps in this pathway. Further metabolic engineering coupled with long-term metabolic evolution is apparently required to overcome the rate-limiting step(s) by activating native *E. coli* genes to channel glucose carbon to butyric acid followed by redirection of the butyryl-CoA to butanol.

Table 5-1. Purification of recombinant NDH produced in *E. coli* with IPTG or arabinose as an inducer.

Induction	Sample	Total [Protein]	Total Activity[a]	Sp. Activity[b]	Purification Fold	Yield %
IPTG	Crude extract	63.83	16.0	0.25	1.00	100.0 %
	Ni-affinity	5.76	4.9	0.85	3.40	30.7 %
	Gel filtration	2.21	5.4	2.4	9.72	33.7 %
Arabinose	Crude extract	157.76	506	3.21	1.00	100.0 %
	Ni-affinity	2.32	501	216	67.4	99.1 %
	Gel filtration	0.72	419	582	181	82.8 %

Activity was determined using 50 mM K-PO_4 buffer pH 7.5, 5 mM benzylviologen (BV), and 1 mM NADH, under anaerobic condition. The reaction was monitored at 600nm (BV reduction) and the activity as calculated from the initial rate of reaction.

[a] Total activity: μmole min^{-1}

[b] Sp. Activity: μmole min^{-1} (mg protein)$^{-1}$

Table 5-2. Specific activity of recombinant *T. vaginalis* hydrogenosome NDH produced in *E. coli* with arabinose as inducer

Electron acceptor	Specific activity (μmole min^{-1} mg $protein^{-1}$)	
	Arabinose-induced	Native[a]
Ferricyanide	604 ± 24	690
Benzyl viologen	582 ± 44	ND
Methyl viologen	392 ± 19	262
Ferredoxin	24 ± 0.2[b]	48[c]

[Reprinted with permission from Do, P.M., A. Angerhofer, I. Hrdy, L. Bardonova, L.O. Ingram, and K.T. Shanmugam. 2009. Engineering *Escherichia coli* for fermentative dihydrogen production: potential role of NADH-ferredoxin oxidoreductase from the hydrogenosome of anaerobic protozoa. Appl Biochem Biotechnol 153:21-33. (Page 27, Table 1)]

[a] Values for the native enzyme isolated from *Trichomonas vaginalis* hydrogenosomes were from Hrdy *et al.*(94).

[b] *Clostridium acetobutylicum* ferredoxin

[c] *T. vaginalis* ferredoxin

ND – not determined.

Table 5-3. Kinetic properties of recombinant *T. vaginalis* hydrogenosome NDH purified from *E. coli*

Induction	Reaction	K_m (donor) (mM NADH)	K_m (acceptor) (mM)	V_{max}[d]	K_{cat} (s^{-1})
IPTG	NADH → BV[a]	0.35	0.41	3.69	4.14
	NADH → MV[a]	0.36	2.41	3.78	4.24
	NADH → KFeCN[a]	ND	ND	ND	ND
Arabinose	NADH → BV[b]	0.10	0.17	645	725
	NADH → MV[b]	0.22	0.44	570	650
	NADH → KFeCN[c]	0.31	0.06	870	1170

K_m for NADH was determined in assay mixture containing 50 mM K-phosphate buffer, pH 7.5 with 5 mM benzyl viologen, 20 mM methyl viologen or 1 mM potassium ferricyanide. K_m for electron acceptors was determined in a reaction mixture containing 50 mM phosphate buffer, pH 7.5, 1 mM NADH and the electron acceptor at various concentrations. The reaction was followed by the reduction of electron acceptor [Adapted from Do, P.M., A. Angerhofer, I. Hrdy, L. Bardonova, L.O. Ingram, and K.T. Shanmugam. 2009. Engineering *Escherichia coli* for fermentative dihydrogen production: potential role of NADH-ferredoxin oxidoreductase from the hydrogenosome of anaerobic protozoa. Appl Biochem Biotechnol 153:21-33 (Page 28, Table 2)]

[a]6.29 µg protein was used in the reduction

[b]0.15 µg protein was used in these assays

[c]0.45 µg protein was used in these reactions

[d]µmole (min mg protein)$^{-1}$

Table 5-4. Specific activities of recombinant enzymes in butanol production pathway

Enzyme	Reaction	Specific Activity (U mg protein^{-1})	K_{cat} (s^{-1})
ThlA	Acetyl-CoA → Acetoacetyl-CoA	14.00 ± 1.88	85.62
ThlB	Acetyl-CoA → Acetoacetyl-CoA	4.09 ± 1.01	23.19
Hbd	Acetoacetyl-CoA→ Hydroxybutyryl-CoA	209.5 ± 15.46 (349)[a]	459.1
Crt	Hydroxybutyryl-CoA→ Crotonyl-CoA	799.5 ± 15.79	1572
Bcd/EtfBA	Crotonyl-CoA→ Butyryl-CoA	ND	ND
CcrA	Crotonyl-CoA→ Butyryl-CoA	7.59 ± 0.68 (2.89)[b]	11.23
Aad	Butyryl-CoA→ Butyraldehyde	ND	ND
	Butyraldehyde → Butanol	ND	ND
AdhE2	Butyryl-CoA→ Butyraldehyde	(0.74)[c]	ND
	Butyraldehyde → Butanol	0.86 ± 0.22 (0.18)[c]	ND

All enzymes were purified from recombinant *E. coli*. The number in parentheses represents reported values for enzymes from the respective native organism. Under the conditions assayed, Bcd/EtfBA had no detectable activity. ND: not detected.

[a] Specific activity of Hbd purified from *C. beijerinckii* (47)

[b] Specific activity of CcrA purified from *S. collinus* (211)

[c] Specific activity of *C. acetobutylicum* AdhE2 purified from *E. coli* (67)

Table 5-5. Specific activity of butanol pathway enzymes in the crude extract of JM107 (pCBEHTCB)

Enzyme Tested	IPTG	Specific Activity (mU mg protein^{-1})
ThlA	+	11.2 ± 2.3
	–	ND
Hbd	+	908.8 ± 81.6
	–	19.47 ± 2.4
Bcd (NADH)	+	ND
	–	ND
CcrA (NADPH)	+	11.8 ± 1.3
	–	ND
BdhB	+	ND
	–	ND

Crude extracts from JM107 bearing pCBEHTCB uninduced and induced with IPTG were assayed for the enzymes indicated. Values are the average of three independent experiments. ND: not detected.

Table 5-6. Specific activity of AtoB and AdhE2 in the crude extracts of JM107 (pAA)

Enzyme Tested	IPTG	Specific Activity (mU mg protein^{-1})
AtoB	+	22,130 ± 802
	–	ND
AdhE2	+	25.62 ± 3.3
	–	ND

Crude extracts from JM107 (pAA) uninduced and induced with IPTG were extracted and assayed for AdhE2 and AtoB. ND: not detected.

Table 5-7. Butanol production by various mutant strains of *E. coli* bearing pCBEHCU and pAA

Strain	Parent Strain	Δ*ldhA*	Δ(*focA-pflB*)	*lpd101**	Δ*mgsA*	Δ*tcdE*	Δ*adhE*	Butanol (mM)
W3110								<0.10
PMD40	W3110	X						0.45 ± 0.13
PMD42	W3110	X	X					ND
PMD46	W3110	X	X	X				ND
PMD47	W3110	X	X	X	X			ND
PMD48	W3110	X	X	X	X	X		ND
JM107								0.21 ± 0.02
PMD50	JM107	X						1.90 ± 0.06
PMD51	JM107	X	X					ND
PMD52	JM107	X	X	X				0.92 ± 0.11[a]
PMD53	JM107	X	X	X		X		ND[a]
PMD54	JM107	X	X	X			X	0.21 ± 0.09[a]

Cultures bearing both pCBEHCU and pAA were grown anaerobically in LB-ampicillin, chloramphenicol with 0.3 % glucose at 37^{o}C for 96 hrs. ND, not detected. (n=3)

[a] Grown in a pH stat at pH 7.0 with O_2-limitation at 37^{o}C.

Table 5-8. Effect of various plasmids on the production of butanol by different *E. coli* strains.

Plasmid(s)	Butanol [mM]		
	PMD50	PMD70[a]	PMD72 [a,b]
No Plasmid	ND	ND	ND
pCBEHCU	0.21 ± 0.01	0.30 ± 0.02	0.16 ± 0.09
pAA	ND	ND	ND
pAA + pCBEHCU	0.17 ± 0.13	0.21 ± 0.05	0.20 ± 0.02
pButanol	1.93 ± 0.05	2.20 ± 0.07	1.15 ± 0.40
pButyrate	1.22 ± 0.02 (1.42 ± 0.03)[c]	1.10 ± 0.05 (1.22 ± 0.03)[c]	0.82 ± 0.23 (0.37 ± 0.02)[c]

Different *E. coli* strains bearing various plasmids were tested for butanol production in LB with 0.3 % glucose at 37^{o}C for 48 hrs. ND, not detected. (n=2)

[a] Contains *but*$^{+}$ chromosomal integration of butanol pathway genes

[b] Cultures were grown micro-aerobically

[c] The values in parentheses represent butyrate concentration

Table 5-9. Effect of a second chromosomal insertion of BCS operon transcriptionally controlled by *pflB* promoters.

Strain	Glucose consumed [mM]	Fermentation Products						
		Succ	Lac	For	Ace	EtOH	Butyrate	BuOH
PMD70 [a]	55.31 ± 0.00	11.6 ± 0.21	ND	ND	38.10 ± 3.26	66.1 ± 4.69	ND	ND
PMD73 [b]	28.20 ± 6.24	4.89 ± 0.03	1.75 ± 0.61	ND	1.86 ± 0.56	18.8 ± 3.42	ND	0.16 ± 0.00
PMD72 [b]	12.52 ± 4.98	7.12 ± 0.21	0.85 ± 0.11	ND	5.84 ± 0.64	0.56 ± 0.34	ND	ND
PMD74 [b]	19.58 ± 2.36	6.03 ± 0.53	1.56 ± 0.12	ND	4.73 ± 1.89	0.32 ± 0.16	0.31 ± 0.11	<0.10

Succ, succinate; lac, lactate; for, formate; ace, acetate; EtOH, ethanol; BuOH, butanol; ND, not detected. (n=2)
[a] Cultured anaerobically in LB-ampicillin, 1.0 % glucose at 37^{o}C for 72hrs
[b] Cultured micro-aerobically in the same medium

Table 5-10. Effect of plasmids encoding intermediate reactions for butyrate production on *E. coli* strain PMD75.

Plasmid	Glucose consumed [mM]	Fermentation Products [mM]						
		Succ	Lac	For	Ace	Acetoin	EtOH	Butyrate
pTrc99a-vector	17.06 ± 4.19	5.58 ± 0.54	1.55 ± 0.02	ND	1.04 ± 0.78	ND	ND	0.20 ± 0.07
pTrc99a-*atoB*	27.18 ± 6.12	2.54 ± 0.51	0.75 ± 0.04	ND	5.84 ± 2.21	ND	ND	0.39 ± 0.04
pTrc99a-*ccrA*-*udhA*	23.21 ± 2.65	2.89 ± 0.02	1.39 ± 0.08	ND	4.72 ± 1.86	ND	ND	0.31 ± 0.02
pTrc99a-*bcd/etfBA*	29.30 ± 3.87	1.05 ± 0.02	1.08 ± 0.09	ND	7.03 ± 2.98	0.28 ± 0.11	ND	3.08 ± 0.21
pButyrate	31.73 ± 4.72	ND	1.64 ± 0.02	ND	12.77 ± 2.11	0.53 ± 0.00	0.68 ± 0.02	2.47 ± 0.10

E. coli strain PMD75 bearing the above plasmids were grown micro-aerobically in LB- ampicillin with 1.0 % glucose in partially filled tubes at 37^{o}C for 72 hrs. Succ, succinate; lac, lactate; for, formate; ace, acetate; EtOH, ethanol; ND, not detected.

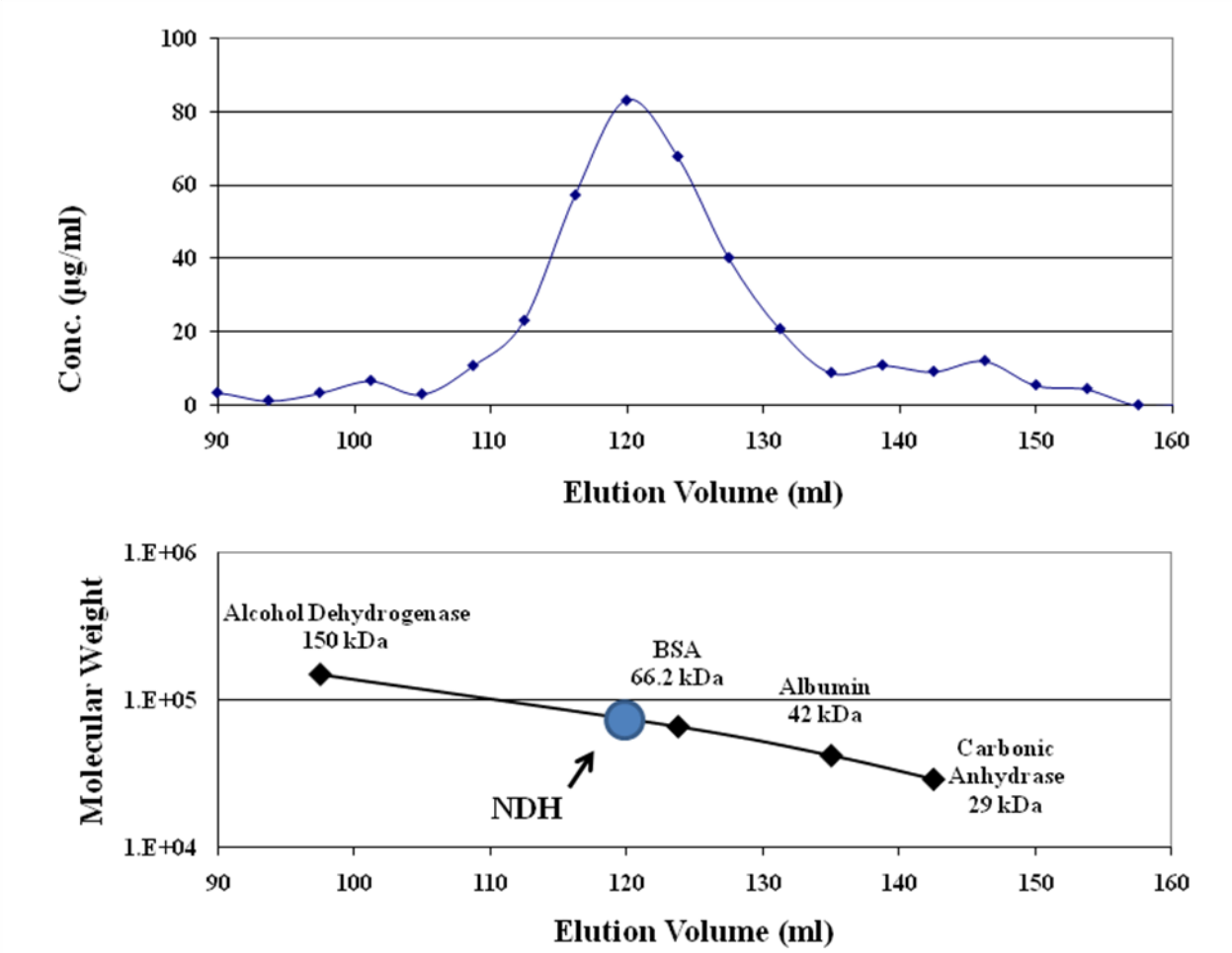

Figure 5-1. Native molecular weight of NDH as determined by gel filtration. Sephacryl S-200 column was pre-equilibrated with 50 mM K-PO_4 buffer pH 7.5, 0.1 M NaCl, and 0.5 mM DTT at 4°C. 5 ml of protein sample was loaded with the flow rate of 0.5 ml min^{-1} and 3.75 ml fractions were collected. NDH eluted as a heterodimer with a measured molecular weight of 69.1 kDa.

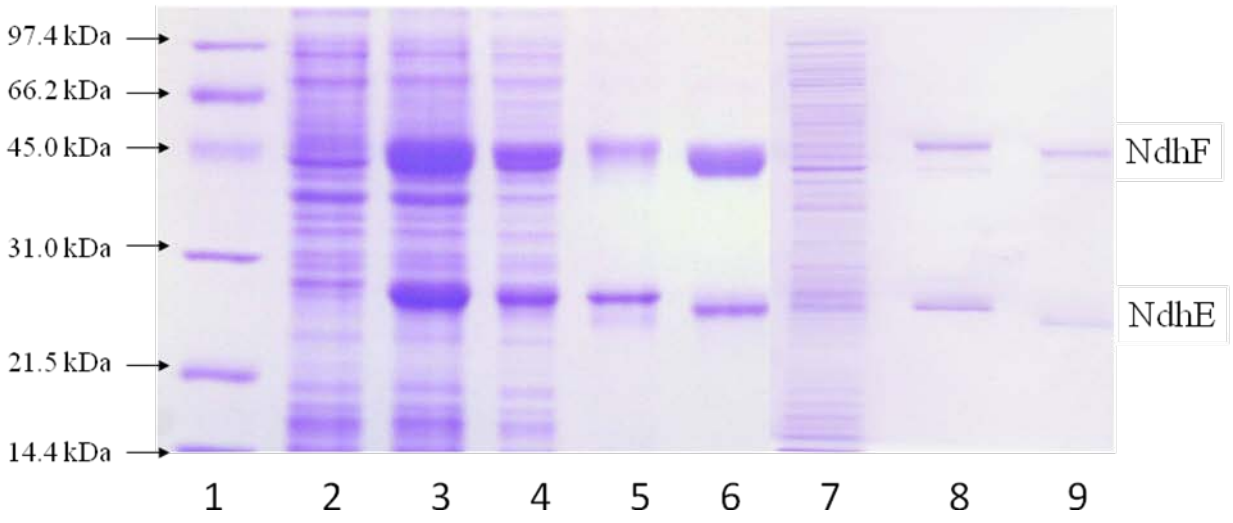

Figure 5-2. SDS-PAGE of recombinant NDH expressed in *E. coli* induced by IPTG or arabinose. Rosetta (λDE3) bearing pPMD40 was induced with IPTG (lanes 1-6) or arabinose (lanes 7-9). Proteins were separated by reducing SDS-PAGE (12.5 % acrylamide). Lane 1, Protein standards; Lane 2, uninduced cells; Lane 3, IPTG induced cells; Lane 4, soluble crude extract (10 µg); Lane 5, after Ni^{2+} column (5 µg); Lane 6, after Thrombin digestion followed by Sephacryl S-200 gel filtration (5 µg); Lane 7, arabinose induced soluble crude extract (5 µg); Lane 8, after Ni^{2+} column (1 µg); Lane 9, after Thrombin digestion followed by Sephacryl S-200 gel filtration (1 µg).

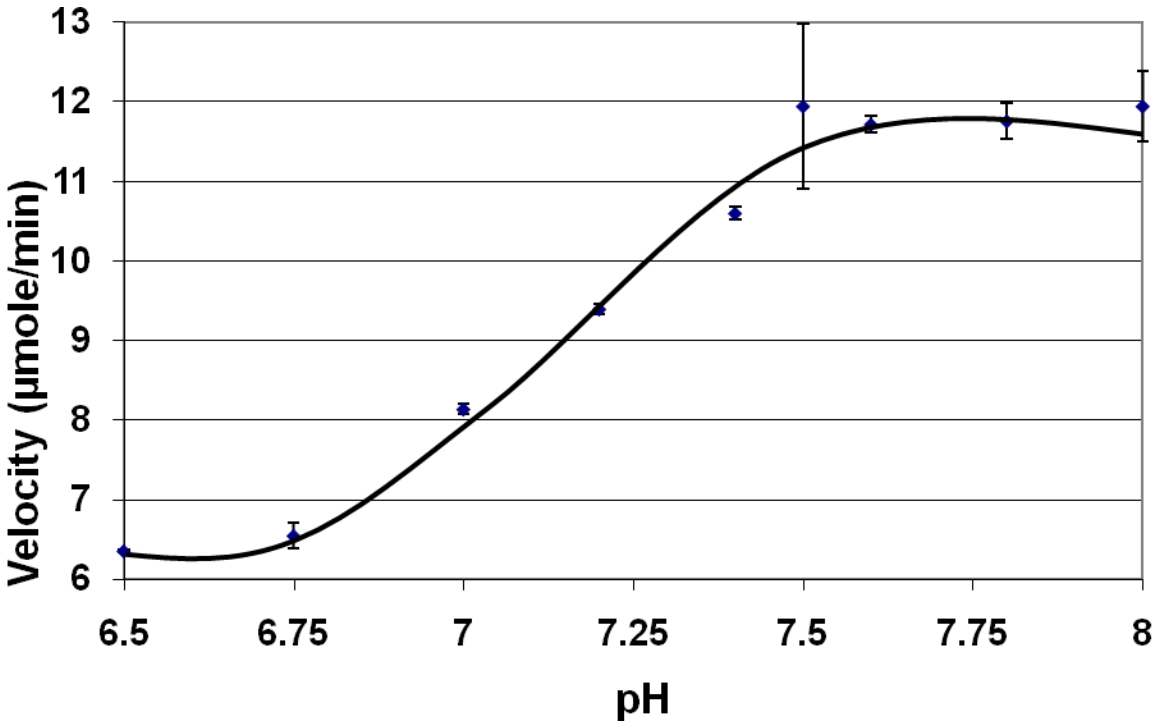

Figure 5-3. pH profile of NDH activity in phosphate buffer. Activity was determined as described in Table 5-1. Optimal pH for NDH activity was determined to be about 7.5 -8.0 in phosphate buffer.

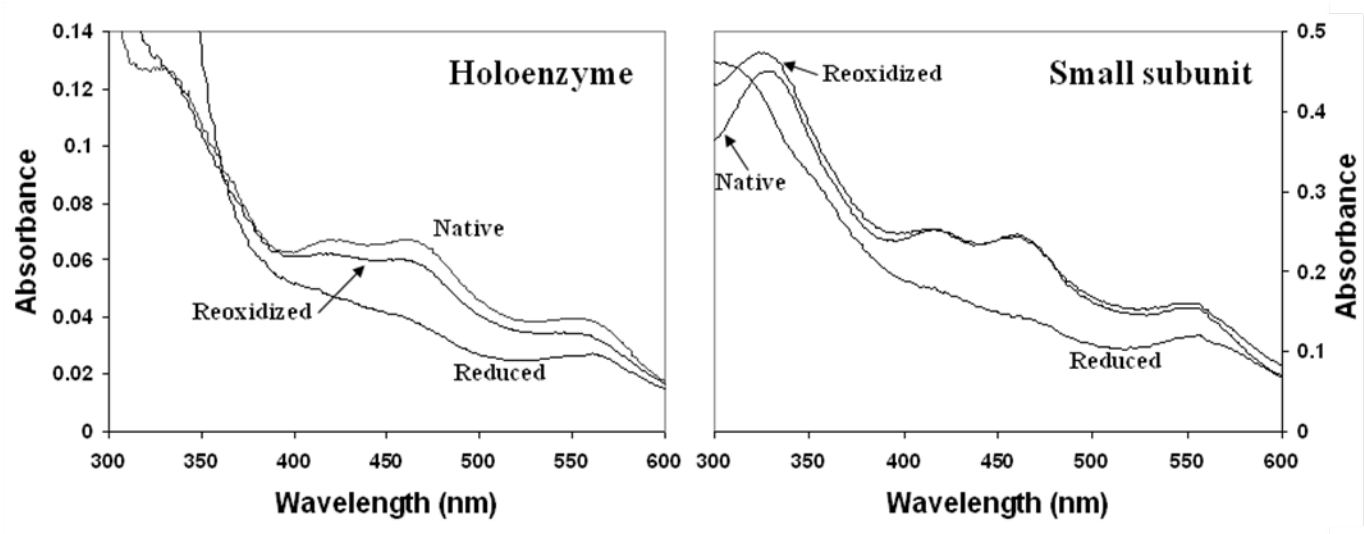

Figure 5-4. Absorption spectrum of recombinant *T. vaginalis* hydrogenosome NDH or NDH-small subunit. Native spectrum represents the protein as purified. Reduced spectrum was obtained after titrating the protein with sodium dithionite. Reoxidized spectrum was obtained after gently mixing the reduced protein with air. [Reprinted with permission from Do, P. M., A. Angerhofer, I. Hrdy, L. Bardonova, L. O. Ingram, and K. T. Shanmugam. 2009. Engineering *Escherichia coli* for fermentative dihydrogen production: potential role of NADH-ferredoxin oxidoreductase from the hydrogenosome of anaerobic protozoa. Appl Biochem Biotechnol 153:21-33. (Page 28, Figure 2)]

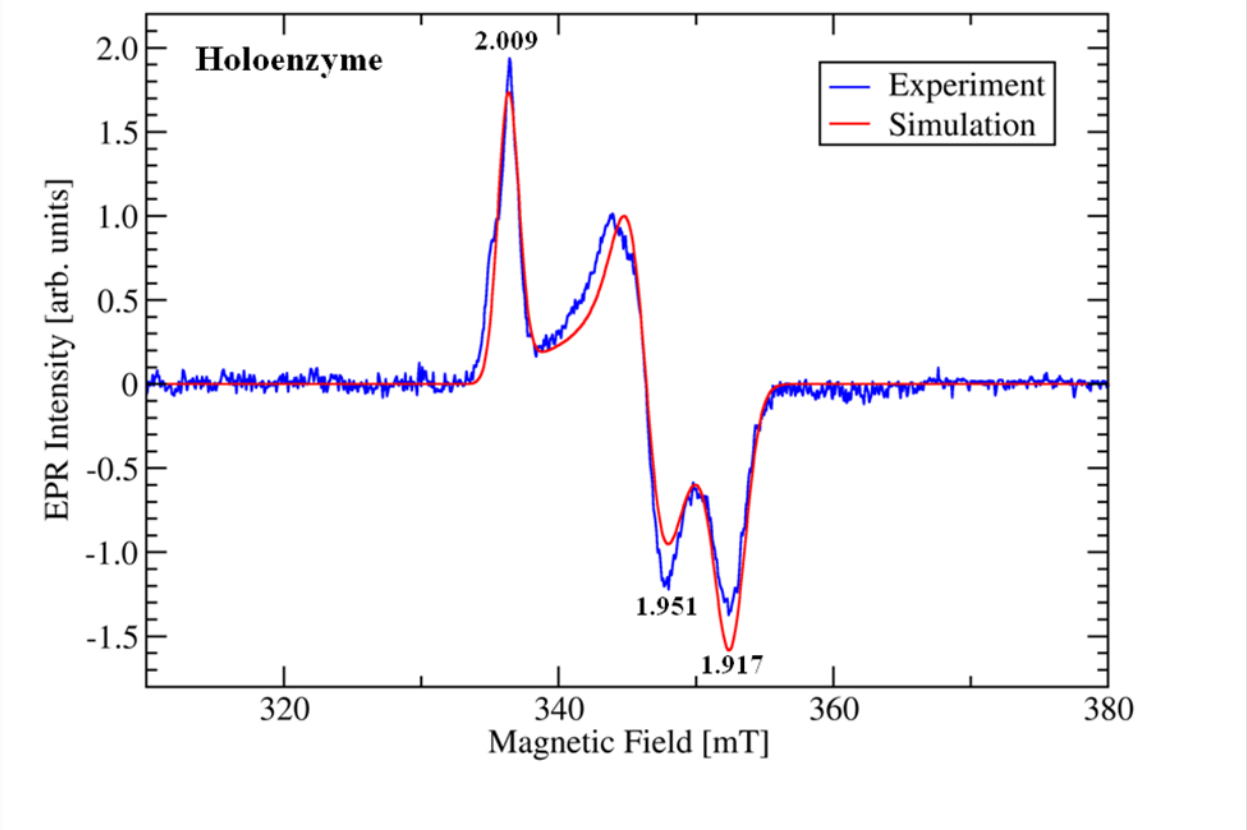

Figure 5-5. EPR spectrum of the recombinant *T. vaginalis* hydrogenosome NDH holoenzyme produced in *E. coli.* Spectrum of the holoenzyme (123.3 µM) was recorded at a microwave power of 2.0 mW after reducing the protein with sodium dithionite. EPR conditions: sample temperature, 25ºK; microwave frequency, 9.45801 GHz; modulation amplitude, 5G; modulation frequency, 100 kHz; time constant, 80 ms; scan rate, 160 ms/data point for 4.9 G/s, 0.78 G/data point, receiver gain 60 dB. Wavy lines represent the experimental data and the smooth line is the simulation of the spectrum. [Reprinted with permission from Do, P. M., A. Angerhofer, I. Hrdy, L. Bardonova, L. O. Ingram, and K. T. Shanmugam. 2009. Engineering *Escherichia coli* for fermentative dihydrogen production: potential role of NADH-ferredoxin oxidoreductase from the hydrogenosome of anaerobic protozoa. Appl Biochem Biotechnol 153:21-33 (Page 29, Figure 3)]

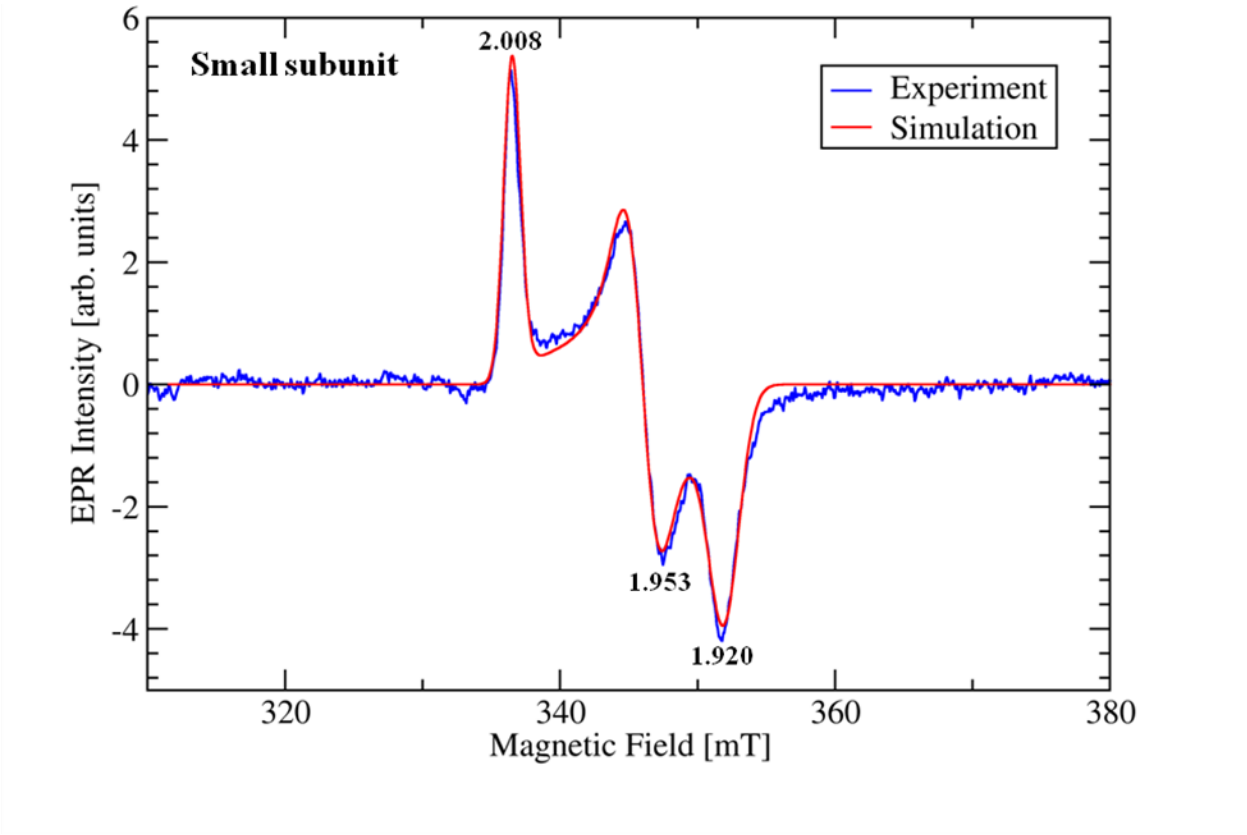

Figure 5-6. EPR spectrum of NdhE (small subunit) of the *T. vaginalis* NDH produced in *E. coli*. Spectrum of the small subunit (121.0 µM) was obtained after reducing the protein with sodium dithionite. Other conditions were as listed for Figure 5-5. [Reprinted with permission from Do, P. M., A. Angerhofer, I. Hrdy, L. Bardonova, L. O. Ingram, and K. T. Shanmugam. 2009. Engineering *Escherichia coli* for fermentative dihydrogen production: potential role of NADH-ferredoxin oxidoreductase from the hydrogenosome of anaerobic protozoa. Appl Biochem Biotechnol 153:21-33 (Page 30, Figure 4)]

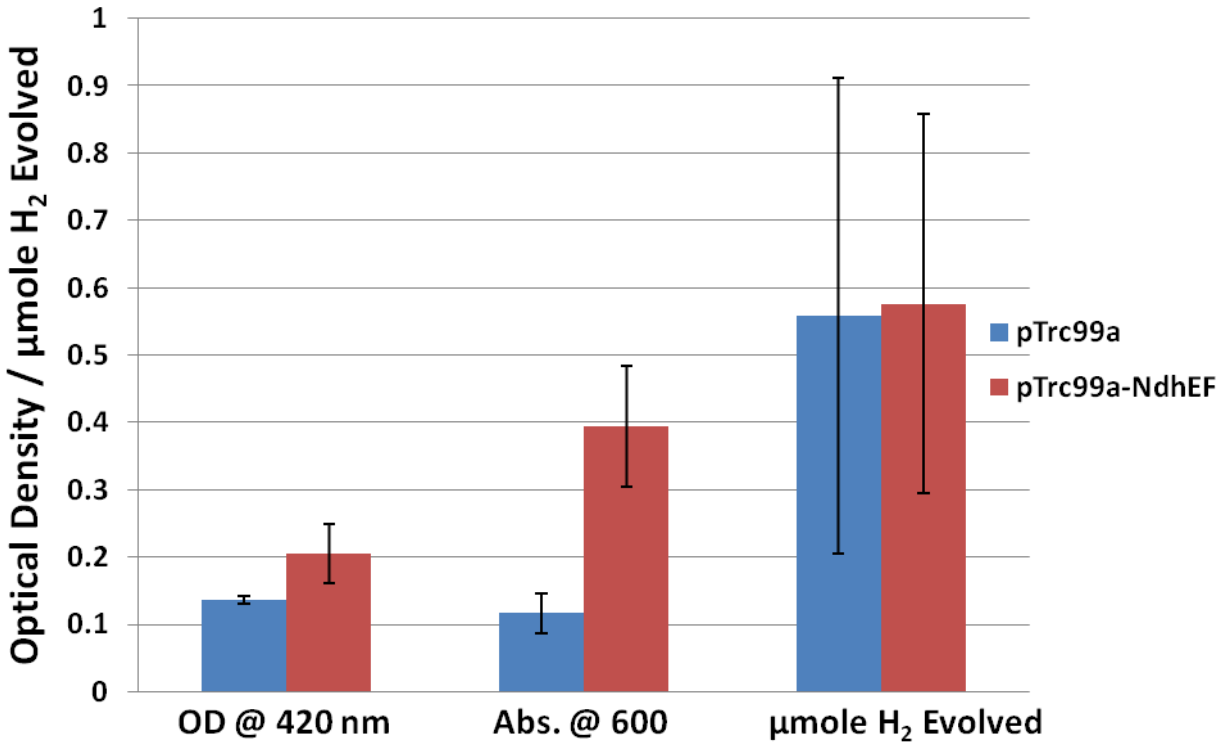

Figure 5-7. Effect of NDH on whole cell reduction of methyl viologen and H_2 evolution in overnight cultures of MV resistant PMD45. MV resistant cells with indicated plasmids were inoculated in 1 ml of LB, 0.3 % glucose, 100 µg ml^{-1} ampicillin, and 1 mM MV in 13 x 100 mm tubes which were sealed with a rubber stopper and N_2 as the gas phase. The cultures were incubated for 17hrs at 37°C. Optical densities of cultures were determined at 420 nm and 600 nm. Since cells naturally scatter light at 600 nm, measurements at 600 nm were adjusted for reduced MV by subtracting the OD contributed by the cells. (n=4)

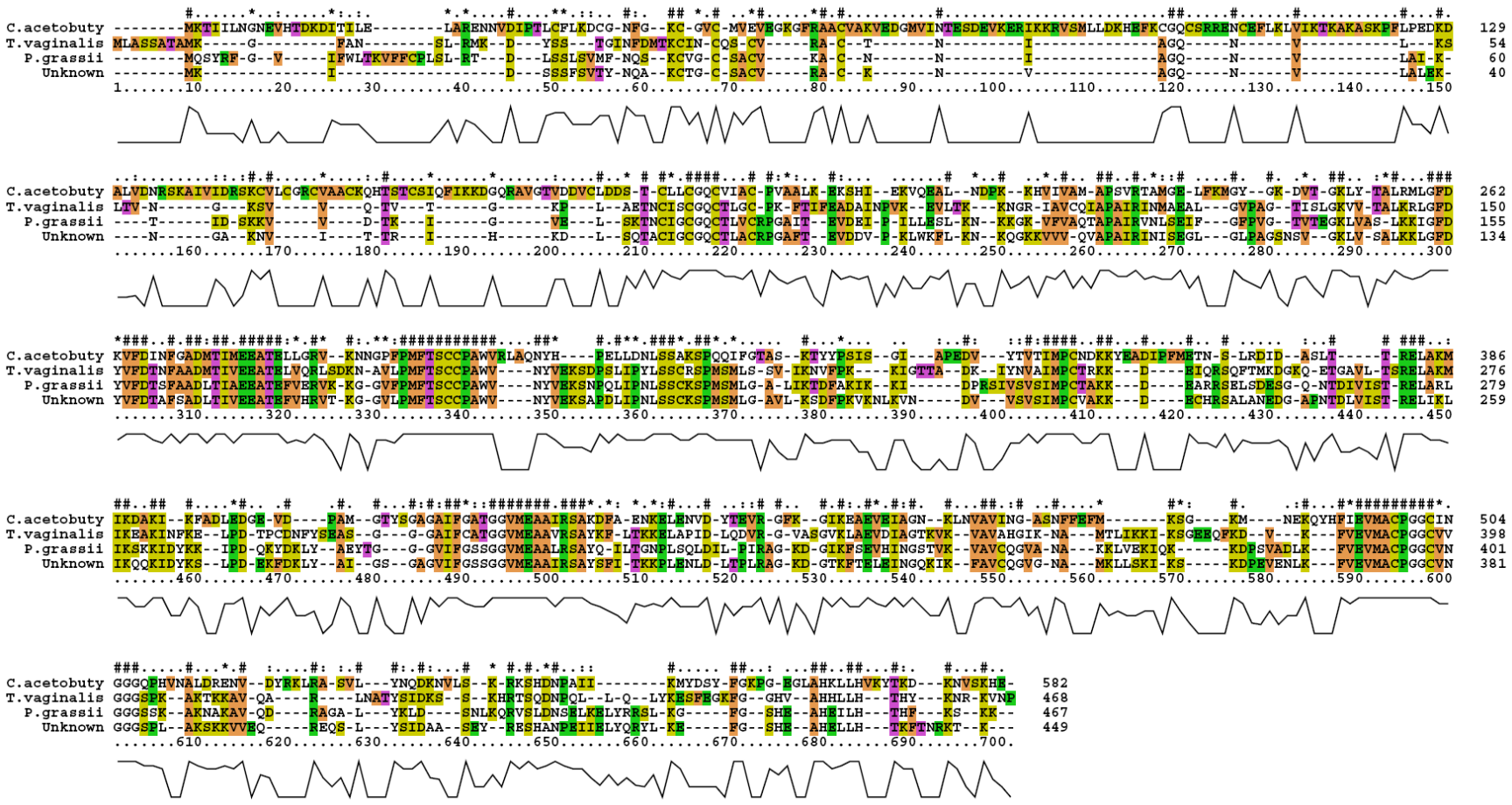

Figure 5-8. Primary sequence alignment of HydA from *C. acetobutylicum*, *T. vaginalis*, *P. grassii*, and a symbiont from the hindgut of *R. flavipes*. The isolated hydrogenase gene from the unknown symbiont had an E_{value} of 4 x 10^{-174} with 67 % amino acid identity and 81 % overall similarity to [Fe]-hydrogenase to *P. grassii.* The isolated hydrogenase also had high similarity to *T. vaginalis* HydA (E_{value} = 1 x 10^{-127}) and to a lesser extent to *C. acetobutylicum* (E_{value} = 3 x 10^{-88}). Protein alignment was performed with ClustalG ver. 1.5. Symbol legend: #, fully conserved; *, highly conserved; :, moderately conserved; ., weakly conserved or not significant; -, gap.

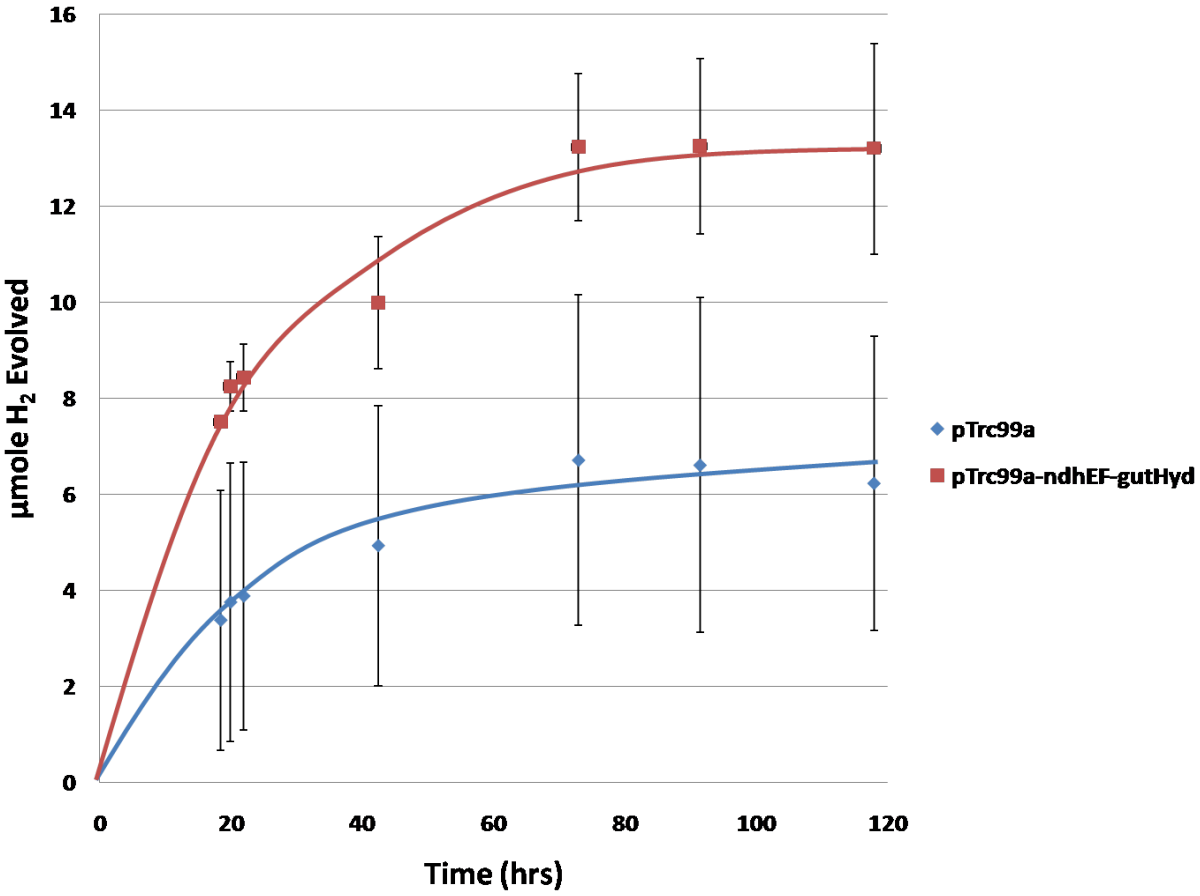

Figure 5-9. Effect of NDH and GutHyd on hydrogen production. *E. coli* strain PMD45 with pTrc99a-*ndhEF-gutHyd* or pTrc99a vector control were grown in 5 ml LB-amp-kan with 0.3 % glucose in 9 ml vial sealed with rubber septum and degassed with N_2. The cultures were incubated at 37^{o}C and H_2 in the gas phase was determined by GC. Fermentation profile of these cultures was determined by HPLC after 120 hrs (Figure 5-10). (n=2)

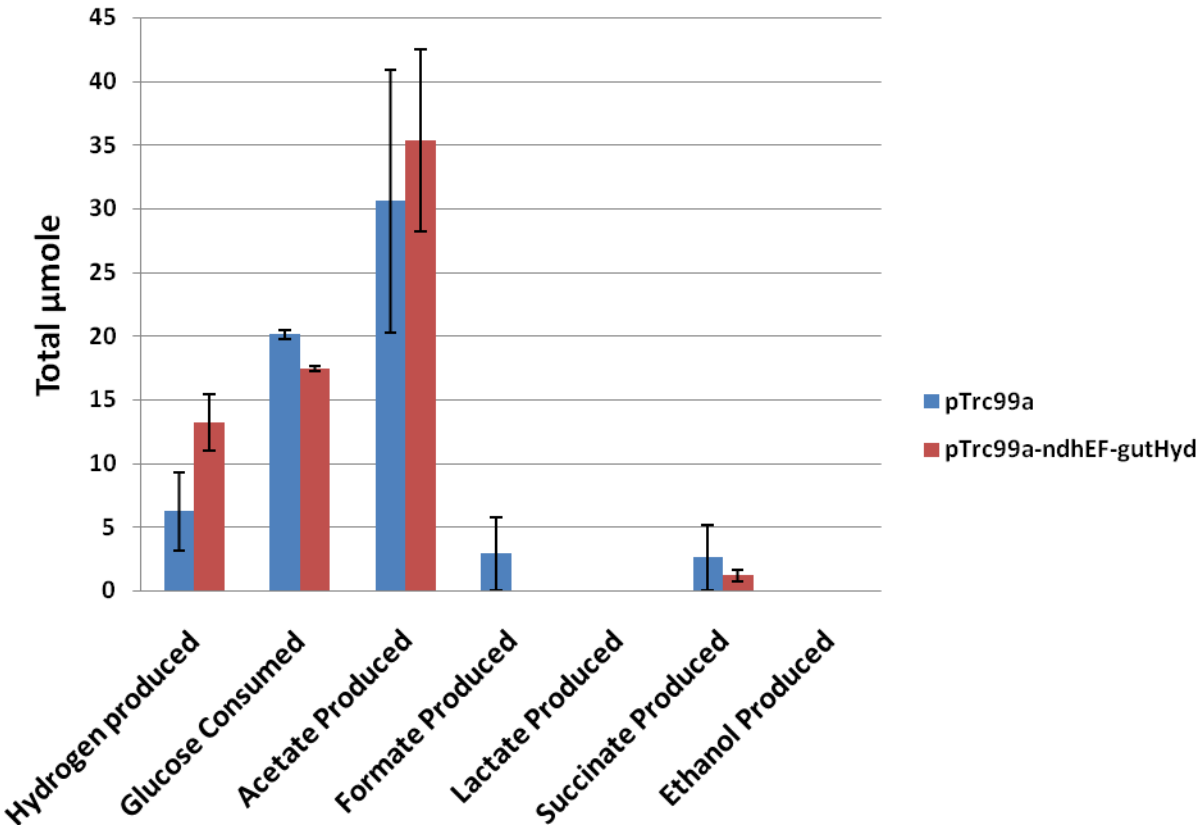

Figure 5-10. Effect of NDH and GutHyd on fermentation profile of *E. coli* strain PMD45. The fermentation products are from cultures after 120 hrs. (Figure 5-9) of incubation at 37^{o}C.

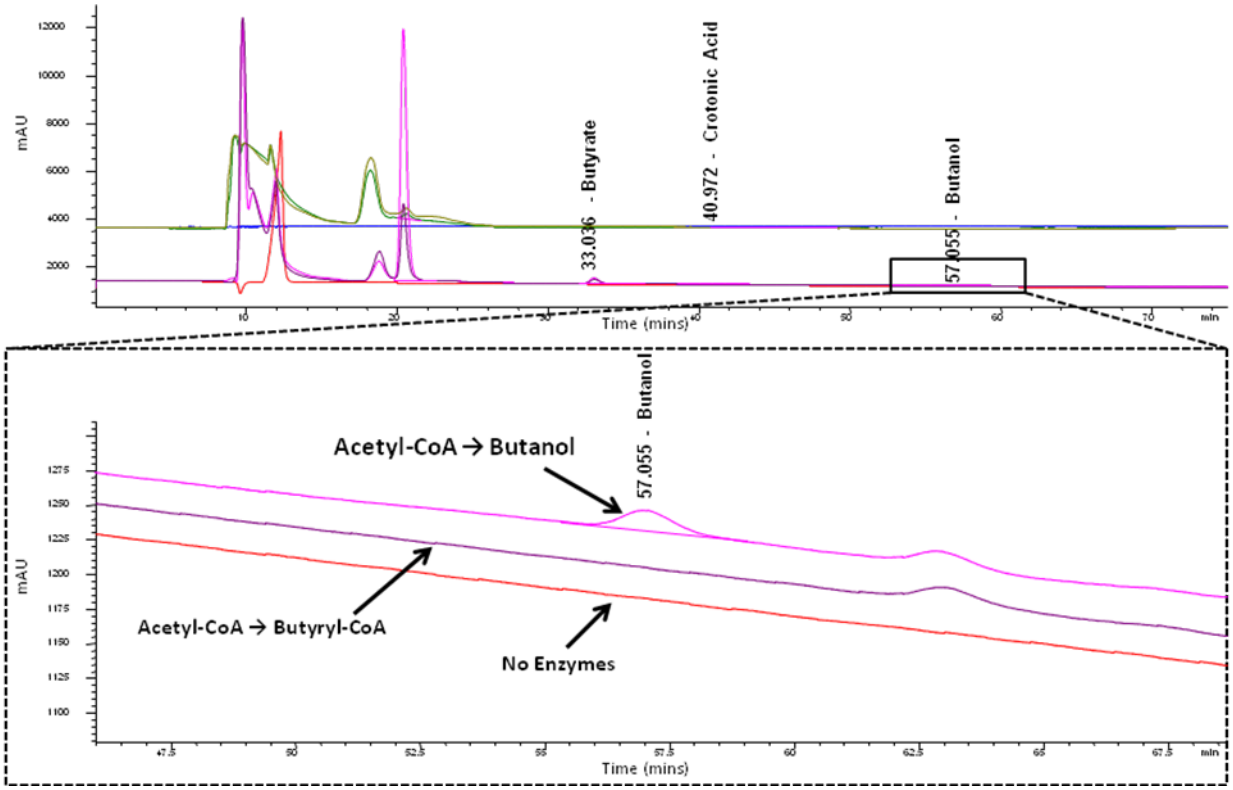

Figure 5-11. HPLC profile of *in vitro* production of 1-butanol from acetyl-CoA. 1 unit (µmole min^{-1}) of each enzyme listed in Table 5-4 minus ThlB and AdhE2 were incubated together in 0.5 ml 50 mM K-PO_4 pH 7.6 assay buffer containing 5 mM acetyl-CoA, 10 mM NADH, and 10 mM NADPH . The reaction mixture was incubated at 37°C for 30 minutes, after which 1 unit of AdhE2 and 10 mM additional NADH were added and the reaction was continued for an additional 30 minutes. Samples were taken before enzymes were added, prior to the addition of AdhE2, and at the end of incubation with all enzymes. HPLC was used to determine the production of butanol and pathway intermediates.

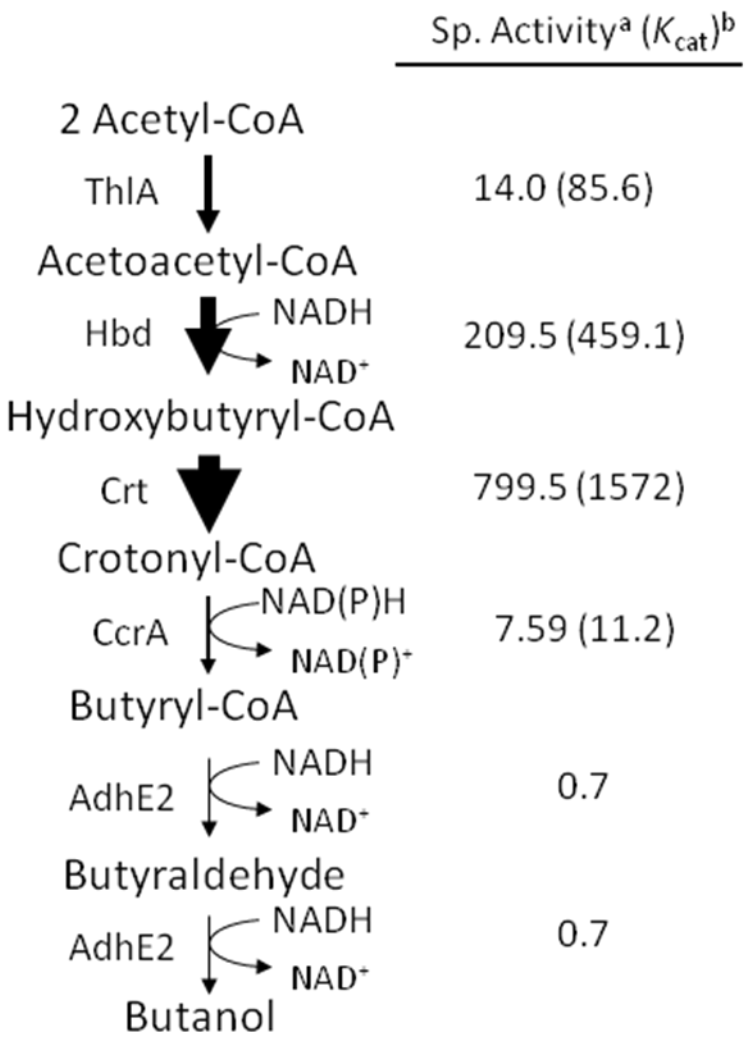

Figure 5-12. Relative specific activities of functionally expressed recombinant enzymes in *E. coli*. Relative activities listed in Table 5-4 are pictorially represented by the thickness of the arrow. Since Bcd/EtfBA had no detectable activity, it was replaced by its analogue, NADPH-dependent CcrA from *S. avermitilis*. The pathway is now complete and can be combined to produce butanol *in vitro*. [a]μmole min^{-1} mg $protein^{-1}$; [b]s^{-1}

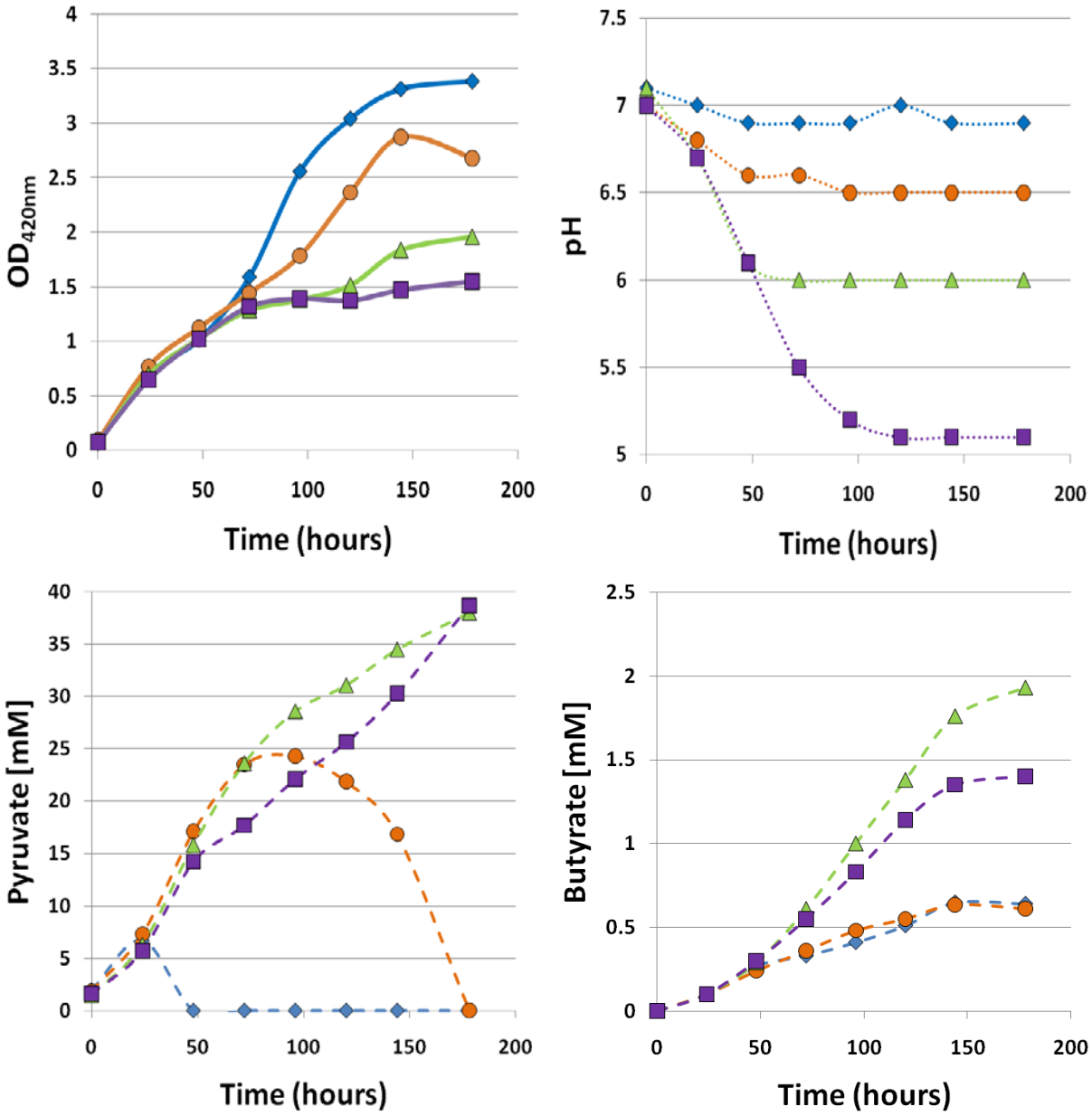

Figure 5-13. Growth, pH, pyruvate, and butyrate production from PMD76 with pH control. Cultures were grown in 1 % glucose minimal medium starting at pH 7.0. pH controllers set to 7.0 (diamonds), 6.5 (circles), 6.0 (triangles), and 5.0 (squares).

CHAPTER 6
SUMMARY AND CONCLUSIONS

Increasing demand for fuel and a finite supply of petroleum reserve dictate that a new alternative renewable energy sources be developed in order to free the world from the bond of fossil fuels. Current use of ethanol as a gasoline additive is an excellent step towards an energy independent country and a "greener" future; however, physical constraints of ethanol as a fuel along with the higher cost of transportation makes ethanol a less desirable transportation fuel. New fuels currently in development that could replace gasoline include hydrogen and higher chain alcohols such as butanol.

Hydrogen

The development of hydrogen as a fuel has been a work in progress for over 30 years. Hydrogen is a highly attractive energy source due to the extremely high energy content and clean combustion producing water as the only product. Currently, hydrogen is primarily produced by steam reforming of methane, a limited fossil fuel. Biological production of hydrogen may serve as a renewable source of fuel since it involves the conversion of solar energy either directly (photosynthetic hydrogen production) or indirectly (fermentative hydrogen production from biomass). Fermentative hydrogen production involves the conversion of sugars, the monomeric units of biomass, to hydrogen.

Fermentative hydrogen production could be economical if yields of 10 H_2 per glucose could be achieved (64); however, maximal theoretical yields of only 2 and 4 H_2 per glucose could be reached by facultative and strict anaerobic microbes, respectively. Facultative anaerobes such as *E. coli* have the natural ability to fully oxidize glucose to CO_2 producing up to 10 NAD(P)H as reducing equivalents. Strict anaerobes such as *C. acetobutylicum* and *T. vaginalis* possess the ability to couple NADH oxidation to hydrogen evolution but cannot fully

oxidize all the carbons from glucose to CO_2. The absence of a complete TCA cycle in strict anaerobes limits the NADH production to only glycolysis. By combining the two systems, NADH-dependent hydrogen production from strict anaerobes with the full TCA cycle from facultative anaerobes, higher hydrogen yields of up to 10 H_2 per glucose could be achieved. Hydrogen production by strict anaerobes generally involves intermediate electron carriers such as ferredoxin transferring electrons to soluble [Fe]-hydrogenase for H_2 evolution. Pyruvate oxidation by PFOR is the primary source of reduced ferredoxin produced in a coupled reaction. The lesser known NFOR could directly couple NADH oxidation to ferredoxin. However, NFOR activity is limited to few anaerobes; *Clostridium* (108, 124, 197) and anaerobic protozoan such as *Trichomonas* (56, 94). Clostridial NFOR activity was recently determined to be a side reaction of Bcd/EtfBA reduction of crotonyl-CoA to butyryl-CoA (55, 124). Since clostridial systems do not have a true NFOR, the only other source of NFOR is the anaerobic protozoan.

The unique ability of this NDH to couple NADH oxidation to directly reduce a broad range of electron acceptors including low potential ferredoxin, MV, and BV makes *T. vaginalis* NDH the only known member of NFOR class of enzymes. NDH is a heterodimer consisting of a small (NdhE) and large (NdhF) subunit which have high homology to mitochondrial 24-kDa and 51-kDa subunits of NADH-dehydrogenase (NDH) of respiratory complex I (94). Recombinant *T. vaginalis* NDH expressed in *E. coli* also reduced these low potential electron acceptors (56).

H_2 production from NADH using MV as an electron carrier may also require recombinant expression of [Fe]-hydrogenase which currently only been accomplished with low activity. Compatibility issues with traditional clostridial [Fe]-hydrogenase due to pH differences makes its use with *T. vaginalis* NDH less ideal. Hydrogenase from *P. grassii* isolated from termite hindgut may serve as a possible alternative (99). The high activity of this hydrogenase without

maturation accessory proteins in *E. coli* may be more compatible with NDH since both enzymes were hydrogenosome based in their native organisms. The best candidate for [Fe]-hydrogenase cloned from symbiont portion of *R. flavipes* hindgut had an E_{value} of 4×10^{-174} with 67 % identity and 81 % overall similarity to [Fe]-hydrogenase from *P. grassii*. This high homology did not translate into functional expression of active enzyme without accessory proteins. It may be essential to clone and express the hydrogenosomal proteins NDH, Fd, Fe-hydrogenase, and accessory proteins together in *E. coli* to establish an NADH to H_2 pathway in *E. coli*.

The thermodynamics of producing H_2 from NADH is unfavorable requiring about +4.62 kcal mol^{-1} (ΔG_o) (Equation 5-1) (Figure 6-1). The [NADH]/[NAD^+] ratio required for thermodynamically favorable reaction is 2390. The internal [NAD^+]/[NADH] ratios appears to be inadequate to shift the reaction to reduce sufficient amount of MV required to drive continuous H_2 evolution by HYD3. Overnight cultures of *E. coli* expressing NDH contained only 0.060 mM reduced MV in a total of 1.0 mM MV. The actual redox potential (E) of MV at this equilibrium ratio is -404 mV (E_o' = -440 mV). NDH needs to generate a MV_{red}/MV_{ox} ratio at least three to four fold higher to drive the electrons to hydrogenase and to H_2 production, at an E_o' of -420 mV.

This study attempted to improve hydrogen production by *E. coli* utilizing hydrogenosome based NDH to couple NADH oxidation to low potential viologen dye reduction. Although reduced methyl viologen failed to support high level of hydrogen production, this study expanded our understanding of hydrogenosomal NDH from *T. vaginalis* by providing an insight of its capability and limitation in heterologous hosts. Future work in this area may involve recombinant expression of enzymes/proteins from the same organism since they normally have better protein-protein interactions than with heterologous enzymes. The expression of *T.*

vaginalis hydrogenosome ferredoxin (-347 mV) and a [Fe]-hydrogenase in an active form may be required to achieve NADH dependent H_2 production; however, given the thermodynamic constraints of the system, *in vivo* NADH to H_2 may still be difficult to accomplish even with continuous H_2 removal.

Butanol

Butanol is a 4-carbon alcohol that has many physical properties similar to gasoline. Its high combustional energy yield and renewable biological production is of great interest in recent years as a gasoline additive or even as a potential gasoline replacement. Butanol is produced by fermentation by some members of the genus *Clostridium*, where the model organism is *C. acetobutylicum*. Production of butanol is always accompanied by co-production of lower energy value compounds such as acetone and ethanol. Attempts to eliminate side products and produce a robust homo-butanol fermentating *Clostridium* had been unsuccessful (44, 87, 88, 120, 145, 234). The limited available genetic tools and fastidious nature of the strict anaerobes makes it a less than ideal organism to engineer. An alternative to engineering clostridia for homo-butanol production is to introduce the entire butanol pathway into a well-known non-producing organism that is easy to manipulate. In this study, I explored the potential of *E. coli* to produce butanol as a sole fermentation product.

The established butanol pathway enzymes were produced in a recombinant *E. coli* and these enzymes did catalyze the sequential reactions from acetyl-CoA to butanol, *in vitro*. However, *in vivo*, crotonyl-CoA reduction was found to be a rate-limiting step in this pathway due to a unique need for alternative electron donor that is yet to be identified. Alternative enzyme such as CcrA is fraught with NADPH requirement since the pool of NADPH in an anaerobic cell is not high enough to drive this reaction towards high butanol yield. However, the *in vitro* production of butanol provided the proof of principle that *E. coli* could functionally

produce the enzymes required for the production of butanol from acetyl-CoA, provided appropriate electron donors can be generated *in vivo*.

pH controlled fermentations revealed the optimal pH for butyrate production was about 6.0 producing about three times more butyrate than at pH 7.0. Multiple copies of *bcd-etfBA* improved butyrate production suggesting that Bcd/EtfBA protein level was not at par with the rest of the pathway. One proposed method for increasing butyrate production was to insert additional copies of *bcd-etfBA* into the chromosome under control of highly expressed promoters.

Directed evolution had been an instrument used for strain development for industrial grade production of compounds and adaptation to less than desirable media conditions (43, 103, 104, 111, 135, 227, 231, 235). Since the chromosomal inserts of the butanol pathway are stable, directed evolution by serial transfers could be implemented to select for improved productivity with the key focus on enhancing Bcd/EtfBA protein level and activity. The recombinant *E. coli* with butanol/butyrate genes produced in this study could be a good platform organism for the evolution of a biocatalyst for butyrate/butanol production.

Future work in this area may include the identification of the specific Bcd/EtfBA electron donor. The expression of clostridial ferredoxin may be required for effective Bcd activity. Li *et al.* demonstrated that the Bcd/EtfBA complex couples NADH-dependent reduction of crotonyl-CoA and ferredoxin (124) and suggest ferredoxin may perhaps serve as an electron bridge between Bcd and EtfBA components. Reduced electron carriers such as MV and DCPIP has been demonstrated to couple to crotonyl-CoA reduction (55). Since *T. vaginalis* NDH reduced these electron carriers, the use of NDH with the appropriate electron carrier may increase Bcd activity. Mutations in *lpdA* has been demonstrated to increase the PDH activity under anaerobic

growth condition supplying an additional 2 NADH (111, 112) that could help maintain redox balance during butanol production. An alcohol dehydrogenase specific for butyryl-CoA/butyraldehyde may need to be engineered to eliminate co-production of ethanol with butanol. Overcoming these rate-limiting steps is expected to yield a microbial biocatalyst that can catalyze the production of butanol as the main fermentation product and at high yield from biomass-derived sugars.

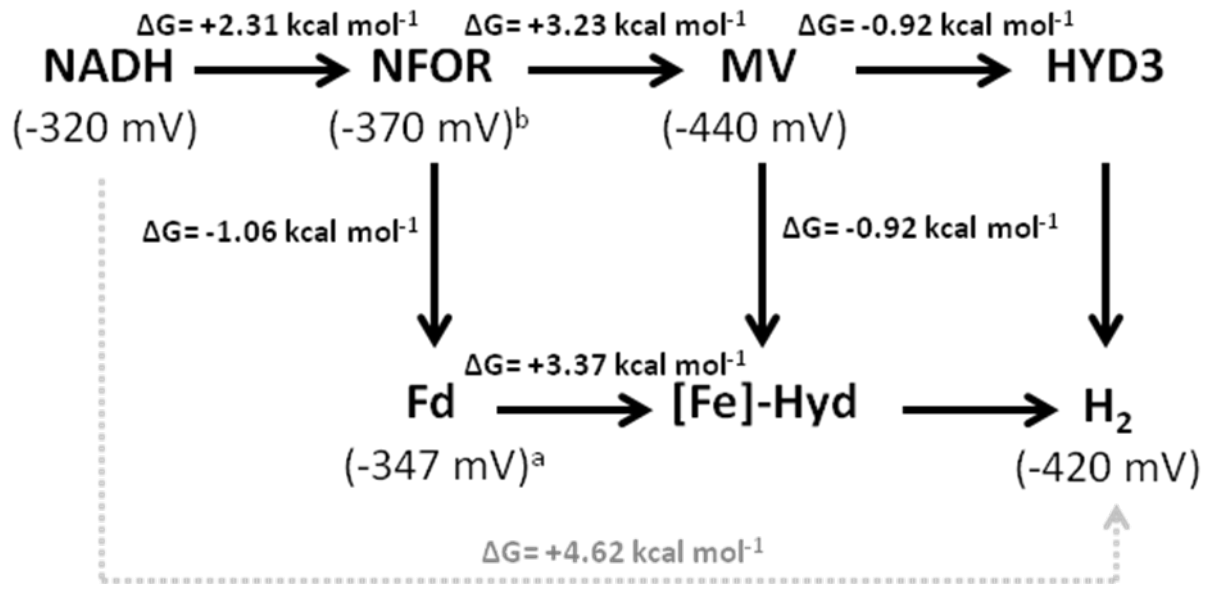

Figure 6-1. Thermodynamics of the NADH-dependent hydrogen production pathway. The values in parentheses represent the standard midpoint potential (E_o') of the respective component. H_2 from NADH is a thermodynamically unfavorable reaction with ΔG of +4.62 kcal mol^{-1}. [a] *T. vaginalis* ferredoxin (205, 206); [b] NDH N1a cluster

APPENDIX
REPRINT PERMISSION OF PUBLISHED MATERIALS

A portion of the Chapter 5: Results - Biochemical Characterization of NFOR (NDH) from *T. vaginalis* was previously published by Springer Science + Business Media and Copyright Clearance Center's Rightslink[1] (56). Written permission from the publisher was given on June 17 and 22, 2009 to reproduce text, excerpts, and figures (Figures 5-4, 5-5, and 5-6 and Tables 5-2 and 5-3) with license numbers 2214350581080, 2211440942274, and 2211440754680, respectively, for use in the doctoral dissertation of Phi Minh Do, the first author of the above publication.

[1] Do, P. M., A. Angerhofer, I. Hrdy, L. Bardonova, L. O. Ingram, and K. T. Shanmugam**.** 2009. Engineering *Escherichia coli* for fermentative dihydrogen production: potential role of NADH-ferredoxin oxidoreductase from the hydrogenosome of anaerobic protozoa. Appl Biochem Biotechnol 153:21-33.

LIST OF REFERENCES

1. **Adams, M. W., and L. E. Mortenson.** 1984. The physical and catalytic properties of hydrogenase II of *Clostridium pasteurianum*. A comparison with hydrogenase I. J Biol Chem **259:**7045-7055.

2. **Adams, M. W., L. E. Mortenson, and J. S. Chen.** 1980. Hydrogenase. Biochim Biophys Acta **594:**105-176.

3. **Alexeeva, S., K. J. Hellingwerf, and M. J. Teixeira de Mattos.** 2003. Requirement of ArcA for redox regulation in *Escherichia coli* under microaerobic but not anaerobic or aerobic conditions. J Bacteriol **185:**204-209.

4. **Almeida, J. R., M. Bertilsson, M. F. Gorwa-Grauslund, S. Gorsich, and G. Liden.** 2009. Metabolic effects of furaldehydes and impacts on biotechnological processes. Appl Microbiol Biotechnol **82:**625-638.

5. **Alsaker, K. V., and E. T. Papoutsakis.** 2005. Transcriptional program of early sporulation and stationary-phase events in *Clostridium acetobutylicum*. J Bacteriol **187:**7103-7118.

6. **Amann, E., B. Ochs, and K. J. Abel.** 1988. Tightly regulated *tac* promoter vectors useful for the expression of unfused and fused proteins in *Escherichia coli*. Gene **69:**301-315.

7. **Amore, R., P. Kotter, C. Kuster, M. Ciriacy, and C. P. Hollenberg.** 1991. Cloning and expression in *Saccharomyces cerevisiae* of the NAD(P)H-dependent xylose reductase-encoding gene (*XYL*1) from the xylose-assimilating yeast *Pichia stipitis*. Gene **109:**89-97.

8. **Asada, Y., Y. Koike, J. Schnackenberg, M. Miyake, I. Uemura, and J. Miyake.** 2000. Heterologous expression of clostridial hydrogenase in the cyanobacterium *Synechococcus* PCC7942. Biochim Biophys Acta **1490:**269-278.

9. **Asada, Y., and J. Miyake.** 1999. Photobiological hydrogen production. J Biosci Bioeng **88:**1-6.

10. **Asadullah, M., S. Ito, K. Kunimori, M. Yamada, and K. Tomishige.** 2002. Energy efficient production of hydrogen and syngas from biomass: development of low-temperature catalytic process for cellulose gasification. Environ Sci Technol **36:**4476-4481.

11. **Atiyeh, H., and Z. Duvnjak.** 2002. Production of fructose and ethanol from sugar beet molasses using *Saccharomyces cerevisiae* ATCC 36858. Biotechnol Prog **18:**234-239.

12. **Atsumi, S., A. F. Cann, M. R. Connor, C. R. Shen, K. M. Smith, M. P. Brynildsen, K. J. Chou, T. Hanai, and J. C. Liao.** 2008. Metabolic engineering of *Escherichia coli* for 1-butanol production. Metab Eng **10:**305-311.

13. **Atta, M., M. E. Lafferty, M. K. Johnson, J. Gaillard, and J. Meyer.** 1998. Heterologous biosynthesis and characterization of the [2Fe-2S]-containing N-terminal domain of *Clostridium pasteurianum* hydrogenase. Biochemistry **37:**15974-15980.

14. **Ausubel, F. M., R. Brent, R. E. Kingston, D. D. Moore, J. A. Smith, J. G. Seidman, and K. Struhl.** 1987. Current Protocols in Molecular Biology. Greene Publishing Associates and Wiley-Interscience, Brooklyn, NY.

15. **Badger, P. C.** 2002. Ethanol from cellulose: A General Review, p. 17-21. *In* J. J. and W. A. (ed.), Trends in new crops and new uses. ASHA Press, Alexandria, VA.

16. **Badziong, W., R. K. Thauer, and J. G. Zeikus.** 1978. Isolation and characterization of *Desulfovibrio* growing on hydrogen plus sulfate as the sole energy source. Arch Microbiol **116:**41-49.

17. **Ballantine, S. P., and D. H. Boxer.** 1986. Isolation and characterisation of a soluble active fragment of hydrogenase isoenzyme 2 from the membranes of anaerobically grown *Escherichia coli*. Eur J Biochem **156:**277-284.

18. **Baranenko, V. I., and V. S. Kirov.** 1989. Solubility of hydrogen in water in a broad temperature and pressure range. Atomic Energy **66:**24-28.

19. **Basso, L. C., H. V. de Amorim, A. J. de Oliveira, and M. L. Lopes.** 2008. Yeast selection for fuel ethanol production in Brazil. FEMS Yeast Res **8:**1155-1163.

20. **Benemann, J.** 1996. Hydrogen biotechnology: progress and prospects. Nat Biotechnol **14:**1101-1103.

21. **Benemann, J. R., J. A. Berenson, N. O. Kaplan, and M. D. Kamen.** 1973. Hydrogen evolution by a chloroplast-ferredoxin-hydrogenase system. Proc Nat Acad Sci **70:**2317-2320.

22. **Benemann, J. R., and A. San Pietro.** 2001. Technical workshop on biological hydrogen production, Final Report to the US Department of Energy, Hydrogen R&D Program, Bethesda, MD.

23. **Berman-Frank, I., P. Lundgren, Y. B. Chen, H. Kupper, Z. Kolber, B. Bergman, and P. Falkowski.** 2001. Segregation of nitrogen fixation and oxygenic photosynthesis in the marine cyanobacterium *Trichodesmium*. Science **294:**1534-1537.

24. **Bernhard, M., B. Benelli, A. Hochkoeppler, D. Zannoni, and B. Friedrich.** 1997. Functional and structural role of the cytochrome b subunit of the membrane-bound hydrogenase complex of *Alcaligenes eutrophus* H16. Eur J Biochem **248:**179-186.

25. **Bettiga, M., B. Hahn-Hagerdal, and M. F. Gorwa-Grauslund.** 2008. Comparing the xylose reductase/xylitol dehydrogenase and xylose isomerase pathways in arabinose and xylose fermenting *Saccharomyces cerevisiae* strains. Biotechnol Biofuels **1:**16.

26. **Black, L. K., C. Fu, and R. J. Maier.** 1994. Sequences and characterization of *hupU* and *hupV* genes of *Bradyrhiobium japonicum* encoding a possible nickel-sensing complex involved in hydrogenase expression. J Bacteriol **176:**7102-7106.

27. **Blankenship, R. E., P. Cheng, T. P. Causgrove, D. C. Brune, S.-H. Wang, J. U. Choh, and J. Wang.** 1993. Redox regulation of energy transfer efficiency in antennas of green photosynthetic bacteria. Photochem Photobiol **57:**103-107.

28. **Böck, A., and G. Sawers.** 1996. Fermentation, p. 262-282. *In* F. C. Neidhardt, et al. (ed.), *Escherichia coli* and *Salmonella*: Cellular and Molecular Biology, 2nd ed. ASM Press, Washington, DC.

29. **Bonaventura, C., and J. Myers.** 1969. Fluorescence and oxygen evolution from *Chlorella pyrenoidosa*. Biochim Biophys Acta **189:**366-383.

30. **Bothast, R. J., N. N. Nichols, and B. S. Dien.** 1999. Fermentations with new recombinant organisms. Biotechnol Prog **15:**867-875.

31. **Bothast, R. J., and M. A. Schlicher.** 2005. Biotechnological processes for conversion of corn into ethanol. Appl Microbiol Biotechnol **67:**19-25.

32. **Boynton, Z. L., G. N. Bennet, and F. B. Rudolph.** 1996. Cloning, sequencing, and expression of clustered genes encoding beta-hydroxybutyryl-coenzyme A (CoA) dehydrogenase, crotonase, and butyryl-CoA dehydrogenase from *Clostridium acetobutylicum* ATCC 824. J Bacteriol **178:**3015-3024.

33. **Boynton, Z. L., G. N. Bennett, and F. B. Rudolph.** 1996. Cloning, sequencing, and expression of genes encoding phosphotransacetylase and acetate kinase from *Clostridium acetobutylicum* ATCC 824. Appl Environ Microbiol **62:**2758-2766.

34. **Bradford, M. M.** 1976. A rapid and sensitive method for the quantitation of microgram quantities of protein utilizing the principle of protein-dye binding. Anal Biochem **72:**248-254.

35. **Brandt, U.** 2006. Energy converting NADH:quinone oxidoreductase (complex I). Annu Rev Biochem **75:**69-92.

36. **Brat, D., E. Boles, and B. Wiedemann.** 2009. Functional expression of a bacterial xylose isomerase in *Saccharomyces cerevisiae*. Appl Environ Microbiol **75:**2304-2311.

37. **Brazzolotto, X., J. K. Rubach, J. Gaillard, S. Gambarelli, M. Atta, and M. Fontecave.** 2006. The [Fe-Fe]-hydrogenase maturation protein HydF from *Thermotoga maritima* is a GTPase with an iron-sulfur cluster. J Biol Chem **281:**769-774.

38. **Brodersen, J., G. Gottschalk, and U. Deppenmeier.** 1999. Membrane-bound $F_{420}H_2$-dependent heterodisulfide reduction in *Methanococcus voltae*. Arch Microbiol **171:**115-121.

39. **Brown, L. C., R. D. Lentsch, G. E. Besenbruch, and K. R. Schultz.** 2003. Alternative flowsheets for the sulfur-iodine thermochemical hydrogen cycle, Spring 2003 National Meeting of American Insitute of Chemical Engineers. GA– A24266, New Orleans, La.

40. **Buhrke, T., O. Lenz, N. Krauss, and B. Friedrich.** 2005. Oxygen tolerance of the H_2-sensing [NiFe] hydrogenase from *Ralstonia eutropha* H16 is based on limited access of oxygen to the active site. J Biol Chem **280:**23791-23796.

41. **Bush, G. W.** 2003. Fact Sheet: Hydrogen Fuel: a clean and secure energy future.:[http://www.whitehouse.gov/news/releases/2003/02/20030206-2.html].

42. **Bush, G. W.** Feb 27, 2003. Statement by the president.: [http://www.whitehouse.gov/news/releases/2003/02/20030227-11.html].

43. **Causey, T. B., K. T. Shanmugam, L. P. Yomano, and L. O. Ingram.** 2004. Engineering *Escherichia coli* for efficient conversion of glucose to pyruvate. Proc Natl Acad Sci **101:**2235-2240.

44. **Chen, C. K., and H. P. Blaschek.** 1999. Acetate enhances solvent production and prevents degeneration in *Clostridium beijerinckii* BA101. Appl Microbiol Biotechnol **52:**170-173.

45. **Cline, J. D.** 1969. Spectrophotometric determination of hydrogen sulfide in natural waters. Limnology and Oceanography **14:**454-458.

46. **Cohen, J., K. Kim, P. King, M. Seibert, and K. Schulten.** 2005. Finding gas diffusion pathways in proteins: application to O_2 and H_2 transport in CpI [FeFe]-hydrogenase and the role of packing defects. Structure **13:**1321-1329.

47. **Colby, G. D., and J. S. Chen.** 1992. Purification and properties of 3-hydroxybutyryl-coenzyme A dehydrogenase from *Clostridium beijerinckii* ("*Clostridium butylicum*") NRRL B593. Appl Environ Microbiol **58:**3297-3302.

48. **Cornillot, E., R. V. Nair, E. T. Papoutsakis, and P. Soucaille.** 1997. The genes for butanol and acetone formation in *Clostridium acetobutylicum* ATCC 824 reside on a large plasmid whose loss leads to degeneration of the strain. J Bacteriol **179:**5442-5447.

49. **Crozier, T. E., and S. Yamamoto.** 1974. Solubility of hydrogen in water, seawater, and NaCl solutions. J Chem Eng Data **19:**242-244.

50. **da Silva Filho, E. A., H. F. de Melo, D. F. Antunes, S. K. dos Santos, A. do Monte Resende, D. A. Simoes, and M. A. de Morais, Jr.** 2005. Isolation by genetic and physiological characteristics of a fuel-ethanol fermentative *Saccharomyces cerevisiae* strain with potential for genetic manipulation. J Ind Microbiol Biotechnol **32:**481-486.

51. **Datsenko, K. A., and B. L. Wanner.** 2000. One-step inactivation of chromosomal genes in *Escherichia coli* K-12 using PCR products. Proc Natl Acad Sci **97:**6640-6645.

52. **de Graef, M. R., S. Alexeeva, J. L. Snoep, and M. J. Teixeira de Mattos.** 1999. The steady-state internal redox state (NADH/NAD) reflects the external redox state and is correlated with catabolic adaptation in *Escherichia coli*. J Bacteriol **181:**2351-2357.

53. **Demple, B.** 1991. Regulation of bacterial oxidative stress genes. Annu Rev Genet **25:**315-337.

54. **Dien, B. S., M. A. Cotta, and T. W. Jeffries.** 2003. Bacteria engineered for fuel ethanol production: current status. Appl Microbiol Biotechnol **63:**258-266.

55. **Diez-Gonzalez, F., J. B. Russell, and J. B. Hunter.** 1997. NAD-independent lactate and butyryl-CoA dehydrogenases of *Clostridium acetobutylicum* P262. Curr Microbiol **34:**162-166.

56. **Do, P. M., A. Angerhofer, I. Hrdy, L. Bardonova, L. O. Ingram, and K. T. Shanmugam.** 2009. Engineering *Escherichia coli* for fermentative dihydrogen production: potential role of NADH-ferredoxin oxidoreductase from the hydrogenosome of anaerobic protozoa. Appl Biochem Biotechnol **153:**21-33.

57. **DOE.** 2005. Property of Fuels. Department of Energy**:** [http://www.eere.energy.gov/afdc/pdfs/fueltable.pdf].

58. **Doherty, G. M., and S. G. Mayhew.** 1992. The hydrogen-tritium exchange activity of *Megasphaera elsdenii* hydrogenase. Eur J Biochem **205:**117-126.

59. **Dross, F., V. Geisler, R. Lenger, F. Theis, T. Krafft, F. Fahrenholz, E. Kojro, A. Duchene, D. Tripier, and K. Juvenal.** 1992. The quinone-reactive Ni/Fe-hydrogenase of *Wolinella succinogenes*. Eur J Biochem **206:**93-102.

60. **Dürre, P.** 2005. Formation of solvents in clostridia, p. 671-685. *In* P. Dürre (ed.), Handbook on Clostridia. CRC Press, Boca Raton.

61. **Dürre, P., M. Bohringer, S. Nakotte, S. Schaffer, K. Thormann, and B. Zickner.** 2002. Transcriptional regulation of solventogenesis in *Clostridium acetobutylicum*. J Mol Microbiol Biotechnol **4:**295-300.

62. **Dürre, P., R. J. Fischer, A. Kuhn, K. Lorenz, W. Schreiber, B. Sturzenhofecker, S. Ullmann, K. Winzer, and U. Sauer.** 1995. Solventogenic enzymes of *Clostridium acetobutylicum*: catalytic properties, genetic organization, and transcriptional regulation. FEMS Microbiol Rev **17:**251-262.

63. **Eady, R. R.** 1996. Structure - function relationships of alternative nitrogenases. Chem. Rev. **96:**3013-3030.

64. **Eggeman, T.** 2004. Boundary analysis for H_2 production by fermentation. National Renewable Energy Laboratory**:**NREL/SR-560-36129.

65. **EIA.** 2009. Appendix A:reference case, p. 109-150, Annual energy outlook 2009: with projections to 2030. Energy Information Administration, Washington D.C. : DOE/EIA-0383(2009).

66. **Elsen, S., A. Colbeau, J. Chabert, and P. M. Vignais.** 1996. The *hupTUV* operon is involved in negative control of hydrogenase synthesis in *Rhodobacter capsulatus*. J Bacteriol **178:**5174-5181.

67. **Fontaine, L., I. Meynial-Salles, L. Girbal, X. Yang, C. Croux, and P. Soucaille.** 2002. Molecular characterization and transcriptional analysis of *adhE2*, the gene encoding the NADH-dependent aldehyde/alcohol dehydrogenase responsible for butanol production in alcohologenic cultures of *Clostridium acetobutylicum* ATCC 824. J Bacteriol **184:**821-830.

68. **Gabriel, C. L.** 1928. Butanol fermentation process. Ind. Eng. Chem. **20:**1063-1067.

69. **Gabriel, C. L., and F. M. Crawford.** 1930. Development of the butyl-acetonic fermentation industry. Ind. Eng. Chem. **22:**1163-1165.

70. **Gaffron, H., and J. Rubin.** 1942. Fermentative and photochemical production of hydrogen in algae. J. Gen. Physiol. **20:**219-240.

71. **Gest, H., and M. D. Kamen.** 1949. Studies on the metabolism of photosynthetic bacteria. J Bacteriol **58:**239-245.

72. **Girbal, L., G. von Abendroth, M. Winkler, P. M. Benton, I. Meynial-Salles, C. Croux, J. W. Peters, T. Happe, and P. Soucaille.** 2005. Homologous and heterologous overexpression in *Clostridium acetobutylicum* and characterization of purified clostridial and algal Fe-only hydrogenases with high specific activities. Appl Environ Microbiol **71:**2777-2781.

73. **Gitlitz, P. H., and A. I. Krasna.** 1975. Structural and catalytic properties of hydrogenase from *Chromatium*. Biochemistry **14:**2561-2568.

74. **Golden, J. W., and H. S. Yoon.** 2003. Heterocyst development in *Anabaena*. Curr Opin Microbiol **6:**557-563.

75. **Grabar, T. B., S. Zhou, K. T. Shanmugam, L. P. Yomano, and L. O. Ingram.** 2006. Methylglyoxal bypass identified as source of chiral contamination in L(+) and D(-)-lactate fermentations by recombinant *Escherichia coli*. Biotechnol Lett **28:**1527-1535.

76. **Gray, C. T., and H. Gest.** 1965. Biological formation of molecular hydrogen. Science **148:**186-192.

77. **Gray, K. A., L. Zhao, and M. Emptage.** 2006. Bioethanol. Curr Opin Chem Biol **10:**141-146.

78. **Grupe, H., and G. Gottschalk.** 1992. Physiological events in *Clostridium acetobutylicum* during the shift from acidogenesis to solventogenesis in continuous culture and presentation of a model for shift induction. Appl Environ Microbiol **58:**3896-3902.

79. **Gutierrez, T., L. O. Ingram, and J. F. Preston.** 2006. Purification and characterization of a furfural reductase (FFR) from *Escherichia coli* strain LYO1--an enzyme important in the detoxification of furfural during ethanol production. J Biotechnol **121:**154-164.

80. **Hahn-Hagerdal, B., K. Karhumaa, M. Jeppsson, and M. F. Gorwa-Grauslund.** 2007. Metabolic engineering for pentose utilization in *Saccharomyces cerevisiae*. Adv Biochem Eng Biotechnol **108:**147-177.

81. **Hallahan, D. L., V. M. Fernandez, and D. O. Hall.** 1987. Reversible activation of hydrogenase from *Escherichia coli*. Eur J Biochem **165:**621-625.

82. **Hallenbeck, P. C.** 2005. Fundamentals of the fermentative production of hydrogen. Water Sci Technol **52:**21-29.

83. **Hans, M., E. Bill, I. Cirpus, A. J. Pierik, M. Hetzel, D. Alber, and W. Buckel.** 2002. Adenosine triphosphate-induced electron transfer in 2-hydroxyglutaryl-CoA dehydratase from *Acidaminococcus fermentans*. Biochemistry **41:**5873-5882.

84. **Happe, T., and J. D. Naber.** 1993. Isolation, characterization and N-terminal amino acid sequence of hydrogenase from the green alga *Chlamydomonas reinhardtii*. Eur J Biochem **214:**475-481.

85. **Happe, T., K. Schutz, and H. Bohme.** 2000. Transcriptional and mutational analysis of the uptake hydrogenase of the filamentous cyanobacterium *Anabaena variabilis* ATCC 29413. J Bacteriol **182:**1624-1631.

86. **Harden, A.** 1901. The chemical action of *Bacillus coli communis* and similar organisms on carbohydrates and allied compounds. J. Chem. Soc **79:**601-618.

87. **Harris, L. M., L. Blank, R. P. Desai, N. E. Welker, and E. T. Papoutsakis.** 2001. Fermentation characterization and flux analysis of recombinant strains of *Clostridium acetobutylicum* with an inactivated *solR* gene. J Ind Microbiol Biotechnol **27:**322-328.

88. **Harris, L. M., R. P. Desai, N. E. Welker, and E. T. Papoutsakis.** 2000. Characterization of recombinant strains of the *Clostridium acetobutylicum* butyrate kinase inactivation mutant: need for new phenomenological models for solventogenesis and butanol inhibition? Biotechnol Bioeng **67:**1-11.

89. **Harvey, A. E. J., J. A. Smart, and E. S. Amis.** 1955. Simultaneous spectrophotometric determination of iron(II) and total Iron with 1,10-phenanthroline. Anal. Chem. **27:**26-29.

90. **Higuchi, Y., H. Ogata, K. Miki, N. Yasuoka, and T. Yagi.** 1999. Removal of the bridging ligand atom at the Ni-Fe active site of [NiFe] hydrogenase upon reduction with H_2, as revealed by X-ray structure analysis at 1.4 Å resolution. Structure **7:**549-556.

91. **Hill, J., E. Nelson, D. Tilman, S. Polasky, and D. Tiffany.** 2006. Environmental, economic, and energetic costs and benefits of biodiesel and ethanol biofuels. Proc Natl Acad Sci **103:**11206-11210.

92. **Homann, P. H.** 2003. Hydrogen metabolism of green algae: discovery and early research - a tribute to Hans Gaffron and his coworkers. Photosynth Res **76:**93-103.

93. **Houchins, J. P., and R. H. Burris.** 1981. Comparative characterization of two distinct hydrogenases from *Anabaena* sp. strain 7120. J Bacteriol **146:**215-221.

94. **Hrdy, I., R. P. Hirt, P. Dolezal, L. Bardonova, P. G. Foster, J. Tachezy, and T. M. Embley.** 2004. *Trichomonas* hydrogenosomes contain the NADH dehydrogenase module of mitochondrial complex I. Nature **432:**618-622.

95. **Ide, T., S. Baumer, and U. Deppenmeier.** 1999. Energy conservation by the H_2:heterodisulfide oxidoreductase from *Methanosarcina mazei* Go1: identification of two proton-translocating segments. J Bacteriol **181:**4076-4080.

96. **Ingram, L. O., H. C. Aldrich, A. C. Borges, T. B. Causey, A. Martinez, F. Morales, A. Saleh, S. A. Underwood, L. P. Yomano, S. W. York, J. Zaldivar, and S. Zhou.** 1999. Enteric bacterial catalysts for fuel ethanol production. Biotechnol Prog **15:**855-866.

97. **Ingram, L. O., T. Conway, D. P. Clark, G. W. Sewell, and J. F. Preston.** 1987. Genetic engineering of ethanol production in *Escherichia coli*. Appl Environ Microbiol **53:**2420-2425.

98. **Ingram, L. O., P. F. Gomez, X. Lai, M. Moniruzzaman, B. E. Wood, L. P. Yomano, and S. W. York.** 1998. Metabolic engineering of bacteria for ethanol production. Biotechnol Bioeng **58:**204-214.

99. **Inoue, J., K. Saita, T. Kudo, S. Ui, and M. Ohkuma.** 2007. Hydrogen production by termite gut protists: characterization of iron hydrogenases of *Parabasalian* symbionts of the termite *Coptotermes formosanus*. Eukaryot Cell **6:**1925-32.

100. **Inui, M., M. Suda, S. Kimura, K. Yasuda, H. Suzuki, H. Toda, S. Yamamoto, S. Okino, N. Suzuki, and H. Yukawa.** 2008. Expression of *Clostridium acetobutylicum* butanol synthetic genes in *Escherichia coli*. Appl Microbiol Biotechnol **77:**1305-1316.

101. **Ito, T., Y. Nakashimada, T. Kakizono, and N. Nishio.** 2004. High-yield production of hydrogen by *Enterobacter aerogenes* mutants with decreased alpha-acetolactate synthase activity. J Biosci Bioeng **97:**227-232.

102. **Jackson, D. D., and J. W. Ellms.** 1896. On odors and taste of surface waters with special reference to *Anabaena*, a microscopical organism found in certain water supplies of Massachusetts. Rep Mass State Board Health.

103. **Jantama, K., X. Zhang, J. C. Moore, K. T. Shanmugam, S. A. Svoronos, and L. O. Ingram.** 2008. Eliminating side products and increasing succinate yields in engineered strains of *Escherichia coli* C. Biotechnol Bioeng **101:**881-893.

104. **Jarboe, L. R., T. B. Grabar, L. P. Yomano, K. T. Shanmugan, and L. O. Ingram.** 2007. Development of ethanologenic bacteria. Adv Biochem Eng Biotechnol **108:**237-261.

105. **Jeffries, T. W.** 2006. Engineering yeasts for xylose metabolism. Curr Opin Biotechnol **17:**320-6.

106. **Jeffries, T. W., and Y. S. Jin.** 2004. Metabolic engineering for improved fermentation of pentoses by yeasts. Appl Microbiol Biotechnol **63:**495-509.

107. **Jones, D. T., and D. R. Woods.** 1986. Acetone-butanol fermentation revisited. Microbiol Rev **50:**484-524.

108. **Jungermann, K., R. K. Thauer, G. Leimenstoll, and K. Decker.** 1973. Function of reduced pyridine nucleotide-ferredoxin oxidoreductases in saccharolytic clostridia. Biochim Biophys Acta **305:**268-280.

109. **Kabus, A., T. Georgi, V. F. Wendisch, and M. Bott.** 2007. Expression of the *Escherichia coli pntAB* genes encoding a membrane-bound transhydrogenase in *Corynebacterium glutamicum* improves L-lysine formation. Appl Microbiol Biotechnol **75:**47-53.

110. **Kern, M., W. Klipp, and J. H. Klemme.** 1994. Increased nitrogenase-nependent H_2 photoproduction by *hup* mutants of *Rhodospirillum rubrum*. Appl Environ Microbiol **60:**1768-1774.

111. **Kim, Y., L. O. Ingram, and K. T. Shanmugam.** 2007. Construction of an *Escherichia coli* K-12 mutant for homoethanologenic fermentation of glucose or xylose without foreign genes. Appl Environ Microbiol **73:**1766-1771.

112. **Kim, Y., L. O. Ingram, and K. T. Shanmugam.** 2008. Dihydrolipoamide dehydrogenase mutation alters the NADH sensitivity of pyruvate dehydrogenase complex of *Escherichia coli* K-12. J Bacteriol **190:**3851-3858.

113. **King, P. W., M. C. Posewitz, M. L. Ghirardi, and M. Seibert.** 2006. Functional studies of [FeFe] hydrogenase maturation in an *Escherichia coli* biosynthetic system. J Bacteriol **188:**2163-72.

114. **Knoshaug, E. P., and M. Zhang.** 2008. Butanol tolerance in a selection of microorganisms. Appl Biochem Biotechnol **153:**13-20.

115. **Kotter, P., R. Amore, C. P. Hollenberg, and M. Ciriacy.** 1990. Isolation and characterization of the *Pichia stipitis* xylitol dehydrogenase gene, *XYL2*, and construction of a xylose-utilizing *Saccharomyces cerevisiae* transformant. Curr Genet **18:**493-500.

116. **Krahn, E., R. Weiss, M. Krockel, J. Groppe, G. Henkel, P. Cramer, X. Trautwein, K. Schneider, and A. Muller.** 2002. The Fe-only nitrogenase from *Rhodobacter capsulatus*: identification of the cofactor, an unusual, high-nuclearity iron-sulfur cluster, by Fe K-edge EXAFS and ^{57}Fe Mossbauer spectroscopy. J Biol Inorg Chem **7:**37-45.

117. **Krasna, A. I.** 1984. Mutants of *Escherichia coli* with altered hydrogenase activity. J Gen Microbiol **130:**779-787.

118. **Laemmli, U. K.** 1970. Cleavage of structural proteins during the assembly of the head of bacteriophage T4. Nature **227:**680-685.

119. **Lambden, P. R., and J. R. Guest.** 1976. Mutants of *Escherichia coli* K12 unable to use fumarate as an anaerobic electron acceptor. J Gen Microbiol **97:**145-160.

120. **Lee, S. Y., J. H. Park, S. H. Jang, L. K. Nielsen, J. Kim, and K. S. Jung.** 2008. Fermentative butanol production by clostridia. Biotechnol Bioeng **101:**209-228.

121. **Lehman, T. C., and C. Thorpe.** 1990. Alternate electron acceptors for medium-chain acyl-CoA dehydrogenase: use of ferricenium salts. Biochemistry **29:**10594-105602.

122. **Leonardo, M. R., Y. Dailly, and D. P. Clark.** 1996. Role of NAD in regulating the *adhE* gene of *Escherichia coli*. J Bacteriol **178:**6013-6018.

123. **Levanon, S. S., K. Y. San, and G. N. Bennett.** 2005. Effect of oxygen on the *Escherichia coli* ArcA and FNR regulation systems and metabolic responses. Biotechnol Bioeng **89:**556-564.

124. **Li, F., J. Hinderberger, H. Seedorf, J. Zhang, W. Buckel, and R. K. Thauer.** 2008. Coupled ferredoxin and crotonyl coenzyme A (CoA) reduction with NADH catalyzed by the butyryl-CoA dehydrogenase/etf complex from *Clostridium kluyveri*. J Bacteriol **190:**843-850.

125. **Liang, L., Y. P. Zhang, L. Zhang, M. J. Zhu, S. Z. Liang, and Y. N. Huang.** 2008. Study of sugarcane pieces as yeast supports for ethanol production from sugarcane juice and molasses. J Ind Microbiol Biotechnol **35:**1605-1613.

126. **Licht, S.** 2005. Thermochemical solar hydrogen generation. Chem Commun (Camb)**:**4635-4646.

127. **Lin, Y., and S. Tanaka.** 2006. Ethanol fermentation from biomass resources: current state and prospects. Appl Microbiol Biotechnol **69:**627-642.

128. **Loach, P. A.** 1968. Oxidation-reduction potentials, aborbance bands and molar absorbance of compounds used in biochemical studies, p. J27-J34. *In* H. A. Sober (ed.),

Handbook of Biochemistry: Selected Data for Molecular Biology. The Chemical Rubber Co., Cleveland, OH.

129. **Logan, B. E., S. E. Oh, I. S. Kim, and S. Van Ginkel.** 2002. Biological hydrogen production measured in batch anaerobic respirometers. Environ Sci Technol **36:**2530-2535.

130. **Ma, K., Z. H. Zhou, and M. W. Adams.** 1994. Hydrogen production from pyruvate by enzymes purified from hyperthermophilic archaeon, *Pyrococcus furiosus*: A key role for NADPH. FEMS Microbio Lett **122:**245-250.

131. **Macarron, R., C. Acebal, M. P. Castillon, J. M. Dominguez, I. de la Mata, G. Pettersson, P. Tomme, and M. Claeyssens.** 1993. Mode of action of endoglucanase III from *Trichoderma reesei*. Biochem J **289 (Pt 3):**867-873.

132. **Mandal, B., K. Nath, and D. Das.** 2006. Improvement of biohydrogen production under decreased partial pressure of H_2 by *Enterobacter cloacae*. Biotechnol Lett **28:**831-835.

133. **Maniatis, T., E. F. Fritsch, and J. Sambrook.** 1982. Molecular Cloning. Cold Spring Harbor Laboratory, New York.

134. **Markov, A. V., A. V. Gusakov, E. G. Kondratyeva, O. N. Okunev, A. O. Bekkarevich, and A. P. Sinitsyn.** 2005. New effective method for analysis of the component composition of enzyme complexes from *Trichoderma reesei*. Biochemistry (Mosc) **70:**657-663.

135. **Martinez, A., T. B. Grabar, K. T. Shanmugam, L. P. Yomano, S. W. York, and L. O. Ingram.** 2007. Low salt medium for lactate and ethanol production by recombinant *Escherichia coli* B. Biotechnol Lett **29:**397-404.

136. **Melis, A., and T. Happe.** 2004. Trails of green alga hydrogen research - from Hans Gaffron to new frontiers. Photosynth Res **80:**401-409.

137. **Melis, A., L. Zhang, M. Forestier, M. L. Ghirardi, and M. Seibert.** 2000. Sustained photobiological hydrogen gas production upon reversible inactivation of oxygen evolution in the green alga *Chlamydomonas reinhardtii*. Plant Physiol **122:**127-136.

138. **Miller, J. H.** 1992. A Short Course in Bacterial Genetics-A Laboratory Manual and Handbook for *Escherichia coli* and Related Bacteria. Cold Spring Harbor Laboratory Press, New York, NY.

139. **Millichip, R. J., and H. W. Doelle.** 1989. Large-scale ethanol production from Mil (Sorghum) using *Zymomonas mobilis*. Process Biochem **24:**141-145.

140. **Mitsui, A., and S. Suda.** 1995. Alternative and cyclic appearance of H_2 and O_2 photoproduction activities under non-growing conditions in an aerobic nitrogen-fixing unicellular cyanobacterium *Synechococcus* sp. Curr Microbio **30:**1-6.

141. **Moock, N., B. Trapp, and D. Gallaspy.** 2005. Presented at the Power-Gen International Conference, Las Vegas, NV.

142. **Mullany, P., C. L. Clayton, M. J. Pallen, R. Slone, A. al-Saleh, and S. Tabaqchali.** 1994. Genes encoding homologues of three consecutive enzymes in the butyrate/butanol-producing pathway of *Clostridium acetobutylicum* are clustered on the *Clostridium difficile* chromosome. FEMS Microbiol Lett **124:**61-67.

143. **Murata, N.** 1969. Control of excitation transfer in photosynthesis. I. Light-induced change of chlorophyll a fluorescence in *Porphyridium cruentum*. Biochim Biophys Acta **172:**242-251.

144. **Nair, R. V., G. N. Bennett, and E. T. Papoutsakis.** 1994. Molecular characterization of an aldehyde/alcohol dehydrogenase gene from *Clostridium acetobutylicum* ATCC 824. J Bacteriol **176:**871-885.

145. **Nair, R. V., E. M. Green, D. E. Watson, G. N. Bennett, and E. T. Papoutsakis.** 1999. Regulation of the *sol* locus genes for butanol and acetone formation in *Clostridium acetobutylicum* ATCC 824 by a putative transcriptional repressor. J Bacteriol **181:**319-330.

146. **Nandi, R., and S. Sengupta.** 1998. Microbial production of hydrogen: an overview. Crit Rev Microbiol **24:**61-84.

147. **Narayanan, N., M. Y. Hsieh, Y. Xu, and C. P. Chou.** 2006. Arabinose-induction of *lac*-derived promoter systems for penicillin acylase production in *Escherichia coli*. Biotechnol Prog **22:**617-625.

148. **Nehring, R., M. zur Hausen, and W. Neumann.** 1980. Process for working up distillation residues from the hydroformylation of propene. US Patent number 4,190,731; Ap. number 05/940,294.

149. **Niba, L. L.** 2005. Carbohydrates: starch. *In* Y. H. Hui (ed.), Handbook of food science, technology, and engineering, vol. 1. Taylor and Francis, New York.

150. **Nicolet, Y., C. Cavazza, and J. C. Fontecilla-Camps.** 2002. Fe-only hydrogenases: structure, function and evolution. J Inorg Biochem **91:**1-8.

151. **Nozaki, M., K. Tagawa, and D. I. Arnon.** 1961. Noncyclic photophosphorylation in photosynthetic bacteria. Proc Natl Acad Sci **47:**1334-1340.

152. **NRC, and NAE.** 2004. The Hydrogen Economy: Opportunities, Cost, Barriers, and R&D Needs. The National Academies Press, Washington, DC.

153. **Ogino, H., T. Miura, K. Ishimi, M. Seki, and H. Yoshida.** 2005. Hydrogen production from glucose by anaerobes. Biotechnol Prog **21:**1786-1788.

154. **Ohnishi, T.** 1998. Iron-sulfur clusters/semiquinones in complex I. Biochim Biophys Acta **1364:**186-206.

155. **Ohta, K., D. S. Beall, J. P. Mejia, K. T. Shanmugam, and L. O. Ingram.** 1991. Genetic improvement of *Escherichia coli* for ethanol production: chromosomal integration of *Zymomonas mobilis* genes encoding pyruvate decarboxylase and alcohol dehydrogenase II. Appl Environ Microbiol **57:**893-900.

156. **Ostergaard, S., L. Olsson, and J. Nielsen.** 2000. Metabolic engineering of *Saccharomyces cerevisiae*. Microbiol Mol Biol Rev **64:**34-50.

157. **Pakes, W. C. C., and W. H. Jollyman.** 1901. The bacterial decomposition of formic acid into carbon dioxide and hydrogen. J. Chem. Soc **79:**386-391.

158. **Patel, M. A., M. S. Ou, R. Harbrucker, H. C. Aldrich, M. L. Buszko, L. O. Ingram, and K. T. Shanmugam.** 2006. Isolation and characterization of acid-tolerant, thermophilic bacteria for effective fermentation of biomass-derived sugars to lactic acid. Appl Environ Microbiol **72:**3228-3235.

159. **Peters, J. W., W. N. Lanzilotta, B. J. Lemon, and L. C. Seefeldt.** 1998. X-ray crystal structure of the Fe-only hydrogenase (CpI) from *Clostridium pasteurianum* to 1.8 angstrom resolution. Science **282:**1853-1858.

160. **Peters, J. W., R. K. Szilagyi, A. Naumov, and T. Douglas.** 2006. A radical solution for the biosynthesis of the H-cluster of hydrogenase. FEBS Lett **580:**363-367.

161. **Petersen, D. J., R. W. Welch, F. B. Rudolph, and G. N. Bennett.** 1991. Molecular cloning of an alcohol (butanol) dehydrogenase gene cluster from *Clostridium acetobutylicum* ATCC 824. J Bacteriol **173:**1831-1834.

162. **Petersen, D. J., R. W. Welch, K. A. Walter, L. D. Mermelstein, E. T. Papoutsakis, F. B. Rudolph, and G. N. Bennett.** 1991. Cloning of an NADH-dependent butanol dehydrogenase gene from *Clostridium acetobutylicum*. Ann N Y Acad Sci **646:**94-98.

163. **Petitdemange, H., C. Cherrier, R. Raval, and R. Gay.** 1976. Regulation of the NADH and NADPH-ferredoxin oxidoreductases in clostridia of the butyric group. Biochim Biophys Acta **421:**334-337.

164. **Posewitz, M. C., P. W. King, S. L. Smolinski, L. Zhang, M. Seibert, and M. L. Ghirardi.** 2004. Discovery of two novel radical S-adenosylmethionine proteins required for the assembly of an active [Fe] hydrogenase. J Biol Chem **279:**25711-25720.

165. **Prince, R. C., and H. S. Kheshgi.** 2005. The photobiological production of hydrogen: potential efficiency and effectiveness as a renewable fuel. Crit Rev Microbiol **31:**19-31.

166. **Qureshi, N., and H. P. Blaschek.** 2001. ABE production from corn: a recent economic evaluation. J Ind Microbiol Biotechnol **27:**292-297.

167. **Rabinowitz, J.** 1972. Preparation and properties of clostridial ferredoxins. Methods Enzymol **24:**431-446.

168. **Ramey, D. E.** 2007. Butanol: the other alternative fuel, p. 137-147, Agricultural Biofuels: Technology, Sustainability and Profitability. ButylFuel, LLC, Blacklick, OH.

169. **Randt, C., and H. Senger.** 1985. Participation of the two photosystems in light dependent hydrogen evolution in *Scenedesmus obliquus*. Photochem. Photobiol. **42:**553-557.

170. **Rogers P. L. K, L. J., Skotnicki M. L. and Tribe D. E.** 1982. Ethanol production by *Zymomonas mobilis*. Advances Biochem. Eng **23:**37-84.

171. **Rubach, J. K., X. Brazzolotto, J. Gaillard, and M. Fontecave.** 2005. Biochemical characterization of the HydE and HydG iron-only hydrogenase maturation enzymes from *Thermatoga maritima*. FEBS Lett **579:**5055-5060.

172. **Sanchez, A. M., J. Andrews, I. Hussein, G. N. Bennett, and K. Y. San.** 2006. Effect of overexpression of a soluble pyridine nucleotide transhydrogenase (UdhA) on the production of poly(3-hydroxybutyrate) in *Escherichia coli*. Biotechnol Prog **22:**420-425.

173. **Sawers, G., and B. Suppmann.** 1992. Anaerobic induction of pyruvate formate-lyase gene expression is mediated by the ArcA and FNR proteins. J Bacteriol **174:**3474-3478.

174. **Sawers, R. G., and D. H. Boxer.** 1986. Purification and properties of membrane-bound hydrogenase isoenzyme 1 from anaerobically grown *Escherichia coli* K12. Eur J Biochem **156:**265-275.

175. **Sazanov, L. A.** 2007. Respiratory complex I: mechanistic and structural insights provided by the crystal structure of the hydrophilic domain. Biochemistry **46:**2275-2288.

176. **Schindelin, H., C. Kisker, J. L. Schlessman, J. B. Howard, and D. C. Rees.** 1997. Structure of ADP · AlF_4^- - stabilized nitrogenase complex and its implications for signal transduction. Nature **387:**370-376.

177. **Schneider, K., and H. G. Schlegel.** 1976. Purification and properties of soluble hydrogenase from *Alcaligenes eutrophus* H 16. Biochim Biophys Acta **452:**66-80.

178. **Shanmugam, K. T., B. B. Buchanan, and D. I. Arnon.** 1972. Ferredoxins in light- and dark-grown photosynthetic cells with special reference to *Rhodospirillum rubrum*. Biochim Biophys Acta **256:**477-486.

179. **Shi, Z., and H. P. Blaschek.** 2008. Transcriptional analysis of *Clostridium beijerinckii* NCIMB 8052 and the hyper-butanol-producing mutant BA101 during the shift from acidogenesis to solventogenesis. Appl Environ Microbiol **74:**7709-14.

180. **Simpson, F. B., and R. H. Burris.** 1984. A nitrogen pressure of 50 atmospheres does not prevent evolution of hydrogen by nitrogenase. Science **224:**1095-1097.

181. **Slininger, P. J., Bothast, R. J. Okos, M. R. and Ladisch, M. R.** 1985. Comparative evaluation of ethanol production by xylose-fermenting yeasts presented high xylose concentrations. Biotechnol. Lett **7:**431-436.

182. **Smith, P. K., R. I. Krohn, G. T. Hermanson, A. K. Mallia, F. H. Gartner, M. D. Provenzano, E. K. Fujimoto, N. M. Goeke, B. J. Olson, and D. C. Klenk.** 1985. Measurement of protein using bicinchoninic acid. Anal Biochem **150:**76-85.

183. **Spiro, S., and J. R. Guest.** 1991. Adaptive responses to oxygen limitation in *Escherichia coli*. Trends Biochem Sci **16:**310-314.

184. **Sprenger, G. A.** 1996. Carbohydrate metabolism in *Zymomonas mobilis*: a catabolic highway with some scenic routes. FEMS. Microbiol Lett **145:**301-307.

185. **Steen, E. J., R. Chan, N. Prasad, S. Myers, C. J. Petzold, A. Redding, M. Ouellet, and J. D. Keasling.** 2008. Metabolic engineering of *Saccharomyces cerevisiae* for the production of n-butanol. Microb Cell Fact **7:**36-42.

186. **Stephenson, M., and L. H. Stickland.** 1931. Hydrogenase: a bacterial enzyme activating molecular hydrogen. I. The properties of the enzyme. Biochem. J **25:**205-214.

187. **Stephenson, M., and L. H. Stickland.** 1932. Hydrogenlyases. Bacterial enzymes liberating molecular hydrogen. Biochem. J. **26:**712-724.

188. **Sticklen, M.** 2006. Plant genetic engineering to improve biomass characteristics for biofuels. Curr Opin Biotechnol **17:**315-319.

189. **Stuart, T. S., and H. Gaffron.** 1972. The mechanism of hydrogen photoproduction by several algae. I. The effect of inhibitors of photophosphorylation. Planta (Berlin) **106:**91-100.

190. **Stuart, T. S., and H. Gaffron.** 1972. The mechanism of hydrogen photoproduction by several algae. II. The contribution of Photosystem II. Planta (Berlin) **106:**101-112.

191. **Sun, Y., and J. Cheng.** 2002. Hydrolysis of lignocellulosic materials for ethanol production: a review. Bioresour Technol **83:**1-11.

192. **Tagawa, K., and D. I. Arnon.** 1962. Ferredoxins as electron carriers in photosynthesis and in the biological production and consumption of hydrogen gas. Nature **195:**537-543.

193. **Takahashi, C. M., D. F. Takahashi, M. L. Carvalhal, and F. Alterthum.** 1999. Effects of acetate on the growth and fermentation performance of *Escherichia coli* KO11. Appl Biochem Biotechnol **81:**193-203.

194. **Takai, M., N. Iwao, T. Tooru, T. Yoshiyuki, U. Hisao, and N. Akio.** 2001. Process for producing aldehyde. US Patent number 6,291,717; Ap. number 09/457,742.

195. **Tatsumi, H., K. Takagi, M. Fujita, K. Kano, and T. Ikeda.** 1999. Electrochemical study of reversible hydrogenase reaction of *Desulfovibrio vulgaris* cells with methyl viologen as an electron carrier. Anal Chem **71:**1753-1759.

196. **Thauer, R. K., K. Jungermann, and K. Decker.** 1977. Energy conservation in chemotrophic anaerobic bacteria. Bacteriol Rev **41:**100-180.

197. **Thauer, R. K., K. Jungermann, E. Rupprecht, and K. Decker.** 1969. Hydrogen formation from NADH in cell-free extracts of *Clostridium kluyveri*. Acetyl coenzyme A requirement and ferredoxin dependence. FEBS Lett **4:**108-112.

198. **Thorpe, E.** 1921. A dictionary of applied chemistry, vol. II. Longmans, Green and Co., London.

199. **Tshiteya, R. M., E. N. Vermiglio, and S. Tice.** 1991. Compatibility of alcohols with other fuels in blends, p. 5-1:5-10. *In* J. H. Ashworth (ed.), Properties of alcohol transportation fuels: alcohol fuels reference work #1. Meridian Corporation, Alexandria, VA.

200. **Ueda, A., F. Yuichi, A. Atsuhiro, and E. Hiroki.** 2002. Process for producing alcohols. US Patent number 6,455,743; App. number 09/450,123.

201. **Valdez-Vazquez, I., E. Rios-Leal, A. Carmona-Martinez, K. M. Munoz-Paez, and H. M. Poggi-Varaldo.** 2006. Improvement of biohydrogen production from solid wastes by intermittent venting and gas flushing of batch reactors headspace. Environ Sci Technol **40:**3409-3415.

202. **van Maris, A. J., D. A. Abbott, E. Bellissimi, J. van den Brink, M. Kuyper, M. A. Luttik, H. W. Wisselink, W. A. Scheffers, J. P. van Dijken, and J. T. Pronk.** 2006. Alcoholic fermentation of carbon sources in biomass hydrolysates by *Saccharomyces cerevisiae*: current status. Antonie Van Leeuwenhoek **90:**391-418.

203. **van Maris, A. J., A. A. Winkler, M. Kuyper, W. T. de Laat, J. P. van Dijken, and J. T. Pronk.** 2007. Development of efficient xylose fermentation in *Saccharomyces cerevisiae*: xylose isomerase as a key component. Adv Biochem Eng Biotechnol **108:**179-204.

204. **Velazquez, I., E. Nakamaru-Ogiso, T. Yano, T. Ohnishi, and T. Yagi.** 2005. Amino acid residues associated with cluster N3 in the NuoF subunit of the proton-translocating NADH-quinone oxidoreductase from *Escherichia coli*. FEBS Lett **579:**3164-3168.

205. **Vidakovic, M., C. R. Crossnoe, C. Neidre, K. Kim, K. L. Krause, and J. P. Germanas.** 2003. Reactivity of reduced [2Fe-2S] ferredoxins parallels host susceptibility to nitroimidazoles. Antimicrob Agents Chemother **47:**302-308.

206. **Vidakovic, M. S., G. Fraczkiewicz, and J. P. Germanas.** 1996. Expression and spectroscopic characterization of the hydrogenosomal [2Fe-2S] ferredoxin from the protozoan *Trichomonas vaginalis*. J Biol Chem **271:**14734-14739.

207. **Vignais, P. M., B. Billoud, and J. Meyer.** 2001. Classification and phylogeny of hydrogenases. FEMS Microbiol Rev **25:**455-501.

208. **Vignais, P. M., and A. Colbeau.** 2004. Molecular biology of microbial hydrogenases. Curr Issues Mol Biol **6:**159-188.

209. **Villa-Komaroff, L., S. Broome, S. P. Naber, A. Efstratiadis, P. Lomedico, R. Tizard, W. L. Chick, and W. Gilbert.** 1980. The synthesis of insulin in bacteria: a model for the production of medically useful proteins in prokaryotic cells. Birth Defects Orig Artic Ser **16:**53-68.

210. **Waldron, M., and T. Welch.** 2004. DOE researchers demonstrate feasibility of efficient hydrogen production from nuclear energy. Department of Energy**:** [http://www.energy.gov/news/1545.htm].

211. **Wallace, K. K., Z. Y. Bao, H. Dai, R. Digate, G. Schuler, M. K. Speedie, and K. A. Reynolds.** 1995. Purification of crotonyl-CoA reductase from *Streptomyces collinus* and cloning, sequencing and expression of the corresponding gene in *Escherichia coli*. Eur J Biochem **233:**954-962.

212. **Walter, K. A., G. N. Bennett, and E. T. Papoutsakis.** 1992. Molecular characterization of two *Clostridium acetobutylicum* ATCC 824 butanol dehydrogenase isozyme genes. J Bacteriol **174:**7149-7158.

213. **Waterson, R. M., and R. S. Conway.** 1981. Enoyl-CoA hydratases from *Clostridium acetobutylicum* and *Escherichia coli*. Methods Enzymol **71 Pt C:**421-430.

214. **Weckbecker, A., and W. Hummel.** 2004. Improved synthesis of chiral alcohols with *Escherichia coli* cells co-expressing pyridine nucleotide transhydrogenase, $NADP^+$-dependent alcohol dehydrogenase and NAD^+-dependent formate dehydrogenase. Biotechnol Lett **26:**1739-1744.

215. **White, D.** 2000. Fermentations, p. 363-383, The Physiology and Biochemistry of Prokaryotes, 2nd ed. Oxford University Press, New York.

216. **Wiedemann, B., and E. Boles.** 2008. Codon-optimized bacterial genes improve L-arabinose fermentation in recombinant *Saccharomyces cerevisiae*. Appl Environ Microbiol **74:**2043-2050.

217. **Winzer, K., K. Lorenz, B. Zickner, and P. Durre.** 2000. Differential regulation of two thiolase genes from *Clostridium acetobutylicum* DSM 792. J Mol Microbiol Biotechnol **2:**531-541.

218. **Wisselink, H. W., M. J. Toirkens, M. del Rosario Franco Berriel, A. A. Winkler, J. P. van Dijken, J. T. Pronk, and A. J. van Maris.** 2007. Engineering of *Saccharomyces cerevisiae* for efficient anaerobic alcoholic fermentation of L-arabinose. Appl Environ Microbiol **73:**4881-4891.

219. **Woodward, J., N. I. Heyer, J. P. Getty, H. M. O'Neill, E. Pinkhassik, and B. R. Evans.** 2002. Efficient hydrogen production using enzymes of the pentose phosphate pathway. Proceedings of the 2002 U.S. DOE Hydrogen Program Review**:**NREL/CP-610-32405.

220. **Woodward, J., M. Orr, K. Cordray, and E. Greenbaum.** 2000. Enzymatic production of biohydrogen. Nature **405:**1014-1015.

221. **Wu, L. F., and M. A. Mandrand-Berthelot.** 1986. Genetic and physiological characterization of new *Escherichia coli* mutants impaired in hydrogenase activity. Biochimie **68:**167-179.

222. **Wu, L. F., and M. A. Mandrand.** 1993. Microbial hydrogenases: primary structure, classification, signatures and phylogeny. FEMS Microbiol Rev **10:**243-269.

223. **Wykoff, D. D., J. P. Davies, A. Melis, and A. R. Grossman.** 1998. The regulation of photosynthetic electron transport during nutrient deprivation in *Chlamydomonas reinhardtii*. Plant Physiol **117:**129-139.

224. **Yang, K. Y., and R. P. Swenson.** 2007. Modulation of the redox properties of the flavin cofactor through hydrogen-bonding interactions with the N(5) atom: role of alpha-Ser254 in the electron-transfer flavoprotein from the methylotrophic bacterium W3A1. Biochemistry **46:**2289-2297.

225. **Yano, T., V. D. Sled, T. Ohnishi, and T. Yagi.** 1996. Expression and characterization of the flavoprotein subcomplex composed of 50-kDa (NQO1) and 25-kDa (NQO2) subunits of the proton-translocating NADH-quinone oxidoreductase of *Paracoccus denitrificans*. J Biol Chem **271:**5907-5713.

226. **Yano, T., V. D. Sled, T. Ohnishi, and T. Yagi.** 1994. Expression of the 25-kilodalton iron-sulfur subunit of the energy-transducing NADH-ubiquinone oxidoreductase of *Paracoccus denitrificans*. Biochemistry **33:**494-499.

227. **Yomano, L. P., S. W. York, and L. O. Ingram.** 1998. Isolation and characterization of ethanol-tolerant mutants of *Escherichia coli* KO11 for fuel ethanol production. J Ind Microbiol Biotechnol **20:**132-138.

228. **Yomano, L. P., S. W. York, S. Zhou, K. T. Shanmugam, and L. O. Ingram.** 2008. Re-engineering *Escherichia coli* for ethanol production. Biotechnol Lett **30:**2097-2103.

229. **Youngleson, J. S., D. T. Jones, and D. R. Woods.** 1989. Homology between hydroxybutyryl and hydroxyacyl coenzyme A dehydrogenase enzymes from *Clostridium acetobutylicum* fermentation and vertebrate fatty acid beta-oxidation pathways. J Bacteriol **171:**6800-6807.

230. **Zaldivar, J., and L. O. Ingram.** 1999. Effect of organic acids on the growth and fermentation of ethanologenic *Escherichia coli* LY01. Biotechnol Bioeng **66:**203-210.

231. **Zaldivar, J., A. Martinez, and L. O. Ingram.** 2000. Effect of alcohol compounds found in hemicellulose hydrolysate on the growth and fermentation of ethanologenic *Escherichia coli*. Biotechnol Bioeng **68:**524-530.

232. **Zhang, X., K. Jantama, J. C. Moore, K. T. Shanmugam, and L. O. Ingram.** 2007. Production of L-alanine by metabolically engineered *Escherichia coli*. Appl Microbiol Biotechnol **77:**355-366.

233. **Zhang, Y. H., B. R. Evans, J. R. Mielenz, R. C. Hopkins, and M. W. Adams.** 2007. High-yield hydrogen production from starch and water by a synthetic enzymatic pathway. PLoS One **2:**e456.

234. **Zhao, Y., C. A. Tomas, F. B. Rudolph, E. T. Papoutsakis, and G. N. Bennett.** 2005. Intracellular butyryl phosphate and acetyl phosphate concentrations in *Clostridium acetobutylicum* and their implications for solvent formation. Appl Environ Microbiol **71:**530-537.

235. **Zhou, S., F. C. Davis, and L. O. Ingram.** 2001. Gene integration and expression and extracellular secretion of *Erwinia chrysanthemi* endoglucanase CelY (*celY*) and CelZ (*celZ*) in ethanologenic *Klebsiella oxytoca* P2. Appl Environ Microbiol **67:**6-14.

BIOGRAPHICAL SKETCH

Phi Minh Do was born in 1981 in Vietnam. Shortly after birth, Phi, accompanied by his parents and two brothers, immigrated to the United States of America as a post-Vietnam War refugee with a port of entry date of February 1982. Phi spent most of his childhood in Panama City, Florida where he graduated from Bay High School in 1999 at the top of his class. He later earned a Bachelor of Science with honors in microbiology and cell science from the Department of Microbiology and Cell Science at the University of Florida in 2003.

Upon graduating with his B.S., Phi was accepted into the Ph.D. graduate program in the same department under the advisement of Dr. K.T. Shanmugam with focus on microbial production of renewable fuels and chemicals. Phi's passion for teaching led to mentoring numerous of undergraduates as well as being guest lecturers in both undergraduate and graduate courses. In addition to his graduate studies, Phi was an advocate for student rights and fought to make changes in departmental policies. In 2006 and 2007, he was elected vice-president and president, respectively, of the Microbiology Society for Graduate Students at the University of Florida where he coordinated the annual Graduate Symposium.

Upon completion of his Ph.D., Phi continued as a post-doctoral research associate with Dr. Lonnie Ingram, a world-renowned expert in the development of biocatalysts for renewable fuels and chemicals, where he hopes to continue the development of his academic career towards making a global impact on renewable energy.